AD NUMBER

AD879736

NEW LIMITATION CHANGE

TO

Approved for public release, distribution unlimited

FROM

Distribution authorized to U.S. Gov't. agencies and their contractors; Critical Technology; JUL 1970. Other requests shall be referred to Air Force Flight Dynamics Laboratory, Attn: FDTR, Wright-Patterson AFB, OH 45433.

AUTHORITY

AFWAL ltr dtd 14 Aug 1980

THIS REPORT HAS BEEN DELIMITED
AND CLEARED FOR PUBLIC RELEASE
UNDER DOD DIRECTIVE 5200.20 AND
NO RESTRICTIONS ARE IMPOSED UPON
ITS USE AND DISCLOSURE.

DISTRIBUTION STATEMENT A

APPROVED FOR PUBLIC RELEASE;
DISTRIBUTION UNLIMITED.

AFFDL-TR-70-106
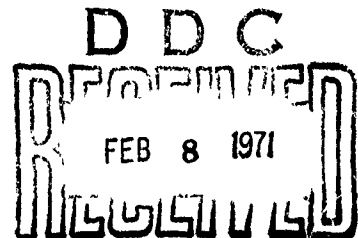
DESIGN MANUAL FOR VERTICAL GUSTS
BASED ON POWER SPECTRAL TECHNIQUES

JOHN C. HOUBOLT

AERONAUTICAL RESEARCH ASSOCIATES OF PRINCETON, INC.

TECHNICAL REPORT AFFDL-TR-70-106

DECEMBER 1970

D D C

FEB 8 1971

B

AIR FORCE FLIGHT DYNAMICS LABORATORY
AIR FORCE SYSTEMS COMMAND
WRIGHT-PATTERSON AIR FORCE BASE, OHIO

NOTICES

When Government drawings, specifications, or other data
are used for any purpose other than in connection with a
definitely related Government procurement operation, the
United States Government thereby incurs no responsibility nor
any obligation whatsoever; and the fact that the government
may have formulated, furnished, or in any way supplied the
said drawings, specifications, or other data, is not to be
regarded by implication or otherwise as in any manner licensing
the holder or any other person or corporation, or conveying any
rights or permission to manufacture, use, or sell any patented
invention that may in any way be related thereto.

DESIGN MANUAL FOR VERTICAL GUSTS BASED ON POWER SPECTRAL TECHNIQUES

JOHN C. HOUBOLT

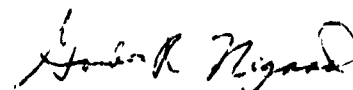*AERONAUTICAL RESEARCH ASSOCIATES OF PRINCETON, INC.*

FOREWORD

This report was prepared by Aeronautical Research Associates of Princeton, Inc., Princeton, New Jersey, under Air Force Contract F33615-69-C-1272. The contract was initiated under Project No. 1367, "Structural Design Criteria," Task No. 136702, "Aerospace Vehicle Structural Loads Criteria." The work was administered under the direction of the Air Force Flight Dynamics Laboratory, Research and Technology Division, Air Force Systems Command, Wright-Patterson Air Force Base, Ohio, Mr. Paul L. Hasty (FDTE), Project Engineer.

The work reported in this study was conducted by Aeronautical Research Associates of Princeton, Inc. with Dr. John C. Houbolt as principal investigator, and covers the period 2 January 1969 to 1 July 1970. The report was submitted by the author in July 1970.

The contractor's report number is A.R.A.P. 147.

This technical report has been reviewed and is approved.

Gordon R. Negaard, Major, USAF
Chief, Design Crite ia Branch
Structures Division

ii

ABSTRACT

Recommended procedures, based on power spectral methods, are given for the design of aircraft for vertical atmospheric turbulence encounter. Four procedures are outlined. The first is a direct preliminary design type, based on specified rigid body results. The second is more detailed and makes use of composite response values, computed either from the rigid body results, or by specific frequency response analysis. A third procedure is based on comparison with a previous successful decign. In the fourth procedure specific loads exceedance curves are derived in accordance with assumed missions. Recommended gust intensity values, proportion of time in turbulence, and scale values are given. For ease in application, detailed step-by-step procedures are listed throughout the manual.

The philosophy and basic for deriving the recommended design values are reviewed in part. Special sections are included throughout which summarize the basic equations that apply to gust analysis, give the means for treating structural interaction effects, and show how the problem of nonuniform spanwise gusts is treated. Appendices are included which give useful conversion and data charts, and which review various means for establishing the frequency response function.

TABLE OF CONTENTS

TABLE OF CONTENTS (Cont.)

ILLUSTRATIONS

SYMBOLS

a	slope of the lift curve
A	structural response quantity as used in $\sigma_x = A\sigma_w$, defined by equation (15)
c	wing chord; generally throughout the report c refers to a reference chord, such as the mean aerodynamic chord
f	frequency, cps
f( )	function notation, generally representing nondimensional exceedance curve
$F_x(\omega)$	Fourier transform of variable x
h	altitude
H	gust gradient distance
$H_x(\omega)$	frequency response function of variable x
i	$\sqrt{-1}$
k	reduced frequency, $k = \frac{\omega c}{2V}$
K_1	Bessel function of the second kind for imaginary argument
K_g	gust alleviation factor for discrete gusts
K_ϕ	spectral gust alleviation factor
L	turbulence scale
m	integers
n	number of crossings with positive slope
N	number of times per second load level x is crossed with positive slope
N_o	number of zero crossings per second with positive slope
$p(x)$ $p(\sigma)$ $p(L)$	probability density functions
P	proportion of time spent in turbulence
s	axial stress

S	wing area
t	time
T	various flight times, including lifetime value
V	flight velocity
w	vertical gust velocity
W	aircraft weight
x	response variable, used generally in the sense of being an increment due to gusts
x_L	limit load value
x_{1-g}	1-g load level
α	constant used in defining exceedance curves
ϵ	spanwise increment of length
η	factor denoting number of standard deviations
λ	wavelength
μ	mass parameter
ν	cross-correlation coefficient
ξ	nondimensional length, $\xi = \frac{m\epsilon}{L}$
ρ	air density
σ_c	r.m.s. value associated with cutoff frequency ω_c
σ_t	truncated r.m.s. value
σ_w	r.m.s. value of vertical gust velocity
σ_x	r.m.s. value of variable x
$\sigma_{\Delta n}$	r.m.s. value of incremental acceleration Δn
τ	shear stress
$\phi_w(\ )$	power spectrum of vertical gust velocities
$\phi_x(\ )$	power spectrum of variable x
$\phi_{xy}(\ )$	cross spectrum between variables x and y

SYMBOLS (Cont.)

ω circular frequency

ω_c cut-off frequency

Ω spatial frequency, $\dfrac{\omega}{V}$

A dot over a symbol represents differentiation with respect to time.

A bar over a symbol denotes the conjugate complex.

SECTION I

INTRODUCTION

Under contract with the Air Force Flight Dynamics Laboratory, Aeronautical Research Associates of Princeton, Inc., has been developing procedures for designing aircraft for gust encounter based on power spectral techniques. Some of the basic results developed are presented in references 1, 2, and 3. A continuing phase of effort has had the objectives of further developing the procedures and in particular distilling all the work that had been accomplished and from this distillation to prepare a manual for the design of aircraft for vertical gust encounter. This report represents the desired gust design manual. It should be noted that although effort was restricted to vertical gusts only, many of the procedures discussed herein can be extended to the cases of horizontal or combined vertical and horizontal gust encounter. The report thus sets the stage for possible manuals on these additional gust encounter situations.

Many of the results presented herein reflect the findings of the past year of effort, but notions of many previous investigations also enter prominently, in particular, those of references 2, 4, and 5. In addition, results of many other gust studies were considered and incorporated wherever possible; these studies include: gust response studies related to the present investigation, references 6, 7, 8; results of the ALLCAT program, references 9-14, and many of the reports dealing with the description of the atmospheric turbulence environment such as references 15-22.

It should be noted that, since this report is in the nature of a manual, much of the information presented is given without details of development and without elaboration of the logic by which some of the choices were made.

1

SECTION II

DESCRIPTION OF MANUAL

Problem treated.- The basic design problem that is treated in this manual is that of an aircraft encountering atmospheric turbulence that is considered to be random in the direction of flight but which is uniform in the spanwise direction, as depicted in the following sketch
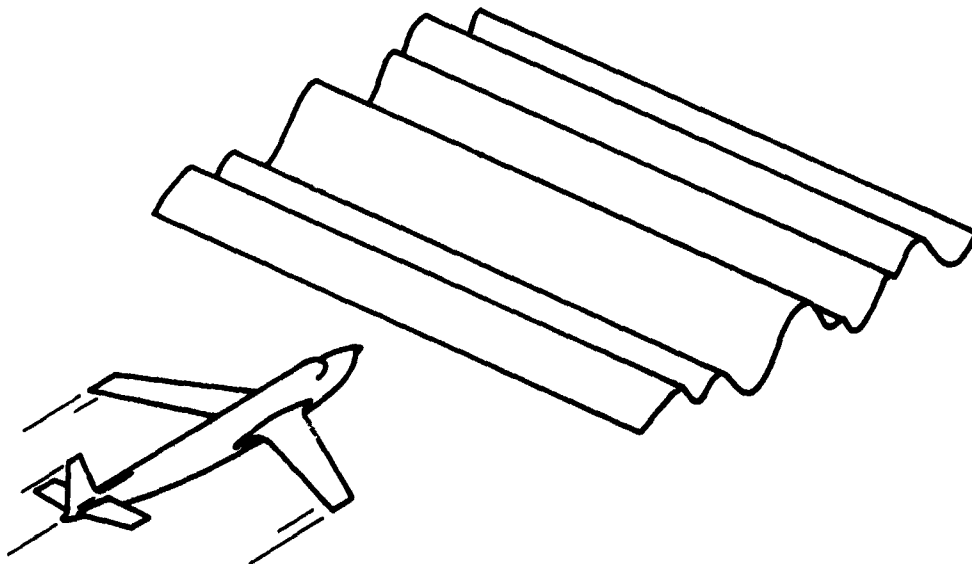
Purpose of manual.- The main purpose of the manual is to outline procedures for establishing gust load levels that are appropriate for use in structural design considerations of the aircraft. A secondary purpose is to give the means for establishing the expected load exceedance curves for possible use in structural fatigue analyses of the aircraft structure.

Basic notions of analytical approach.- The intent of the manual is to specify more realistic gust design procedures through use of the power spectral methods of generalized harmonic analysis. Basic ingredients are essentially as follows. Modelling of the atmospheric turbulence environment is made in terms of a spectrum shape, a r.m.s. gust intensity variable σ_w , a scale of turbulence L , and the parameter P depicting the proportion of flight time spent in turbulence. The response is treated in the frequency plane instead of the time plane, involving mainly the familiar linear equation

$$\phi_x(\omega) = \left| H_x(\omega) \right|^2 \phi_w(\omega)$$

3

which relates the output spectra of the response variable x to the input spectra of gust velocities w through the frequency response function H_x, defined as the response x that results from a sinusoidal gust encounter of unit amplitude. This response equation leads to the two basic structural response quantities A and N_o, where A relates the r.m.s. output value σ_x to the r.m.s. gust input value through the relation

$$\sigma_x = A\sigma_w$$

and N_o defines the number of zero crossings of x with positive slope per second. Load exceedance curves having the form

$$N = PN_o \ f(\frac{x}{\sigma_x})$$

are in turn developed for use in establishing design loads. The environmental parameters P, σ_w, and L, the structural response parameters A and N_o, and the generalized load exceedance curves are thus the basic ingredients of the procedures.

Credibility.- It is felt appropriate to give the following foreword on the development of this manual before giving a synopsis of its contents. Many of the results and procedures given herein were established by reasonably sound mathematical analysis. Because uncertainty still exists with respect to some of the quantities which characterize atmospheric turbulence, however, such as the magnitude and distribution of turbulence intensities and scale, there are places where specified values cannot be regarded with certainty. In these places, recourse was placed on reasoning, judgment, and hypothesis.

Goal.- An underlying goal in the preparation of this manual was to make the procedures as simple as possible. Essentially, procedures no more involved than the discrete-gust design method were sought. The design approach evolved is basically as follows: check the design by the simplified procedures given (which are analogous to the discrete-gust design method); if the design passes the check, no further work is necessary; if design uncertainties are revealed by the simplified procedures, then proceed in the more detailed way outlined, but only for those points of the structural design which appear to be questionable. It should be noted specifically that the procedures given herein do not depend on notions such as probability of failure or failure rate. There is no need to introduce these concepts, and they are thus avoided.

4

Contents.- The breakdown and nature of the contents of the report are essentially as follows. Section III lists the various spectral relations that apply. Section IV defines the atmospheric input spectrum that is recommended. Section V covers the practical aspects of establishing the basic structural response quantities A and N_o . Section VI presents the basic spectral results for gust loads that apply to a rigid airplane with the single degree of freedom of vertical translation; these results form the basis of the simplified procedures.

Section VII is the heart of the report. It shows how, with the use of Section VI, to identify the design conditions, how to make the preliminary design check, and then how to proceed with the cases that are found to need detailed design treatment. Section VIII outlines the procedures for establishing the basic load exceedance curves.

The intent of Section IX is to show that the procedures given herein essentially include the considerations of discrete-gust design. Section X shows why limit load values are chosen as the base for design, and why ultimate load considerations are avoided. The manner of handling structural interaction effects is covered in Section XI. Although not intended as part of the presently recommended design procedure, Section XII is given to show the means for handling the more general gust encounter case, wherein the gusts are random in the spanwise direction as well as the direction of flight. The section is included because it may be desirable to look into this situation for some of the very large aircraft.

Appendix A presents some general data and conversion charts that are useful in spectral considerations. Appendix B reviews the various aspects that are involved in determining the frequency response functions for the aircraft, the function which is central in any spectral treatment of response.

5

SECTION III

BASIC SPECTRAL RELATIONS

The basic spectral relations that are of concern in the treatment of gust loads are presented in this section. The equations are presented in terms of the frequency argument ω, but it should be understood that equivalent expressions may also be written in terms of other frequency arguments. Note that theoretically a value of infinity should be used for the upper limit in the integrals presented; for practical purpose, however, a cutoff frequency ω_c is used. The means for establishing this cutoff frequency is given in Section V. Figure 1, taken from reference 4, serves well to illustrate the physical significance of some of the relations given in this section; the notions of this figure are by now quite well known, but they are so basic that reproduction of the figure here is considered merited.

Definitions:

w   represents the input gust function w(t)

x or y represents the response functions x(t) and y(t)

$\dot{x}$ or $\dot{y}$ represents the response functions $\dot{x}(t)$ and $\dot{y}(t)$

$$H_x(\omega) = A_x(\omega) + i\, B_x(\omega)$$

$$H_y(\omega) = A_y(\omega) + i\, B_y(\omega)$$

where H_x and H_y are the frequency response functions for the variables x and y due to a sinusoidal gust encounter of unit amplitude; note the A functions are symmetrical with respect to the argument ω, while the B functions are antisymmetrical. Various frequency arguments are as follows:

$$\omega = 2\pi f$$

$$\Omega = \frac{\omega}{V}$$

$$k = \frac{\omega c}{2V}$$

Frequency response

$$H_{\dot{x}} = i\omega H_x \tag{1}$$

$$H_{\dot{y}} = i\omega H_y \tag{2}$$

7

Basic input-output relations

$$\phi_x = |H_x|^2 \, \phi_w \tag{3}$$

$$\phi_{\dot{x}} = \omega^2 |H_x|^2 \, \phi_w \tag{4}$$

Basic cross-spectral relations

$$\phi_{xy} = \bar{\phi}_{yx} = \bar{H}_x H_y \phi_w = \frac{H_y}{H_x} \phi_x = \frac{\bar{H}_x}{\bar{H}_y} \phi_y \tag{5}$$

$$\phi_{wx} = H_x \, \phi_w \tag{6}$$

$$\phi_{\dot{x}\dot{y}} = \omega^2 \bar{H}_x H_y \, \phi_w \tag{7}$$

r.m.s. values and correlation coefficients

$$\sigma_w^2 = \int_0^\infty \phi_w(\omega) \, d\omega \tag{8}$$

$$\sigma_x^2 = \int_0^{\omega_c} \phi_x(\omega) \, d\omega = \int_0^{\omega_c} |H_x|^2 \, \phi_w \, d\omega \tag{9}$$

$$\sigma_y^2 = \int_0^{\omega_c} \phi_y(\omega) \, d\omega = \int_0^{\omega_c} |H_y|^2 \, \phi_w \, d\omega \tag{10}$$

$$\rho \sigma_x \sigma_y = \frac{1}{2} \int_{-\omega_c}^{\omega_c} \phi_{xy}(\omega) \, d\omega = \int_0^{\omega_c} \mathrm{Re}(\bar{H}_x H_y) \phi_w \, d\omega$$

$$= \int_0^{\omega_c} (A_x A_y + B_x B_y) \, \phi_w \, d\omega \tag{11}$$

8

$$\sigma^2_{\dot{x}} = \int_0^{\omega_c} \omega^2 |H_x|^2 \, \phi_w \, d\omega \tag{12}$$

$$\sigma^2_{\dot{y}} = \int_0^{\omega_c} \omega^2 |H_y|^2 \phi_w \, d\omega \tag{13}$$

$$\nu \sigma_{\dot{x}} \sigma_{\dot{y}} = \frac{1}{2} \int_{-\omega}^{\omega_c} \phi_{\ddot{x}\ddot{y}}(\omega) \, d\omega$$

$$= \int_0^{\omega_c} \omega^2 (A_x A_y + B_x B_y) \, \phi_w \, d\omega \tag{14}$$

Basic structural response quantities A and N_o

$$A = \frac{\sigma_x}{\sigma_w} = \left[\frac{\int_0^{\omega_c} |H_x|^2 \phi_w \, d\omega}{\int_0^{\infty} \phi_w \, d\omega} \right]^{1/2} \tag{15}$$

$$N_o = \frac{1}{2\pi} \frac{\sigma_{\dot{x}}}{\sigma_x} = \frac{1}{2\pi} \left[\frac{\int_0^{\omega_c} \omega^2 |H_x|^2 \phi_w \, d\omega}{\int_0^{\omega_c} |H_x|^2 \phi_w \, d\omega} \right]^{1/2} \tag{16}$$

9
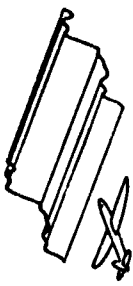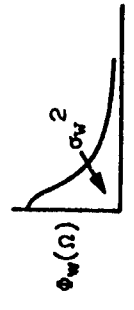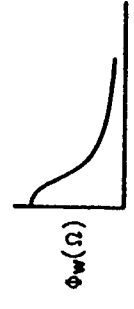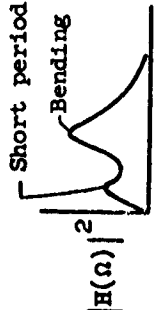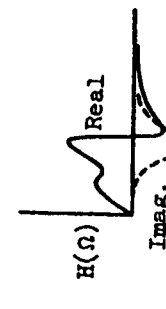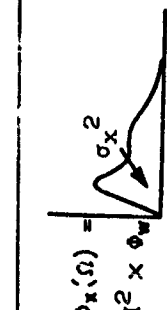
	Power-spectrum approach (Amplitude information only)	Cross-spectrum approach (Phase as well as amplitude information)
Input: Characterizes the atmosphere $\sigma_w^2 =$ Mean-square value of gust velocity	$\Phi_w(\Omega)$ σ_w^2	$\Phi_w(\Omega)$
Frequency-response: Characterizes the airplane	$\lvert H(\Omega)\rvert^2$ Short period Bending	$H(\Omega)$ Real Imag.
Output: Characterizes the response $\sigma_x^2 =$ Mean-square value of response	$\Phi_x'(\Omega) = H^2 \times \Phi_w$ σ_x^2 $\Omega = \dfrac{2\pi}{\lambda}$	$\Phi_{wx}(\Omega) = H \times \Phi_w$ Ω

Spectral conversions

$$\omega = 2\pi f = V\Omega = V\,\frac{2\pi}{\lambda}$$

$$\Phi(\omega) = \frac{1}{2\pi}\,\Phi(f) = \frac{1}{V}\,\Phi(\Omega)$$

Figure 1. Input-Output Relations for Gust Response

SECTION IV

INPUT SPECTRUM AND SHAPE VARIATIONS

The recommended spectrum for the input vertical gust is shown in figure 2 and is given by the equation

$$\phi_W(L\Omega) = \frac{\sigma_w^2}{\pi} \frac{1 + \frac{8}{3}(1.339 \ L\Omega)^2}{\left[1 + (1.339 \ L\Omega)^2\right]^{11/6}} \tag{17}$$

Expressions for this spectrum in terms of other frequency arguments appear as

$$\left.\begin{aligned}
\phi_W(f) &= \frac{2\pi L}{V} \ \phi_W(L\Omega) \\[2mm]
\phi_W(\omega) &= \frac{L}{V} \ \phi_W(L\Omega) \\[2mm]
\phi_W(\Omega) &= L \ \phi_W(L\Omega) \\[2mm]
\phi_W(k) &= \frac{2L}{c} \ \phi_W(L\Omega)
\end{aligned}\right\} \tag{18}$$

The value for the turbulence scale L has been a very elusive quantity. Estimates have ranged from 200 ft to over 5000 ft . Recent studies made by the principal investigator of this report, reference 23, aimed at deducing scale value by means other than those commonly used, have indicated that scale values may be smaller than those often quoted. On the basis of these studies, the value for the effective scale of turbulence L is recommended as $L = 750$ ft for all altitudes. Note the scale is not really known to within the accuracy of 50 ft , or even to within 100 ft . The choice is made simply to make the quantity $2L/c$, which is frequently encountered, expressible in a rounded-off number form; thus, the following ratio is recommended

$$\frac{2L}{c} = \frac{1500}{c}$$

Useful information related to the spectrum shown in figure 2 is shown in figures 3 through 6. Figure 3 is the type of plot that should be kept in mind for all response spectra that are given herein and for any that are derived in design studies. Plots of this type can be quite significant; thus, when the spectrum values are multiplied by the frequency and the results are plotted with a linear scale vertically and a log scale horizontally, then the geometric area one sees visually under the curve shows what frequency range is contributing most to the total power, or mean square value. This result is demonstrated as follows

11

$$\sigma_w^2 = \int_0^\infty \phi_w(\omega) \, d\omega$$

$$= \int_0^\infty \omega \phi_w(\omega) \, \frac{d\omega}{\omega}$$

$$= \int_0^\infty \omega \, \phi_w(\omega) \, d\chi$$

where $d\chi = d\omega/\omega$ or $\chi = \log \omega$.

Figures 4 and 5 give the truncated r.m.s. and zero crossing values of the gust spectrum as a function of cutoff frequency as established by the following equations

$$\sigma_c^2 = \int_0^{(L\Omega)_c} \phi_w(L\Omega) \, d(L\Omega)$$

$$(L\Omega)_0 = \left[\frac{\int_0^{(L\Omega)_c} (L\Omega)^2 \, \phi_w(L\Omega) \, d(L\Omega)}{\sigma_c^2} \right]^{1/2}$$

which are similar to equations (8) and (16). Figure 5 indicates that the "zero crossings" value increases monotonically with cutoff frequency. The reason is that equation (17) is intended to apply only in the turbulence inertial subrange. A leveling of the curve would occur if a more appropriate equation were used at the high frequencies (frequency components having wavelengths smaller than one or two centimeters). From a response point of view, however, the aerodynamics and structural behavior of the aircraft tend to wash out the effects of high frequency gust components even in the inertial subrange. Thus, only frequencies below some cutoff frequency are of practical concern in response calculations. Section V on A and N_0 determination develops this point specifically.

Figure 6 gives a second truncated r.m.s. value of the gust spectrum, often used in the experimental deduction of scale value, as defined by

$$\sigma_t^2 = \int_{(L\Omega)_c}^\infty \phi_w(L\Omega) \, d(L\Omega)$$

Note that

$$\sigma_w^2 = \sigma_c^2 + \sigma_t^2$$

This section is closed with some comment on the variations in shape of gust input spectra. In general, too much attention has been placed on trying to fit various forms of spectral equations to gust data. Often the raw data are wrong cr unreliable to begin with, and often the deduced spectral values are in error because of the distortions that are produced by the numerical analysis procedure used. Usually there is little or no attempt to investigate how errors in the data or in the processing can influence the spectral results, particularly at the low frequency end. Thus, apparent changes in the spectrum shape may, in reality, not be there. It should be realized that considerable variations in the apparent gust spectrum shape can be had even using equation (17) as the basic ingredient. As the r.m.s. value of gust intensity varies from one turbulence encounter to another, so too can the scale be expected to vary. Thus, if a distribution curve $p(L)$ is considered for scale L, see figure 7(a), analogous to the introduction of a probability density distribution for σ_w, then an effective spectrum shape may be deduced using equation (17) as a base according to the equation

$$\frac{\phi(\Omega)}{\sigma_w^2} = \int_{L_1}^{L_2} p(L) \frac{\phi_w(\Omega)}{\sigma_w^2} \, dL \tag{19}$$

This deduction is recognized as being quite similar to the deduction of the familiar peak count relation $e^{-x/\sigma}$ from the peak count expression for normal processes $e^{-\frac{1}{2}\frac{x^2}{\sigma^2}}$. The following example, taken from reference 24, illustrates the use of equation (19). Consider that $p(L)$ is given by the expression

$$p(L) = .75 \, \delta(L - 400) + .25 \, \delta(L - 2000)$$

Effectively, this expression indicates that a normalized spectra $\frac{\phi(\Omega)}{\sigma_w^2}$ having a scale of 400 feet is added to a normalized spectra having a scale of 2000 feet, with a weighting factor of .75 on the first and .25 on the second. Results obtained from this expression through use of equations (17)-(19) are shown in figure 7(b). The effective spectrum so deduced is seen to contrast markedly with the spectrum given by equation 17, curve B, even though this equation was the basic building block of the derived results. The effective scale value of the combined spectra is $L = 800$ ft. By this

13

process many different results of the type indicated by curve A may be deduced. The results shown in figure 7 thus indicate that care must be taken when atmospheric spectral data are interpreted. Often it is stated that the data being presented differs from other data; the interpretation is given, for example, that the spectra seem to exhibit a "mild knee" behavior. In reality the results may simply be indicating that a mixture of data of several scales is being presented. Effectively, the results are probably reflecting the fact that the data are not stationary.

$$\phi(L\Omega) = \frac{\sigma_w^2}{\pi} \frac{1+\frac{8}{3}(1.339L\Omega)^2}{\left[1+(1.339L\Omega)^2\right]^{\frac{11}{6}}}$$
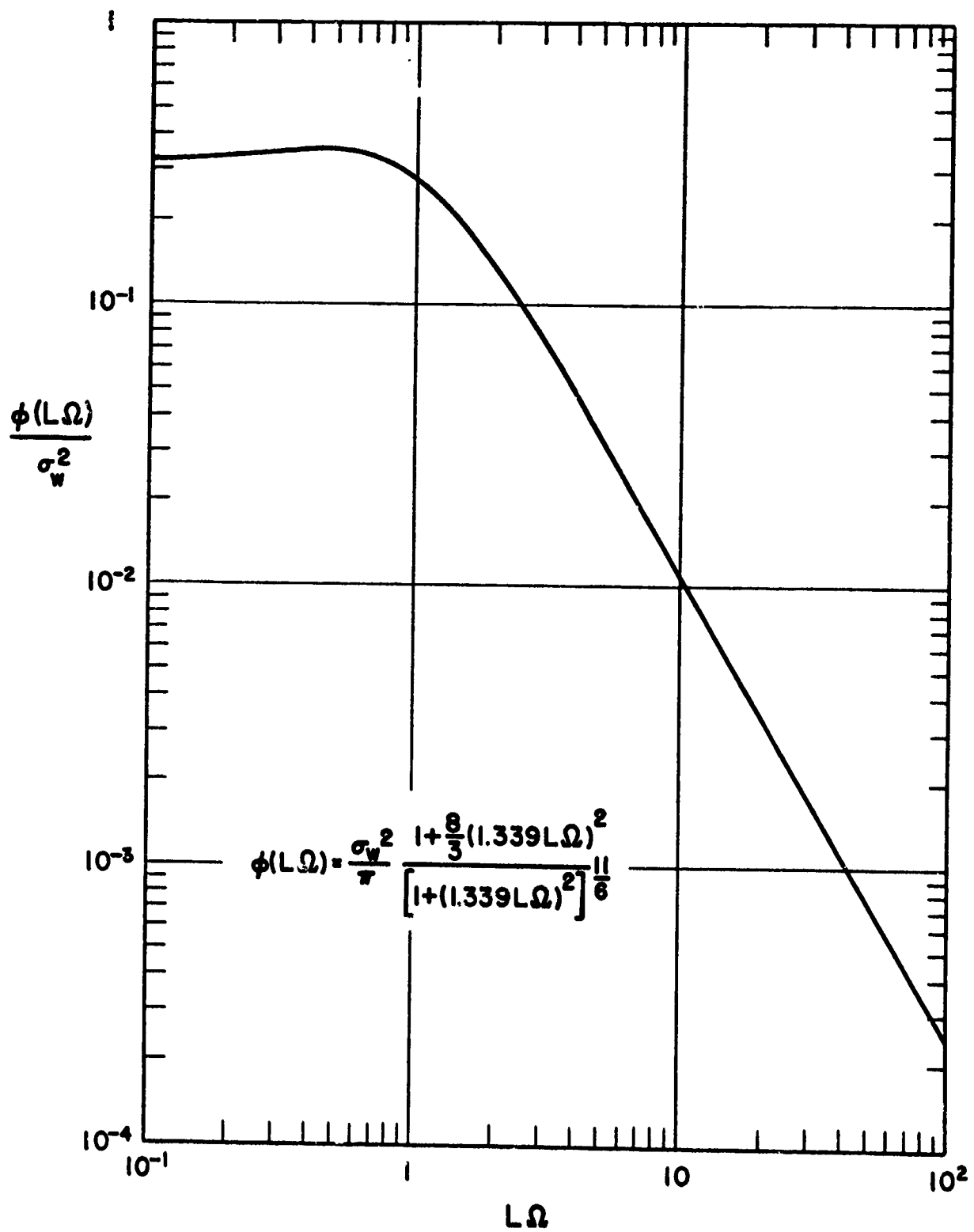
Figure 2. Gust Spectrum Function

15
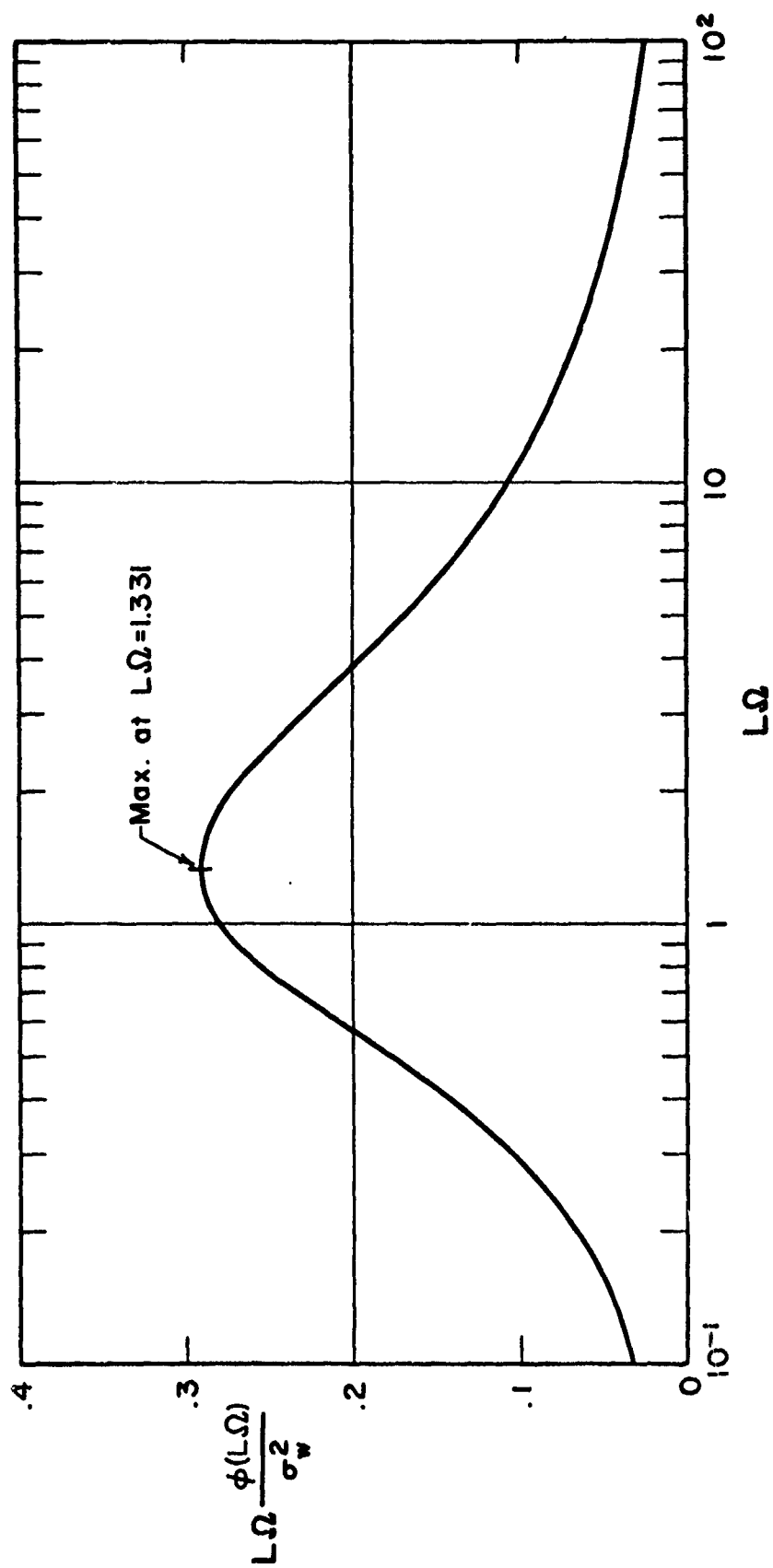
Figure 3. Distribution of σ_w^2 with Frequency

16
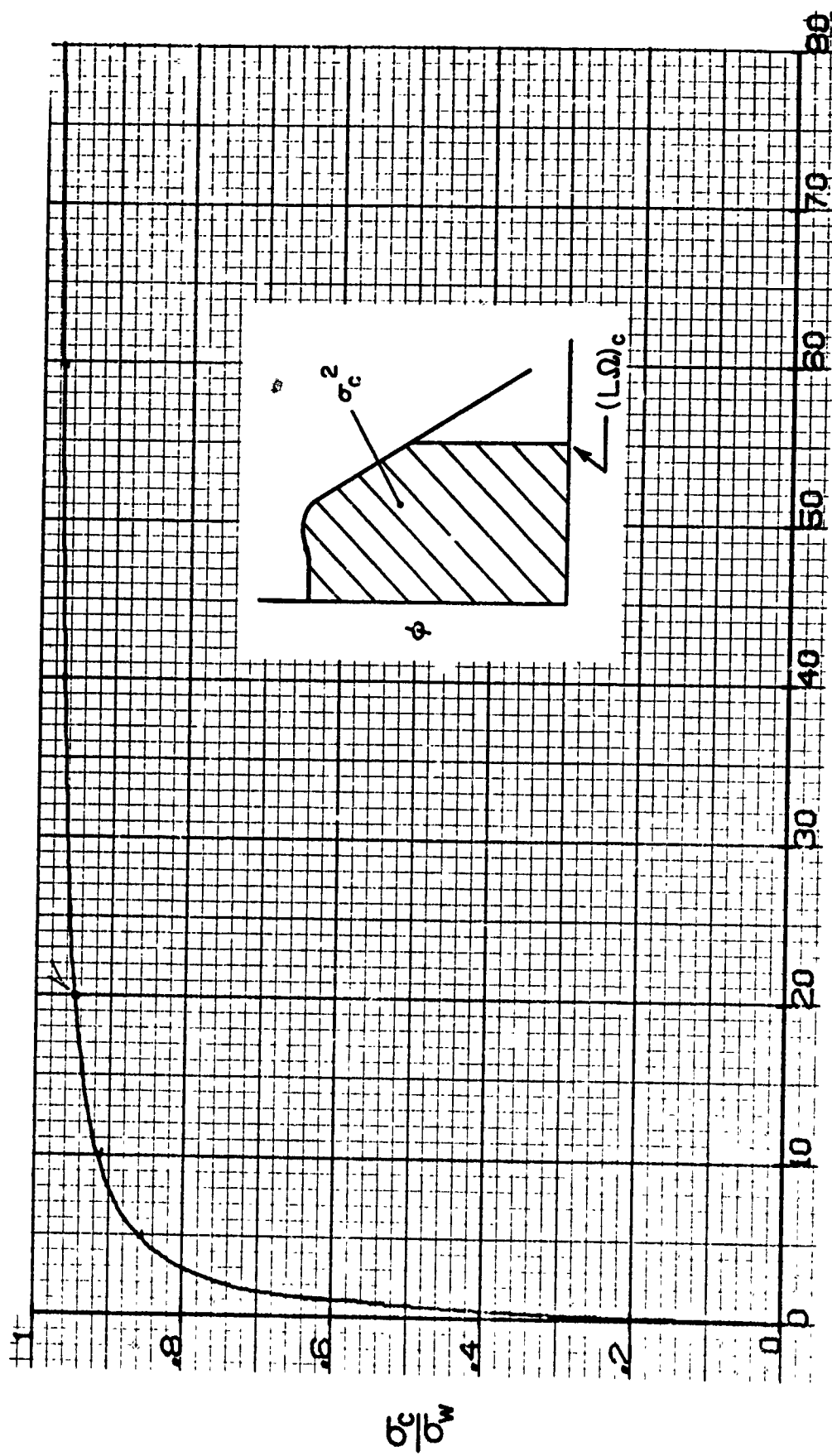
Figure 4. Variation of $\frac{\sigma_c}{\sigma_w}$ with $(L\Omega)_c$
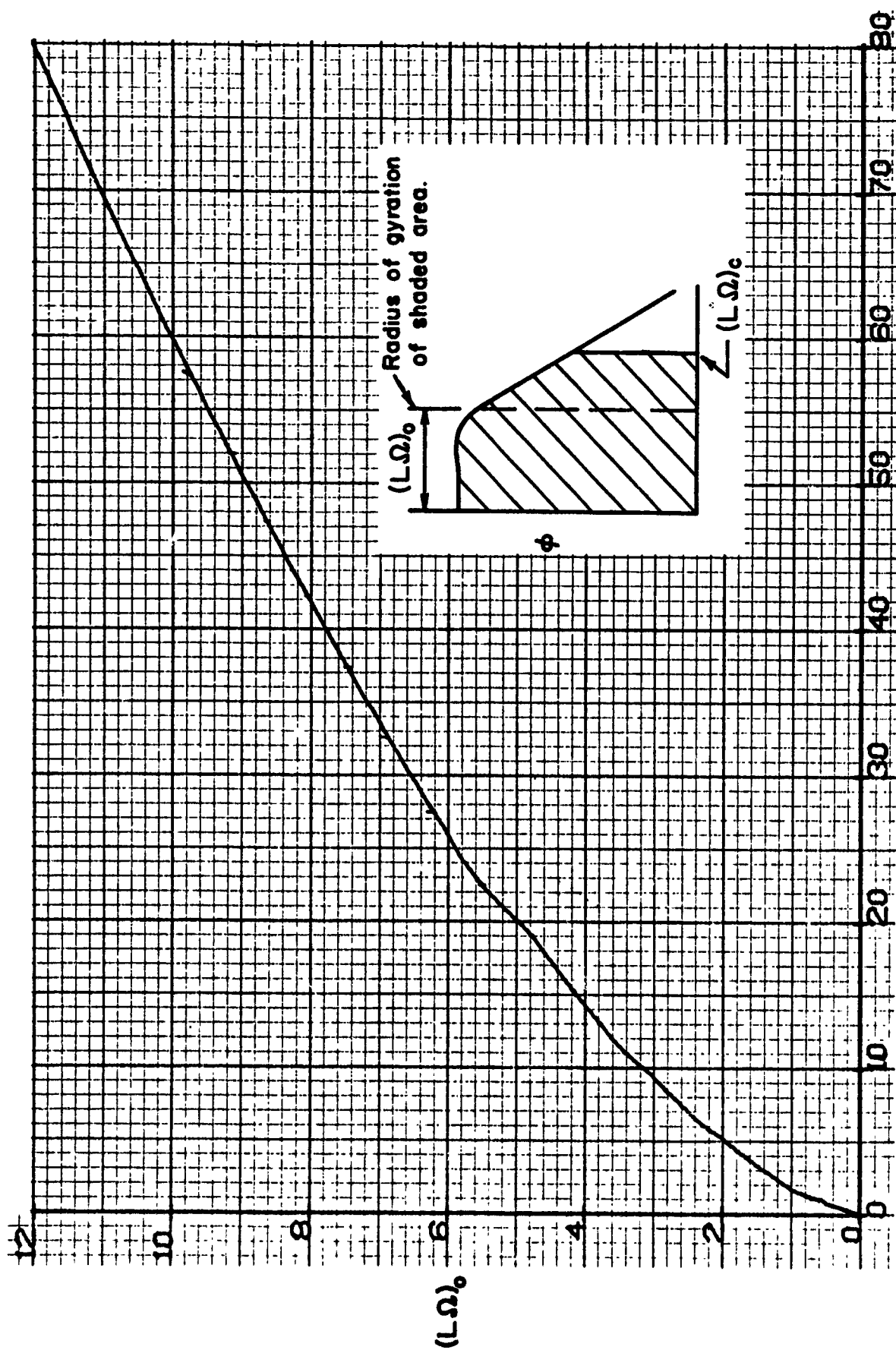
Figure 5. Zero-Crossing Frequencies for Gust Spectrum
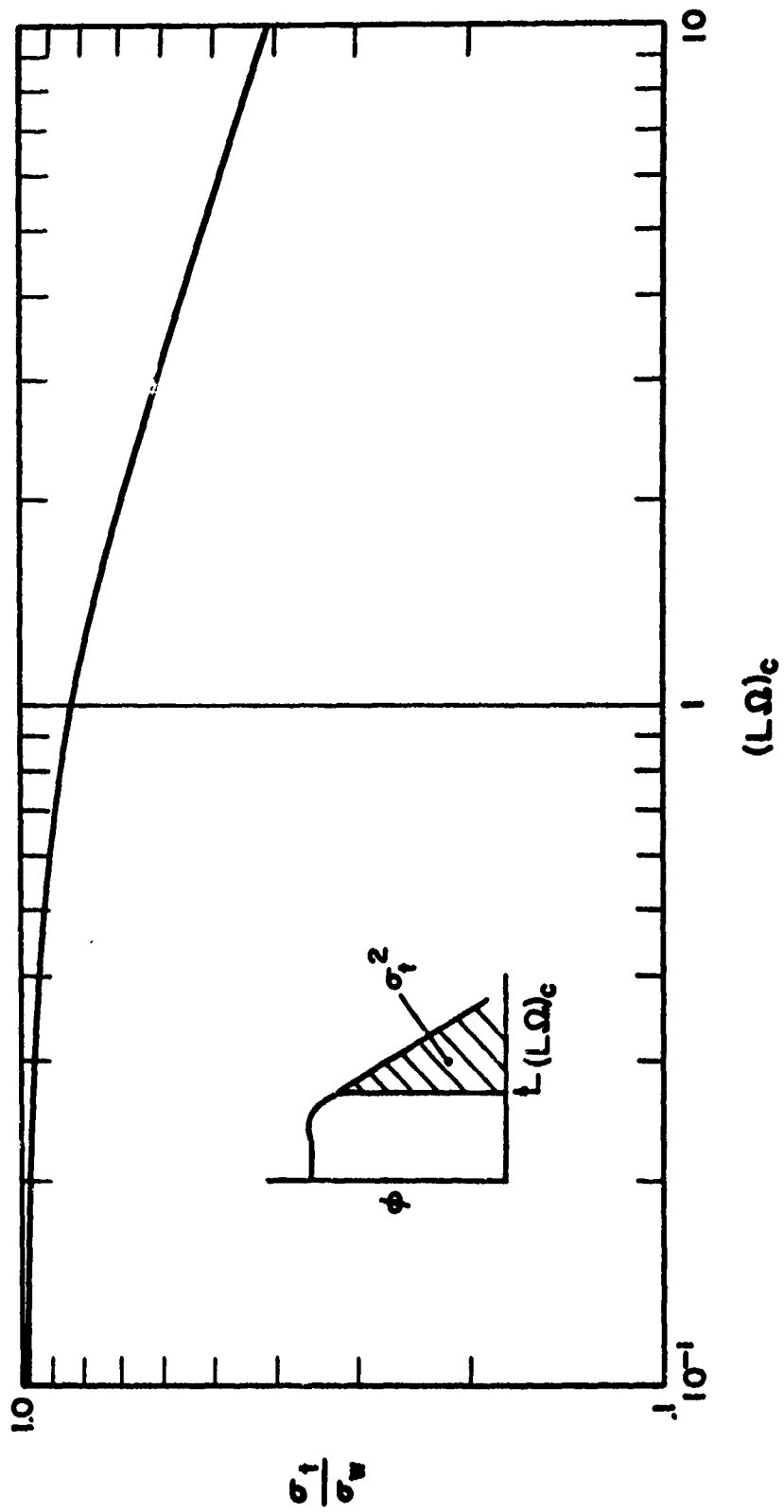
Figure 6. Truncated r.m.s. Value σ_t

19
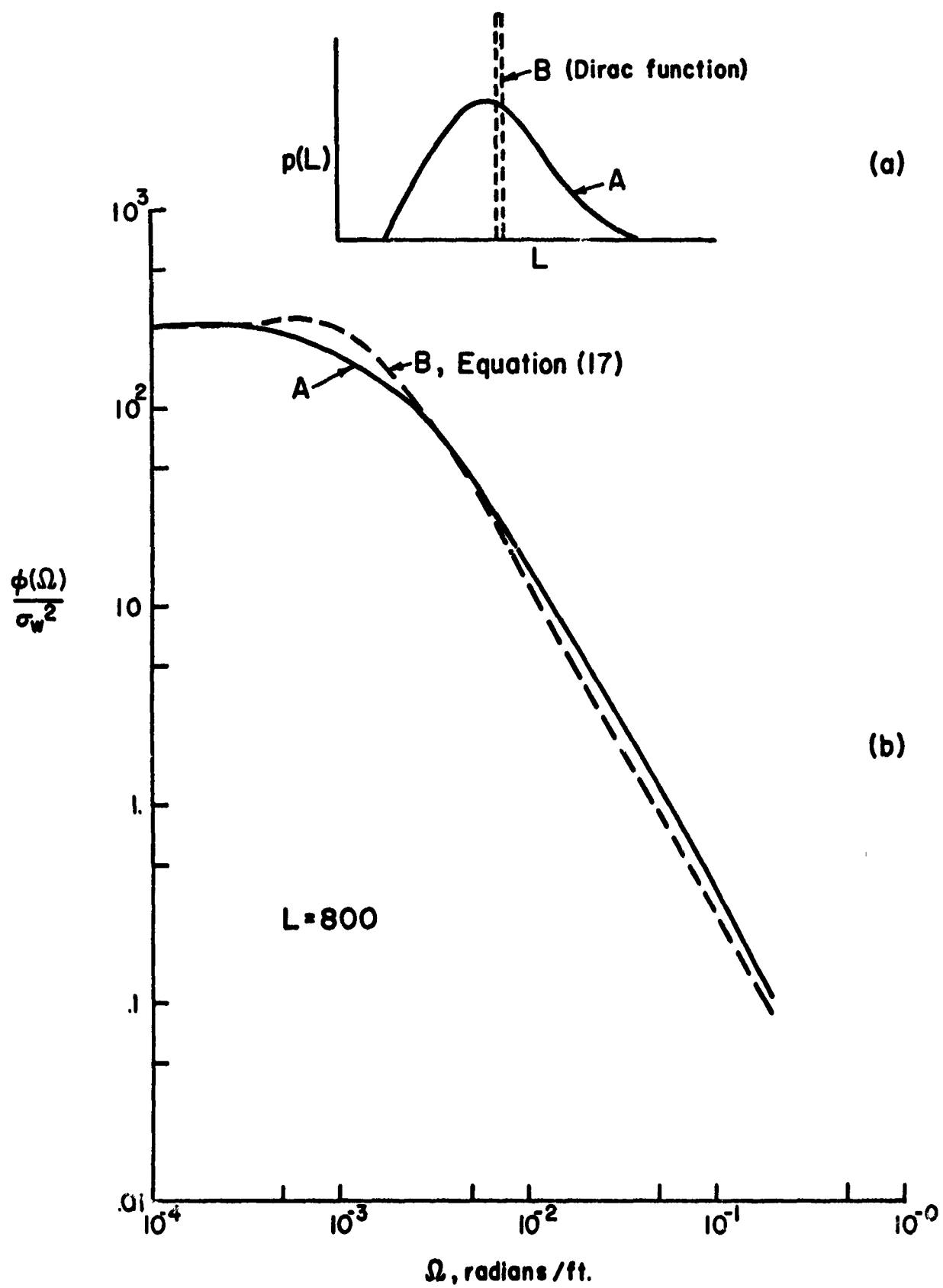
Figure 7. Example Composite Gust Spectrum

20

SECTION V

DETERMINATION OF A & N_O

Upper limit ω_c.- Practical aspects for determining A and N_O by equations (15) and (16) are discussed in this section. In general, plots of A and N_O should be made as a function of the upper limit of integration ω_c. In some cases, no particular difficulty is encountered in establishing the values of A and N_O. Results may appear, for example, as shown in figure 8(a); the values of A and N_O are taken as the values where the functions have leveled off. In other cases, particularly depending on the type of aerodynamics used in the establishment of the frequency response functions, there does not seem to be a limiting value for N_O (as in the case of figure 5 for the gust spectra). The manner for handling these cases is shown in figure 8(b). The top of the knee of the A curve is found; N_O is then taken at the frequency value associated with this knee. Essentially, this choice limits concern to only those frequency components which are significant in contributing to the overall response. The knee of the curve may be tied in with practical observations. Thus, when a record is taken of some response quantity such as stress, high frequency components can usually be seen in the record trace, provided the instrumentation and recording system is sufficiently precise. The high frequency components may be interpreted to be mainly a "hash" or noise; they contribute little to the r.m.s. value, but greatly affect the N_O count. The choice of the top of the knee has the effect of ignoring or by-passing this high frequency "hash" content of the record.

Typical examples from actual aircraft applications, illustrating both of the situations depicted in figure 8, are shown in figures 9 through 11. These practical applications serve also to bring out two facts of significance. It is noted that the value of A is quite sensitive to the value of scale used, generally the higher the scale the lower the A value. Thus, A values should not be compared unless the same L value is used. In contrast, the value of N_O is noted to be quite insensitive to the value of scale.

21
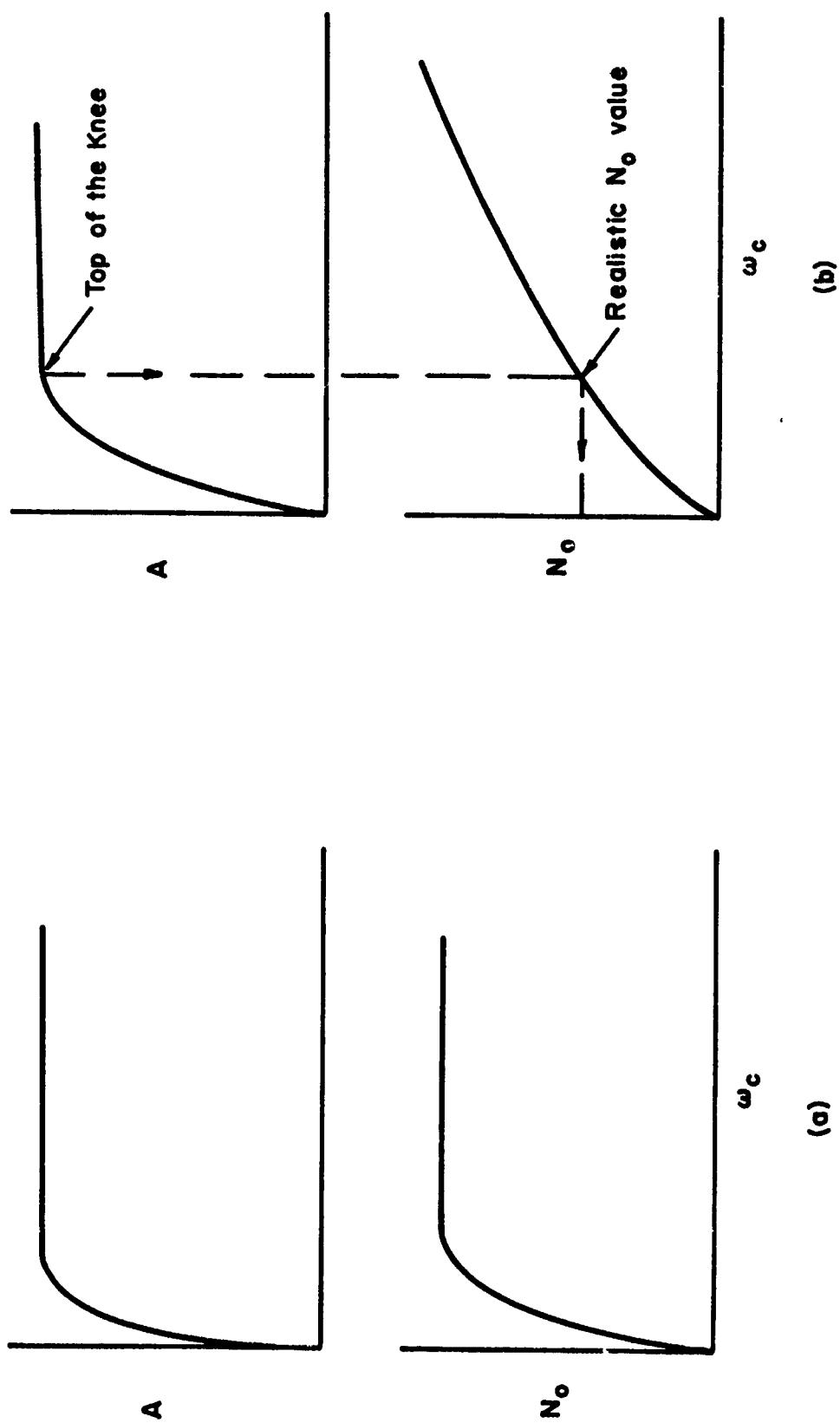
Figure 8. Establishment of A and N_O

22
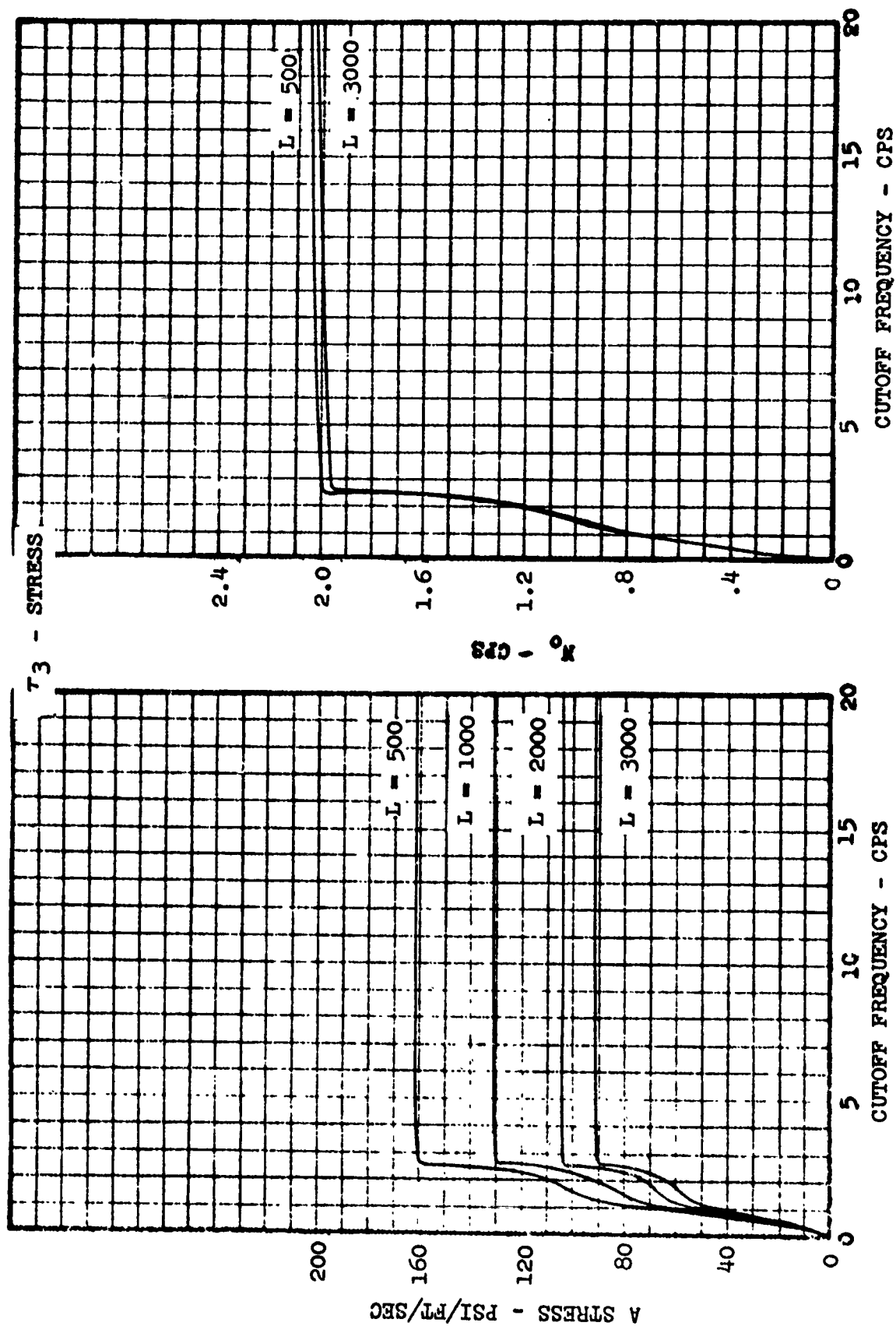
Figure 9. Example A and N_o Values Found for the B-58 Airplane. 155,000 lb G.W. (Taken from Ref. 6)

23
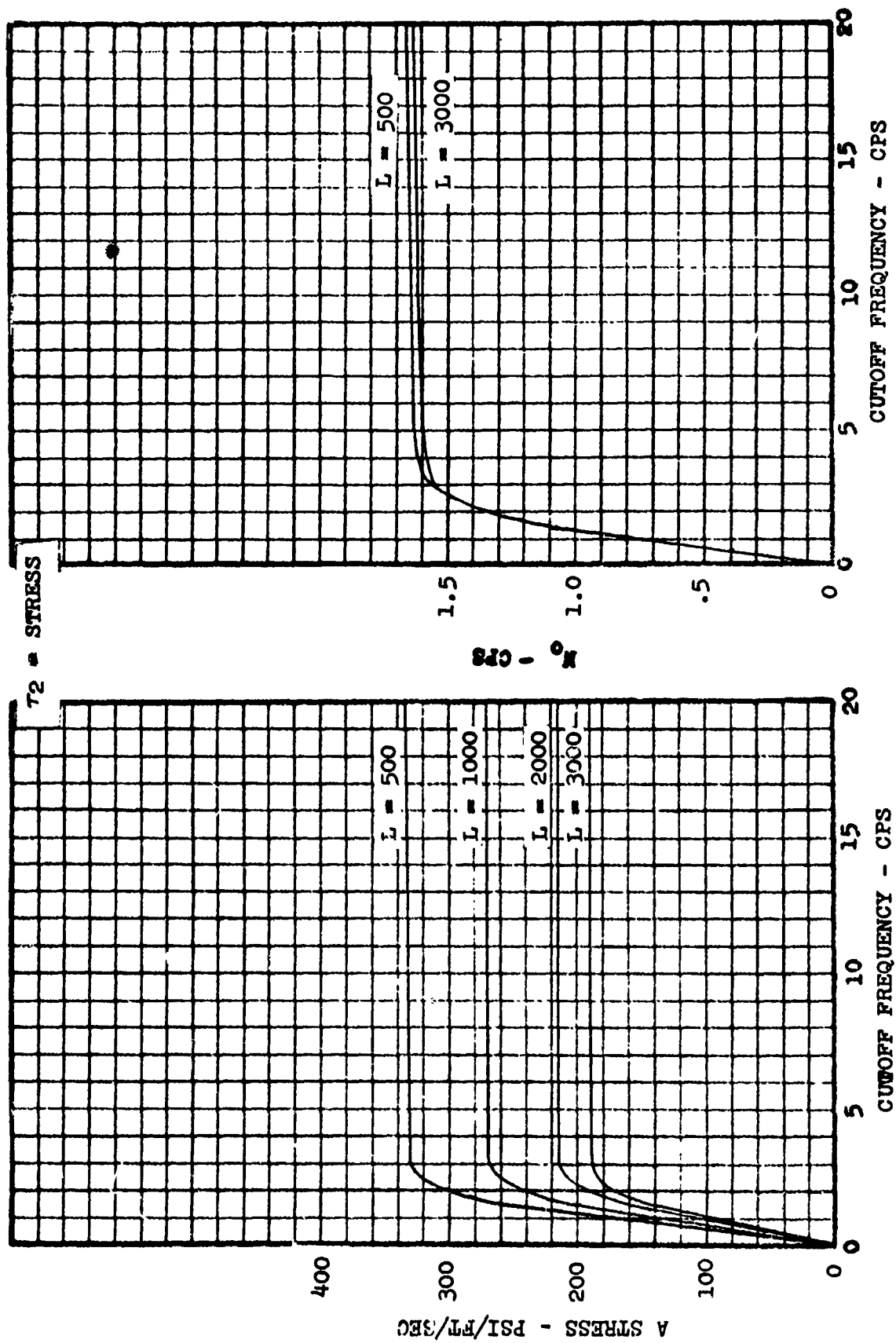
Figure 10. Example A and N_o Values Found for the B-58 Airplane, 5% Fuel, 50,000 Ft. (Taken from Ref. 6)

24
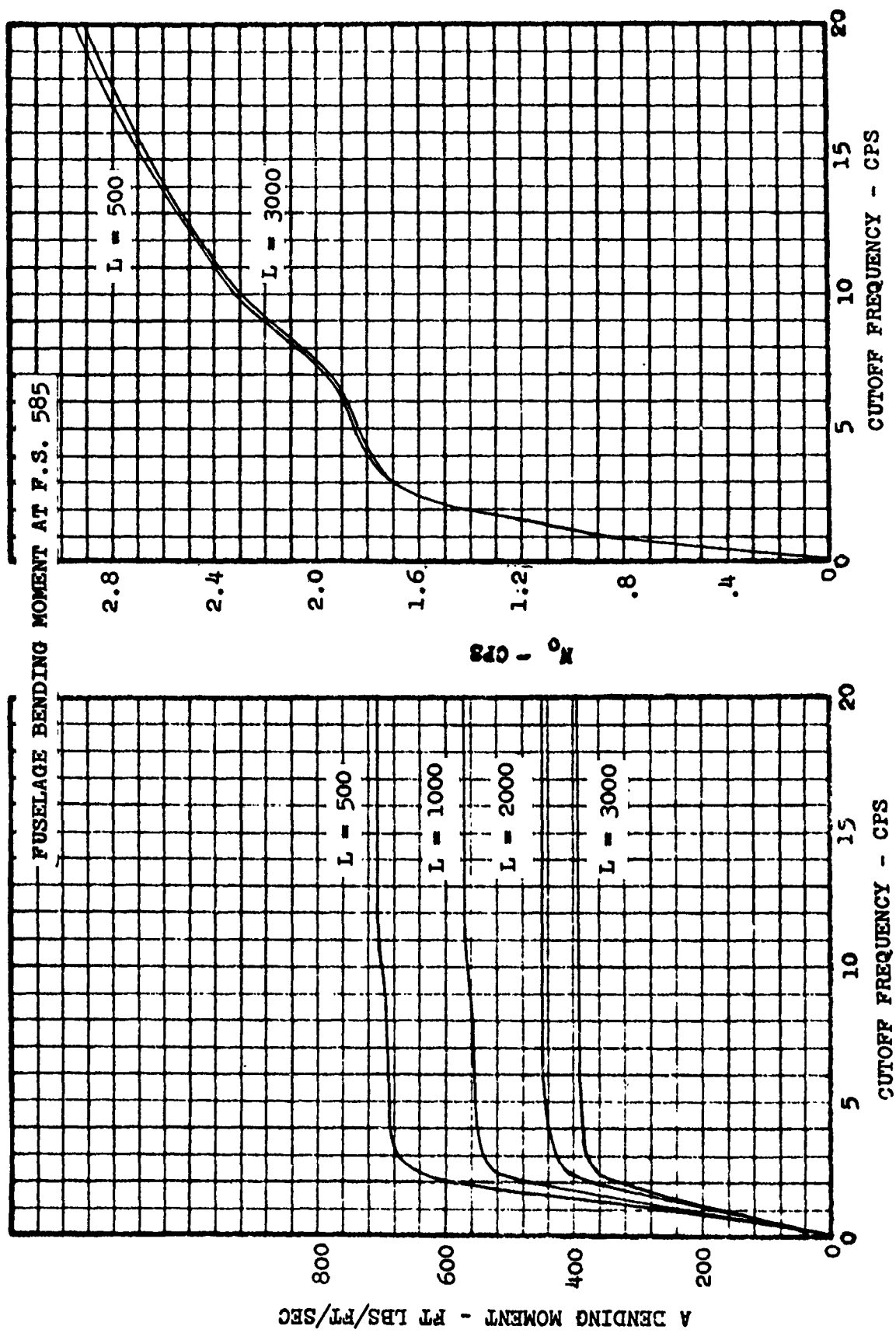
Figure 10. (Concluded)
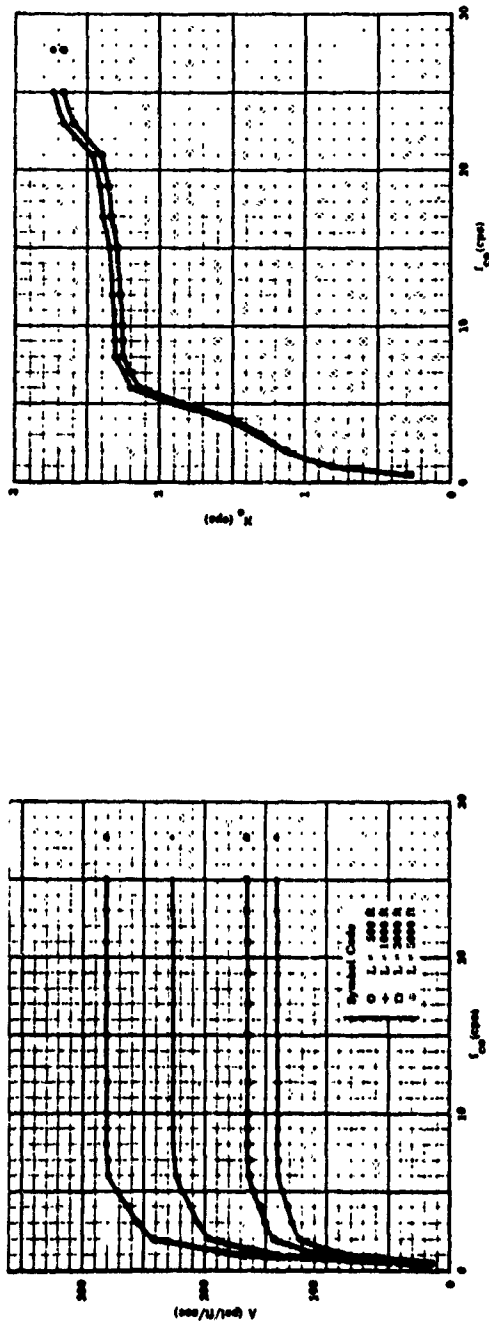
(a) Stress S-4, Configuration 1
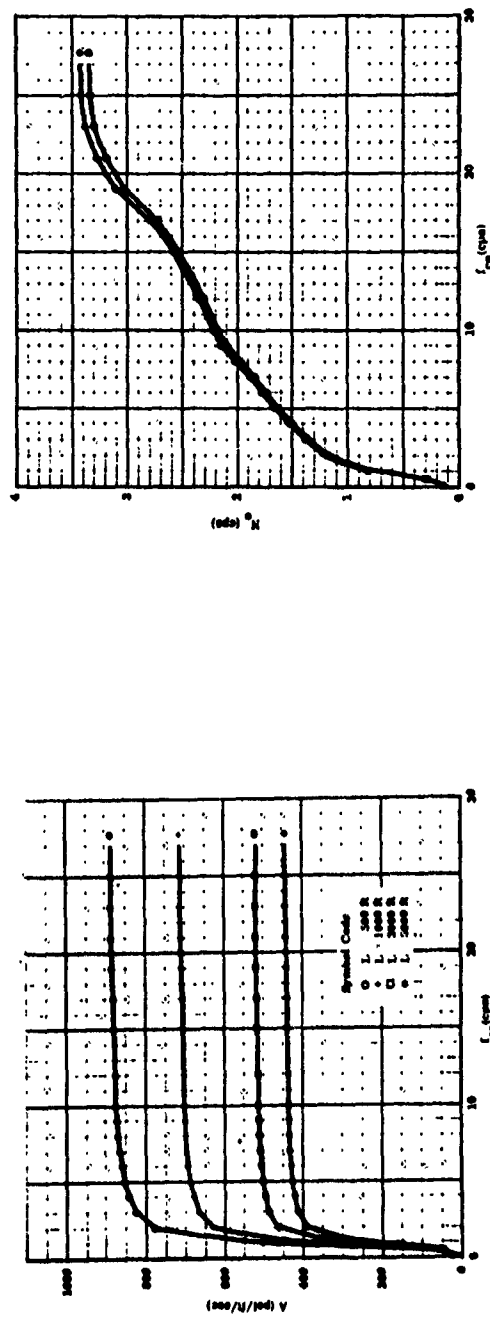
(b) Stress S-25, Configuration 1

Figure 11. Example A and N_0 Values Found for the F-5A Airplane (taken from Ref.8)

26

SECTION VI

BASIC SINGLE DEGREE-OF-FREEDOM RESULTS

The case of a rigid airplane with the single degree of freedom of vertical translation is treated in this section. Response results for cg vertical acceleration in g-units are established; these results form the basis of the preliminary design consideration. For 2-dimensional incompressible flow, the square of the modulus of the frequency response function for this case can be shown to be (see reference 25)

$$|H(k)|^2 = \left(\frac{a\rho SV}{2W}\right)^2 f_1(k) \; f_2(k) \tag{20}$$

where

$$f_1(k) = \frac{16\mu^2}{\left(\frac{2F}{k}\right)^2 + \left(4\mu + \frac{2G}{k}\right)^2}$$

$$f_2(k) = P^2 + Q^2$$

in which

$$\mu = \frac{2W}{a\rho cgS}$$

$$k = \frac{\omega c}{2V}$$

The function F and G in f_1 refer to the Theodorsen functions, as used in oscillatory treatment of 2-dimensional airfoils, while P and Q in f_2 are corresponding type functions for sinusoidal gust encounter. For solution the function f_2, as given in reference 26, for $M = .2$ was used, specifically

$$f_2(k) = \frac{\beta^2}{\beta^2 + 1.5\pi k + \pi^2 M k^2} \quad ; \quad \beta^2 = 1 - M^2$$

$$= \frac{1}{1 + 4.92k + 2.06k^2} \quad ; \quad M = .2$$

The output spectra for this case follows as

$$\phi_{\Delta n}(k) = \left(\frac{a \rho S V}{2W}\right)^2 f_1(k) f_2(k) \phi_w(k)$$

$$= \left(\frac{a \rho S V}{2W}\right)^2 \sigma_w^2 \phi_1(k) \tag{21}$$

where $\phi_1 = f_1 f_2 \dfrac{\phi_w}{\sigma_w^2}$. From this equation the r.m.s. value for cg acceleration in g-units is found to be

$$\sigma_{\Delta n} = \frac{a \rho S V}{2W} K_\phi \ \sigma_w \tag{22}$$

where

$$K_\phi = \left[\int_0^{k_c} \phi_1(k) \, dk \right]^{\frac{1}{2}}$$

Equation (22) is recognized as being analogous to the discrete-gust design formula. The response parameter A for this case is seen to be

$$A_r = \frac{\sigma_{\Delta n}}{\sigma_w} = \frac{a \rho S V}{2W} K_\phi \tag{23}$$

which also may be expressed in the interesting form

$$A_r = \frac{V}{cg} \frac{K_\phi}{\mu} \tag{24}$$

The various results obtained for this case are shown in figures 12 through 18. Figure 12 shows the plots of $k\phi_1(k)$ vs k ; the curves of this figure are significant because they show the ranges of k which contribute mainly to the response. The k values associated with the maximum values of the $k\phi_1(k)$ curves, the location where there is maximum contribution to the r.m.s. value of response, are shown in figure 13. The k_u values shown in this figure are discussed subsequently.

28

Figures 14 and 15 show, respectively, the variation of K_ϕ and k_0 with cutoff frequency. Maximum values of the K_ϕ curves of figure 14 form the gust alleviation factor K_ϕ for the spectral approach; these maximum values are shown in figure 16. For comparison, the gust factor K_g as used in discrete-gust studies, reference 27, is also shown. Figure 17 gives the values of $\dfrac{K_\phi}{\mu}$ as used in the alternate response equation given by equation (24).

Figure 15 shows the variation of k_0 with cutoff frequency as established by equation (16). The "realistic" zero-crossing values of k_0, as established from the K_ϕ and k_0 curves of figures 14 and 15, through use of the top of the knee procedure described in Section V, are shown in figure 18. This figure allows for the quick evaluation of rigid body N_0 values. The k_u curves shown on the right of figure 13 designate the frequency values that were chosen for the top of the knee. Essentially k_u designates the upper value of the range of k that is significant for response; that is, there is little contribution to the r.m.s. value for response beyond these values. To be systematic in selecting the top of the knee for this study, the top of the knee was specifically selected at the point on the K_ϕ curve where the K_ϕ value was two percent less than the maximum K_ϕ value of the curve.

It is of interest to note that the k_0 values of figure 18 are probably closely related with the concept of gust gradient distance that has been used in interpreting gust encounter in a discrete gust sense; specifically, the average gust gradient that has been noted is felt to be a reflection of the k_0 values. From $k_0 = \dfrac{\omega c}{2V}$, and that fact the $\dfrac{\omega}{V}$ is related to wavelength by $\dfrac{\omega}{V} = \dfrac{2\pi}{\lambda}$, the following relation of "equivalent" gust gradient distance in chords results

$$\frac{H}{c} = \frac{\pi}{4k_0}$$

where H refers to $\dfrac{1}{4}$ the wavelength λ. By this expression the k_0 values of figure 18 have been converted to the $\dfrac{H}{c}$ values shown in figure 19. It is noted that for μ around 20, which is representative of some of the mass parameters used in early gust studies, that $\dfrac{H}{c}$ of about 10 is indicated, in good agreement with the gust gradient distances that were noted in the past studies. The chart indicates that the average gust gradient distance can be expected to be greater for larger μ values, and smaller for the small μ values.

29

The results presented in this section are intended to show the character and make-up of the acceleration response for the rigid airplane treated, and are given for ready reference purposes in connection with any response study that may be made. Equation (23) and figures 16 and 18, or alternatively equation (24) and figure 17, are the significant results of this section; they form the basis of the preliminary design treatment given in the subsequent section.
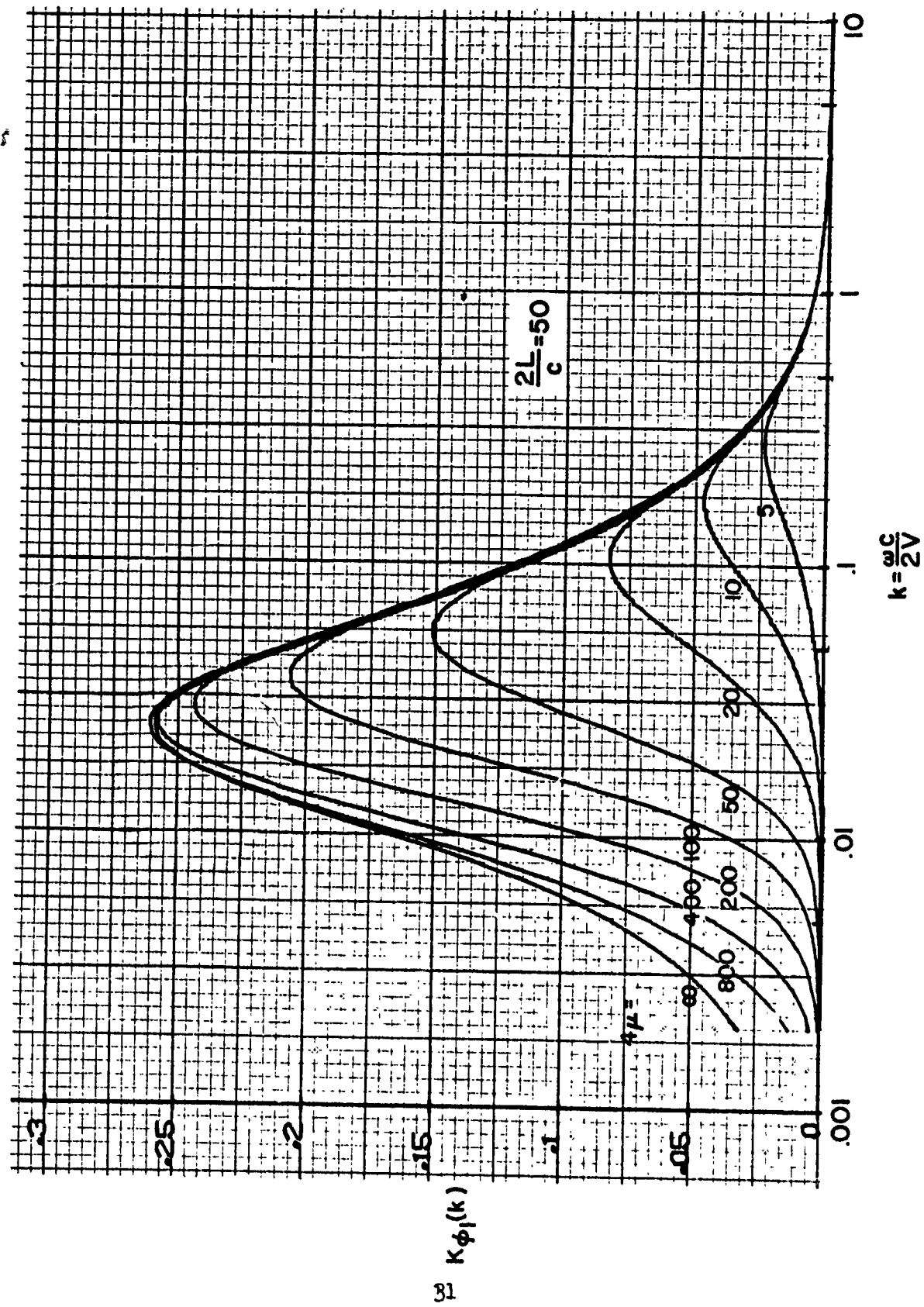
Figure 12. Distribution of $c_{\Lambda n}$ as shown by $k\phi_1$ curves

31

Figure 12. (Cont.)

32

Figure 12. (Cont.)

33

Figure 12. (Concluded)

34
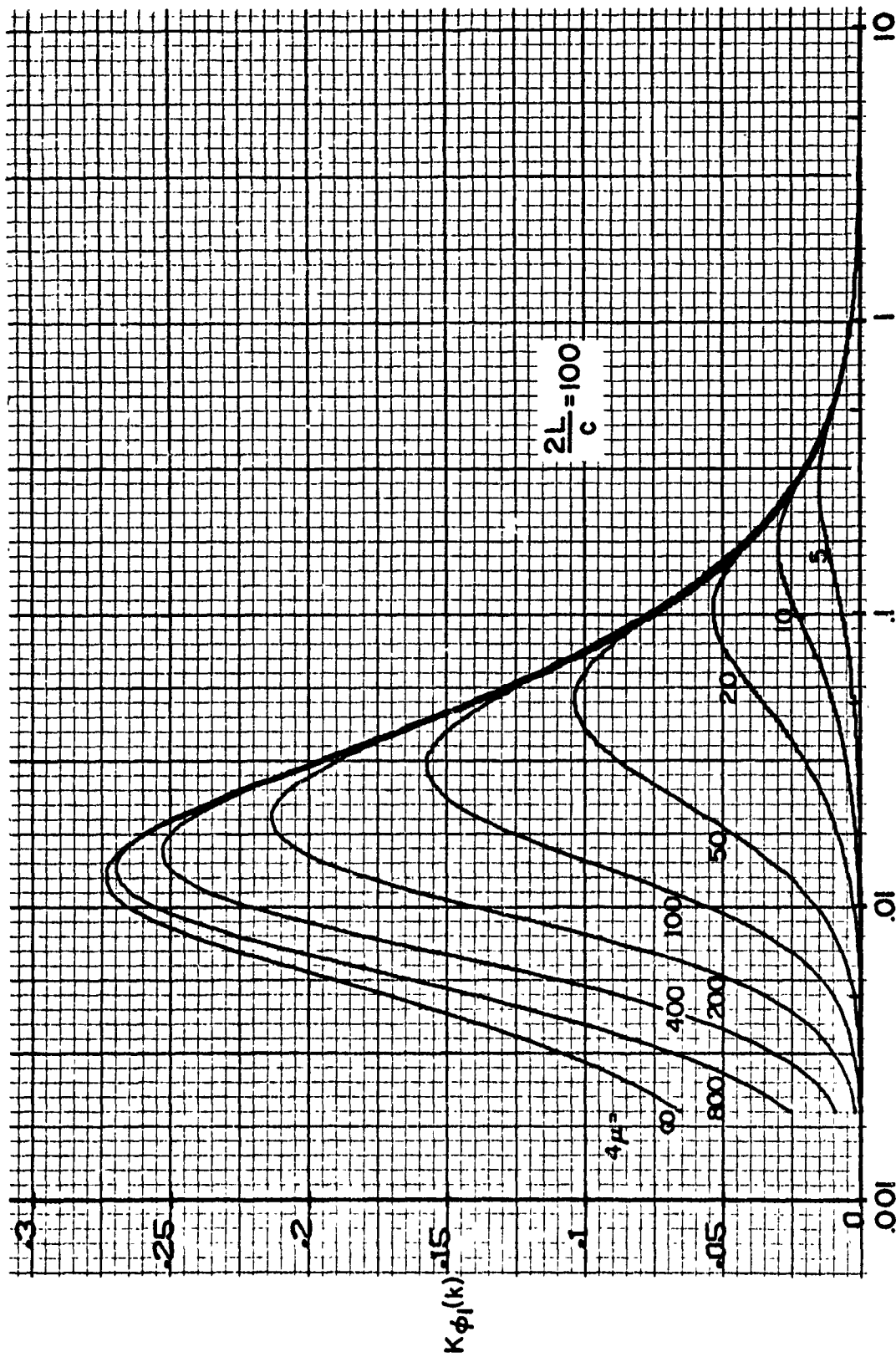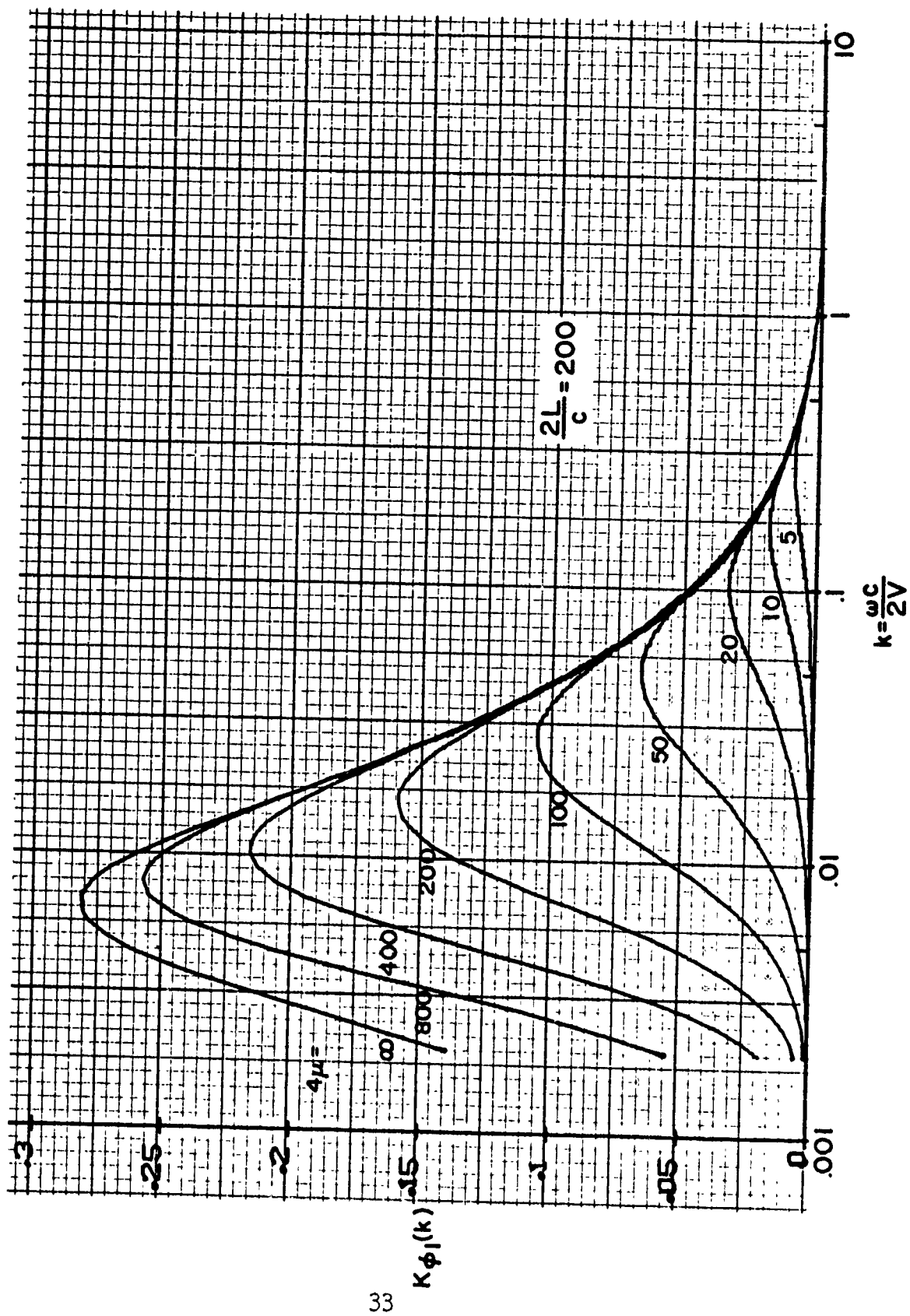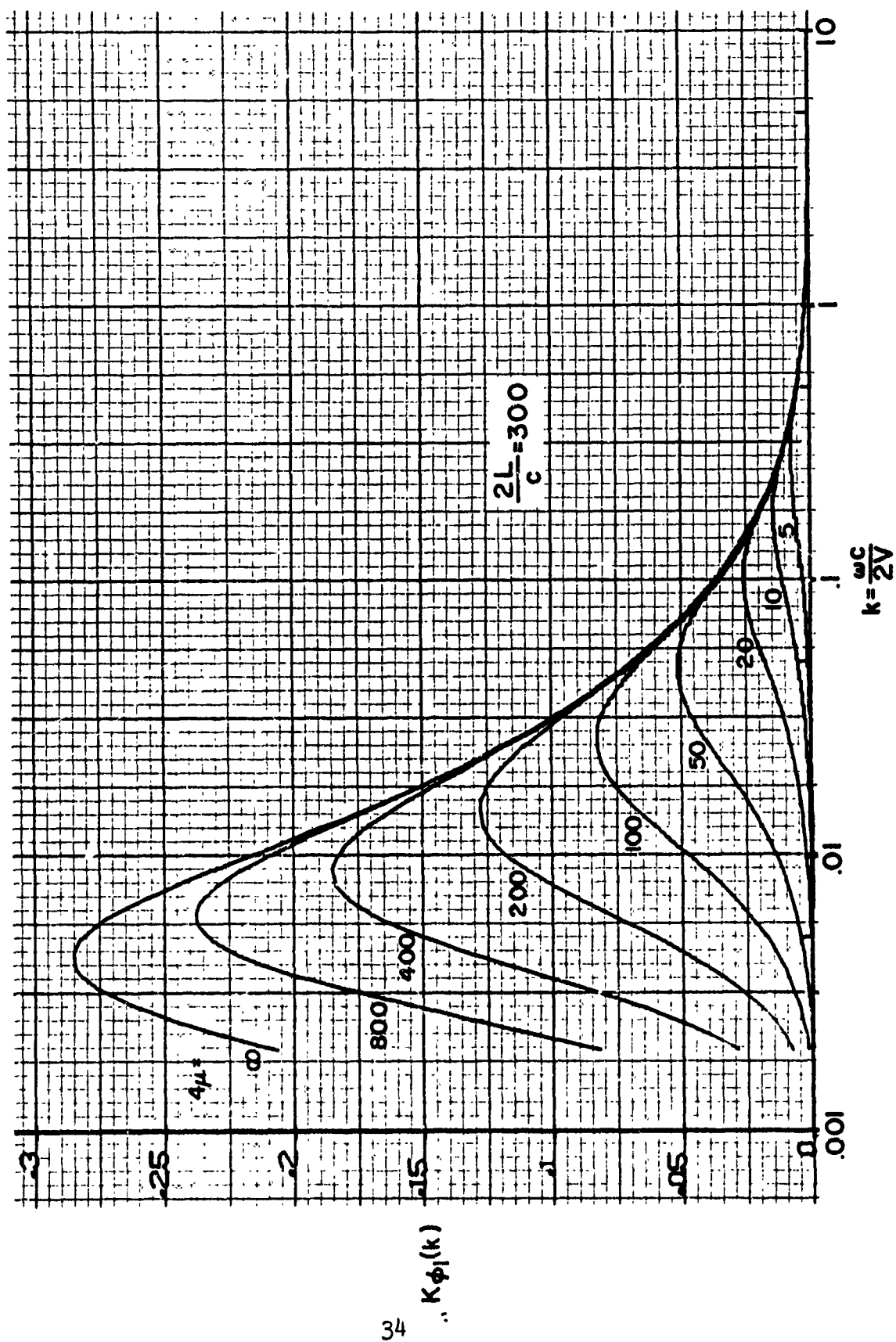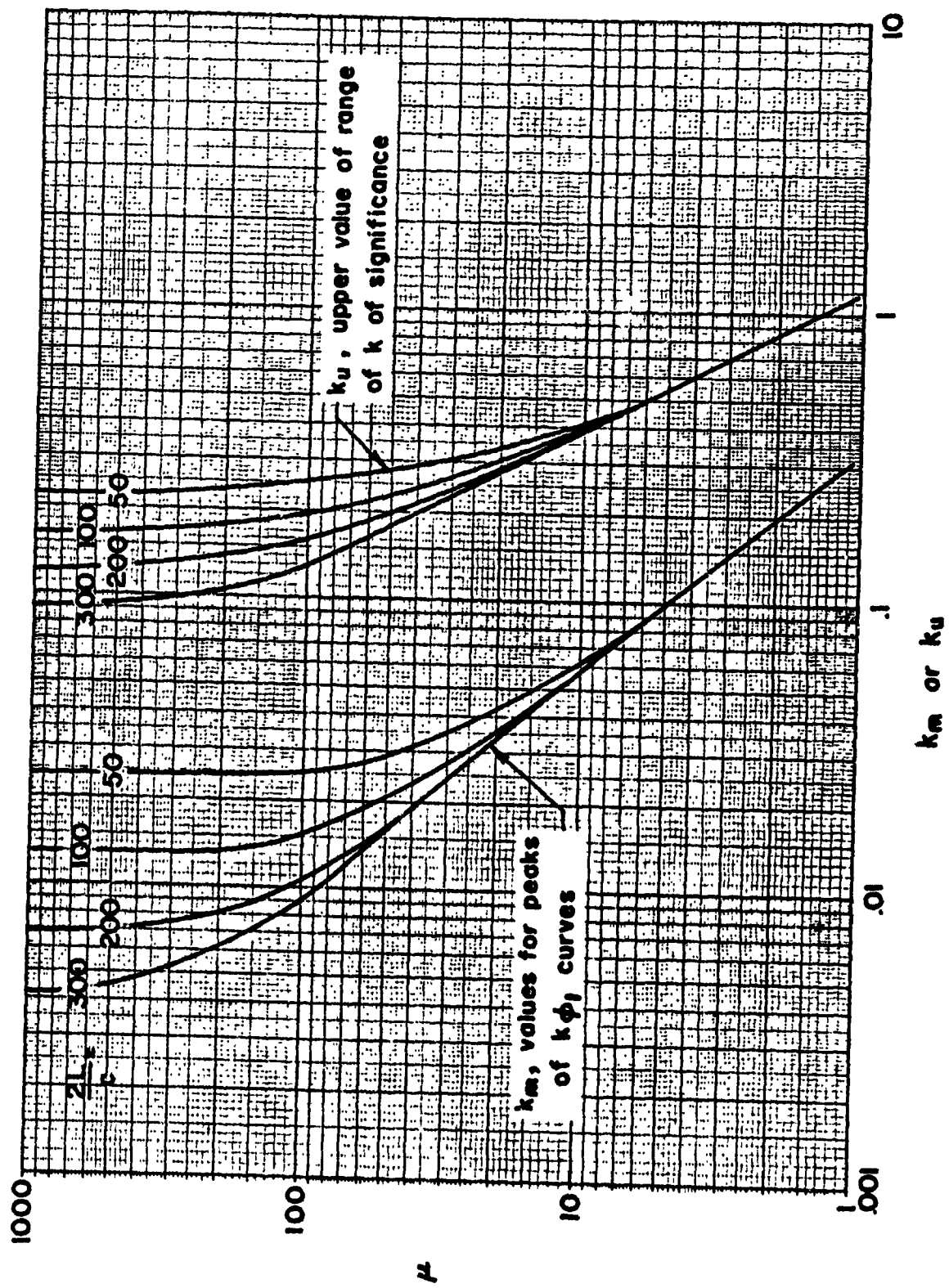
Figure 13. Frequencies Associated with Peaks of the $k\phi_1(k)$ Curves
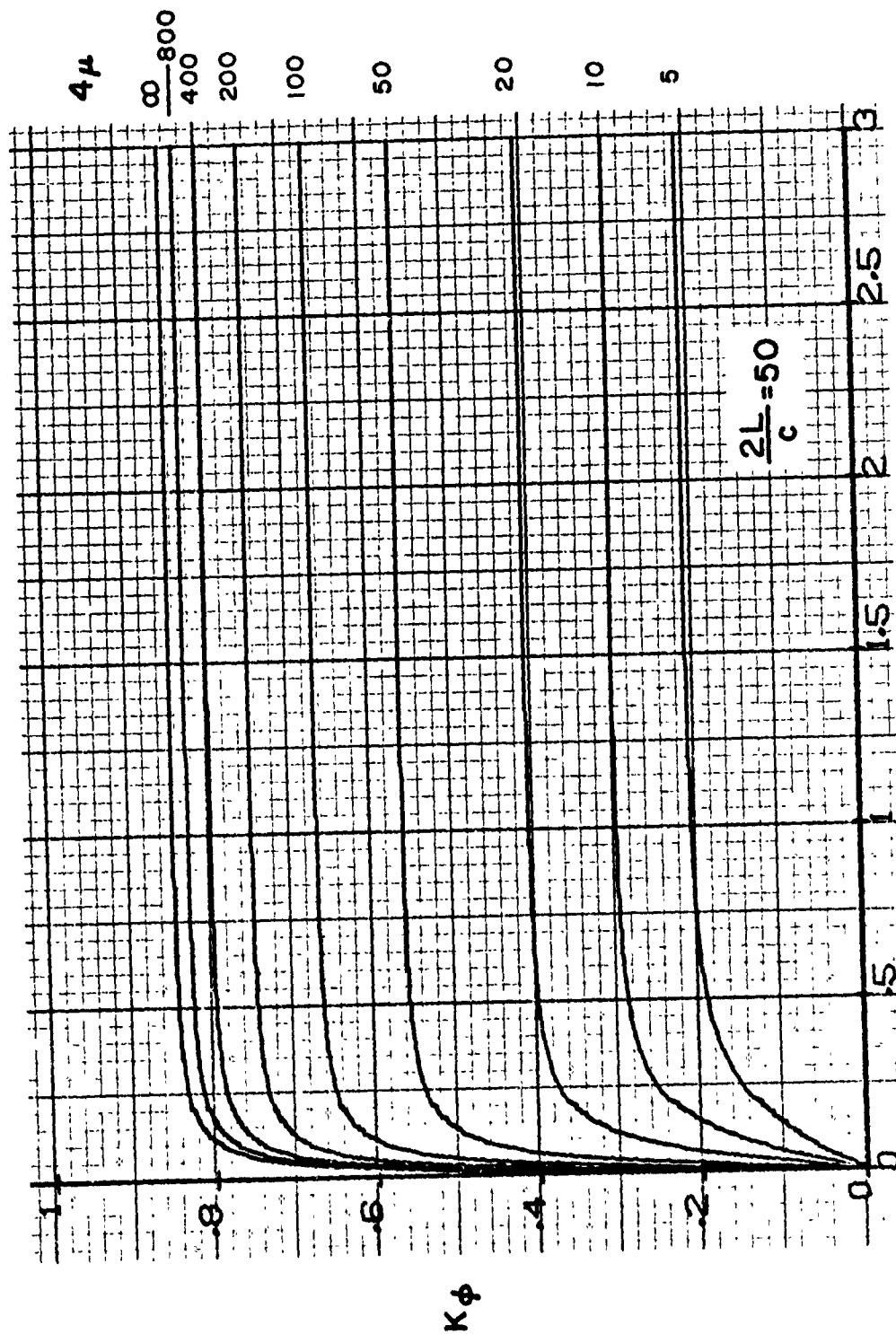
Figure 14. Variation of K_ϕ with k_c

$k_c = \dfrac{\omega c}{2V}$

K_ϕ

$\dfrac{2L}{c} = 20$

4μ
1000 400
200
100
50
20
10
5

35

Figure 14 . (Cont.)

37

Figure 14 . (Cont.)

Figure 14. (Cont.)

Figure 14. (Cont.)

40
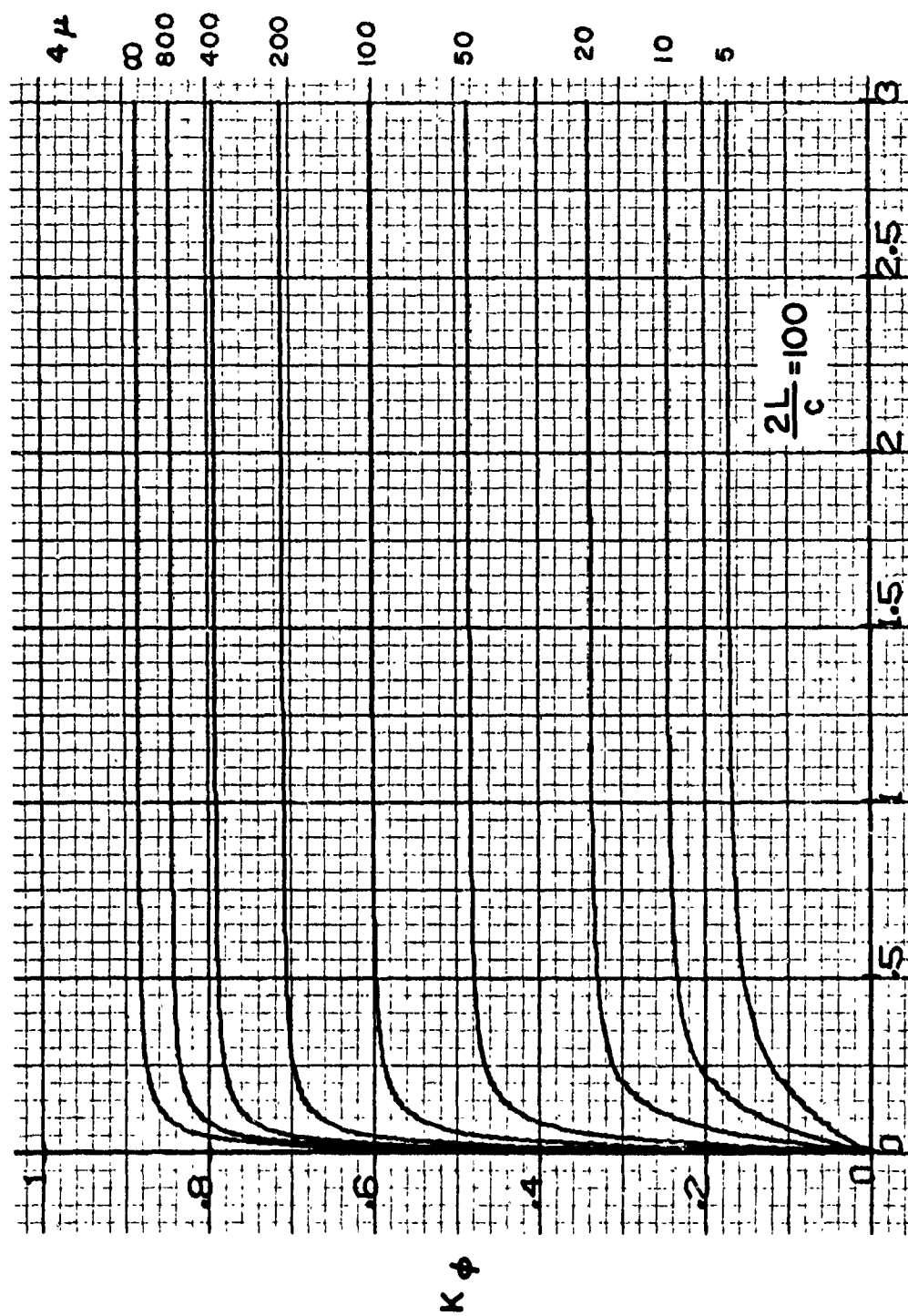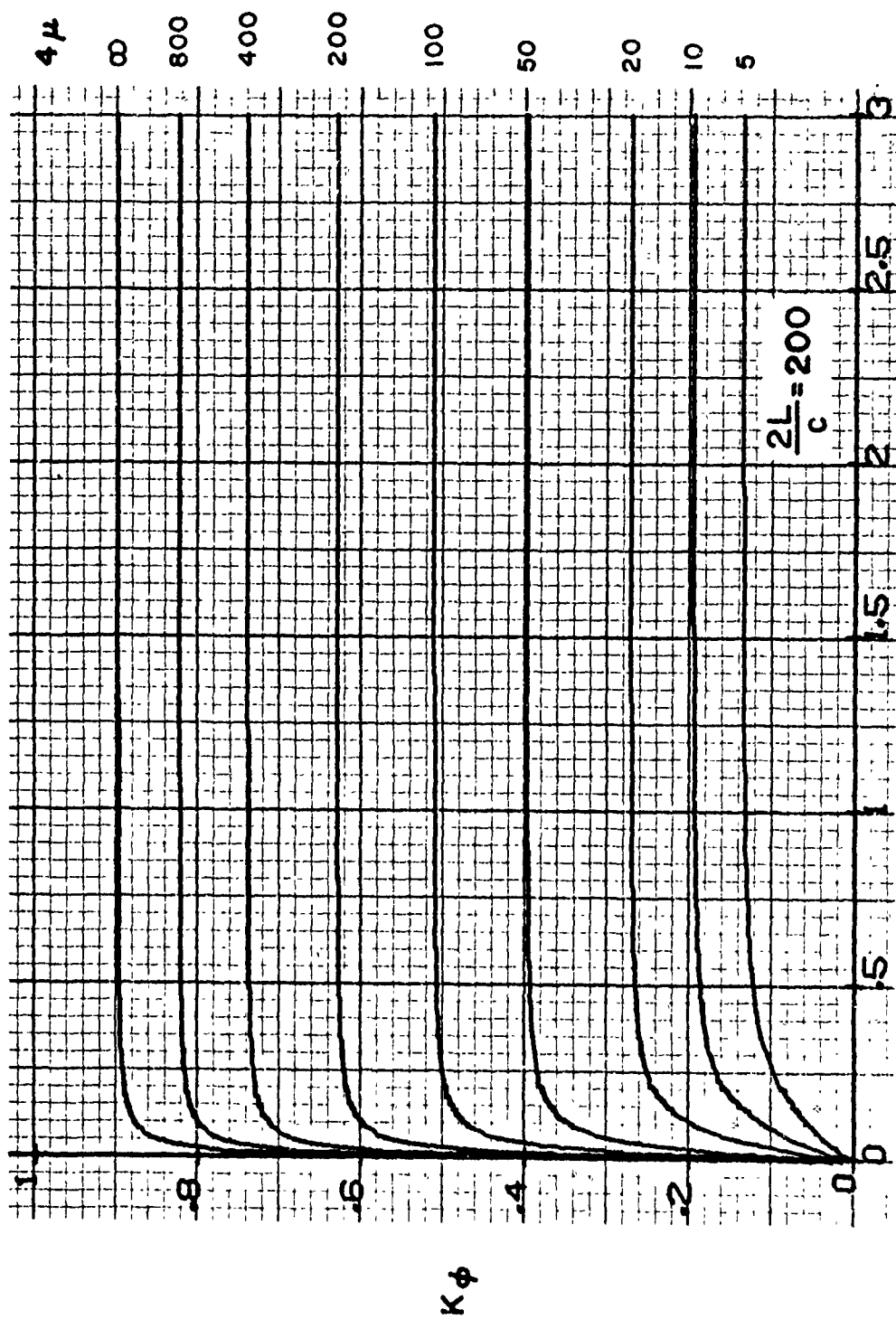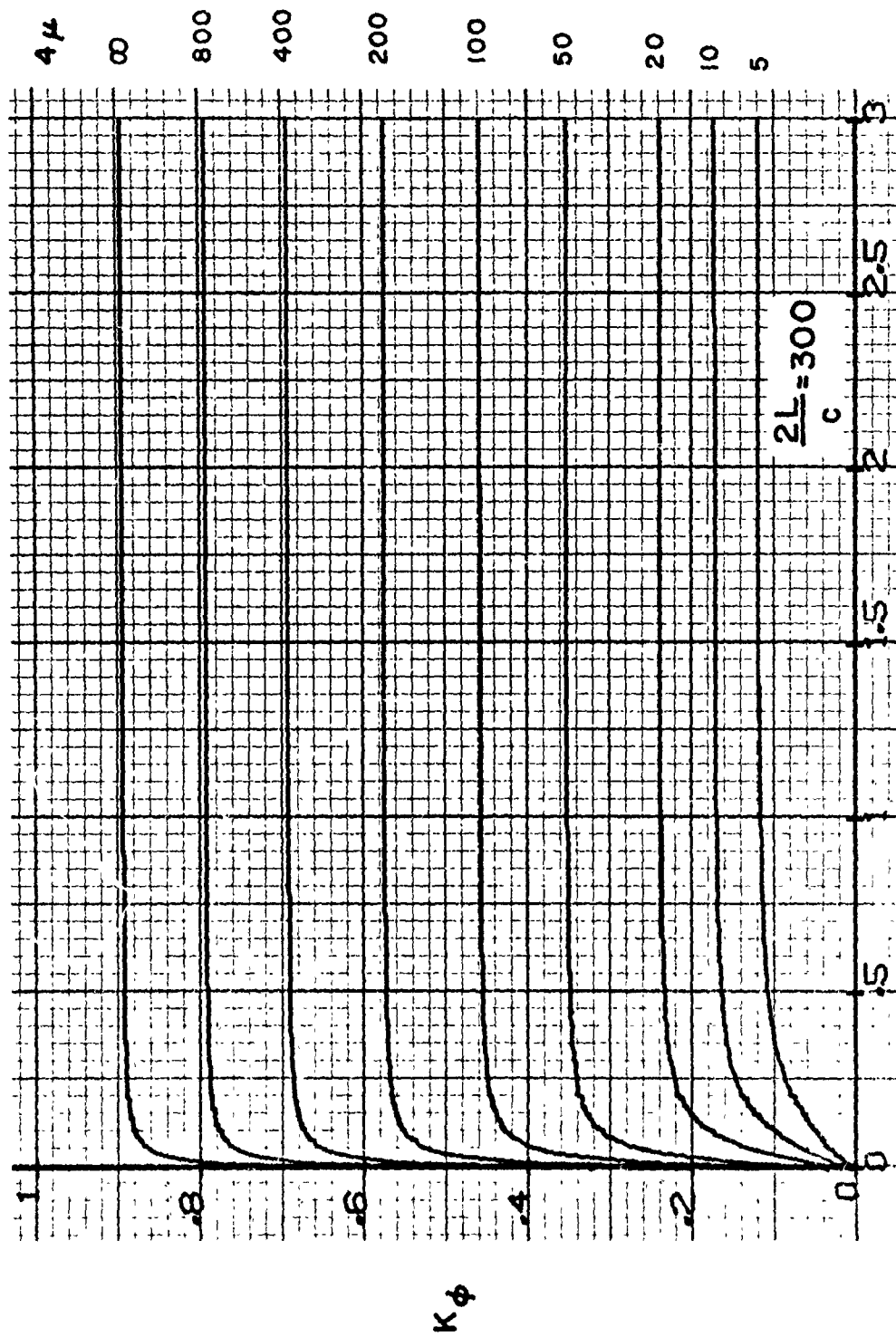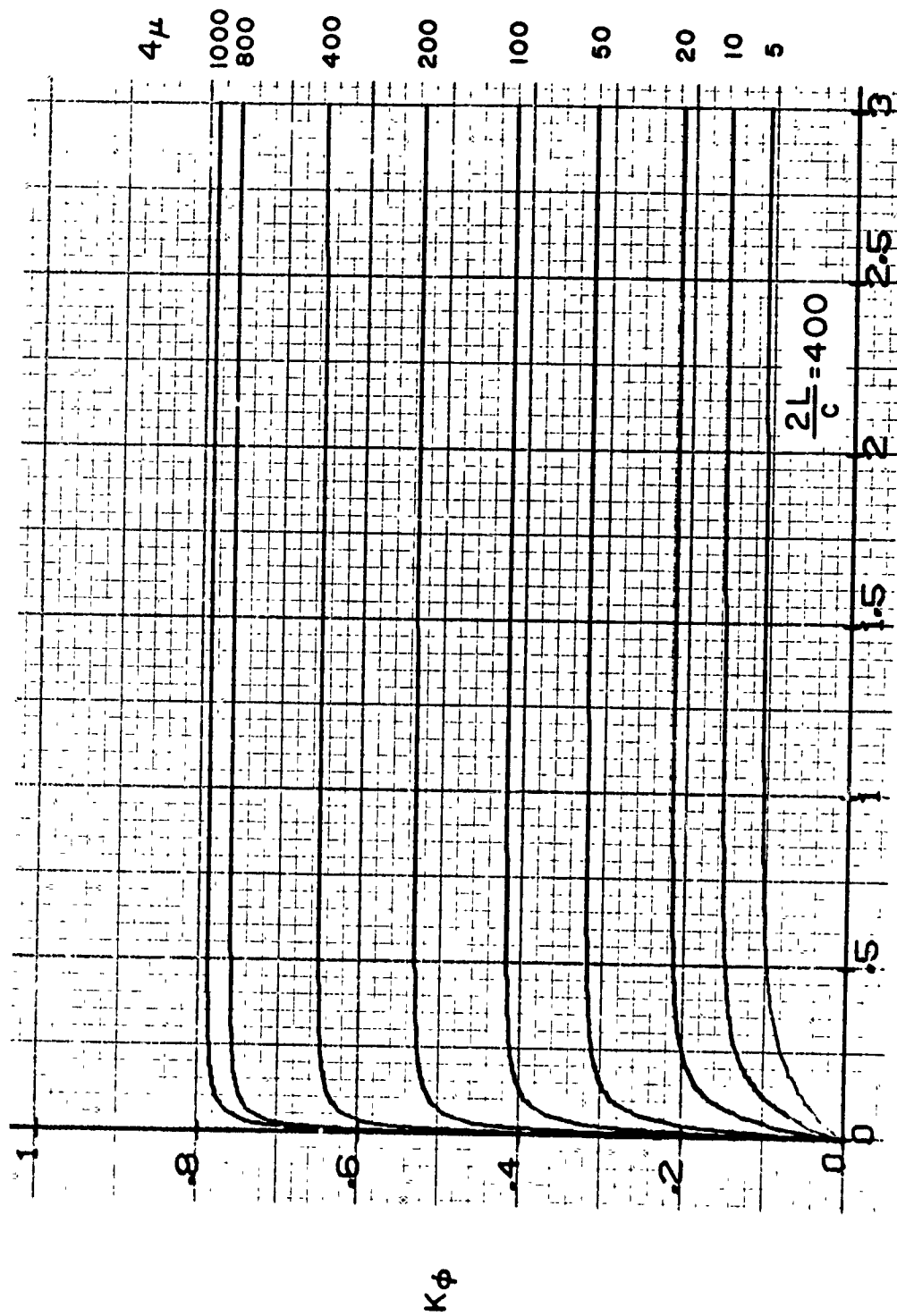
Figure 14. (Concluded)
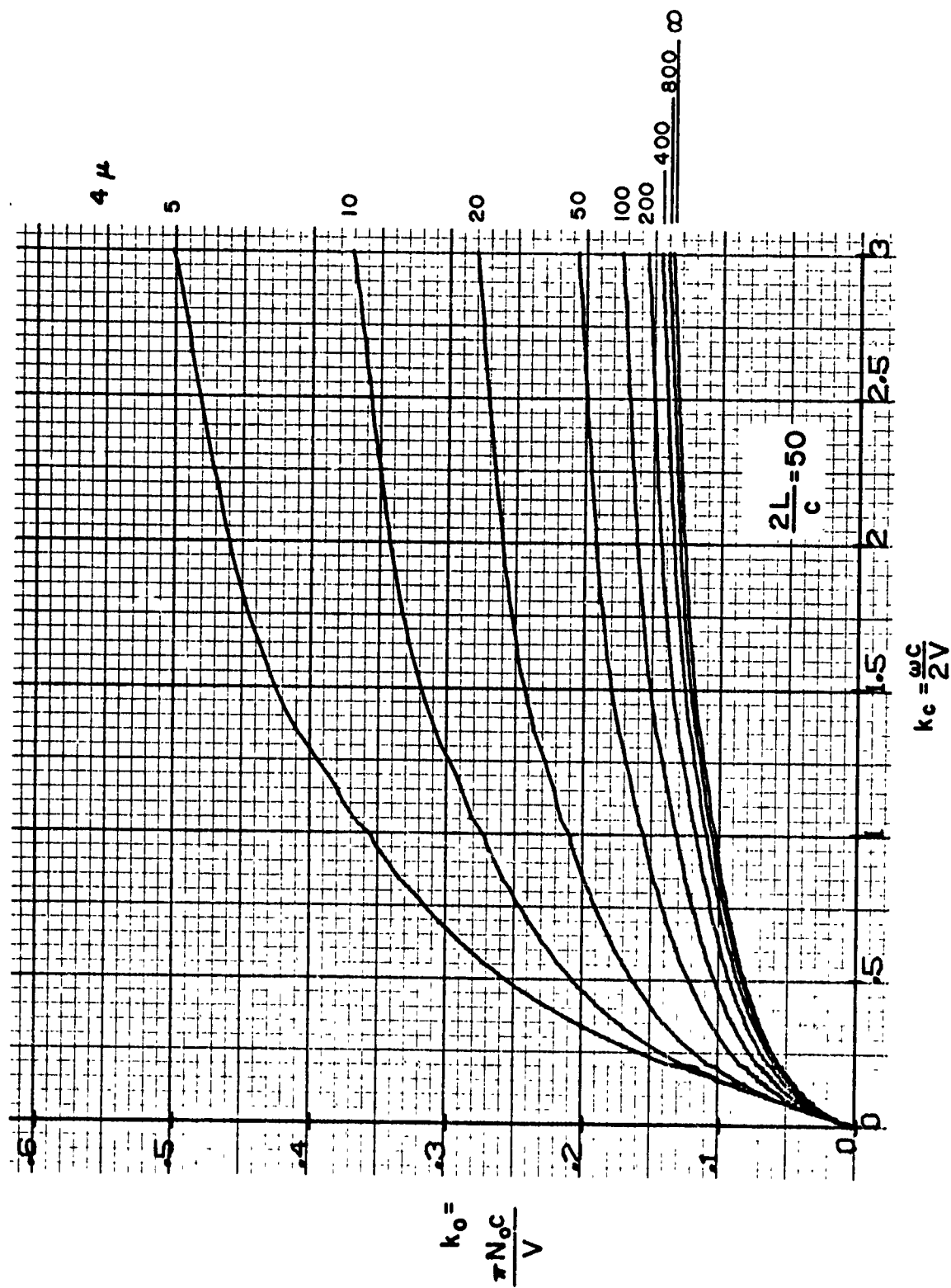
Figure 15. Variation of k_o with k_c

Figure 15 . (Cont.)

43

Figure 15 . (Cont.)

44
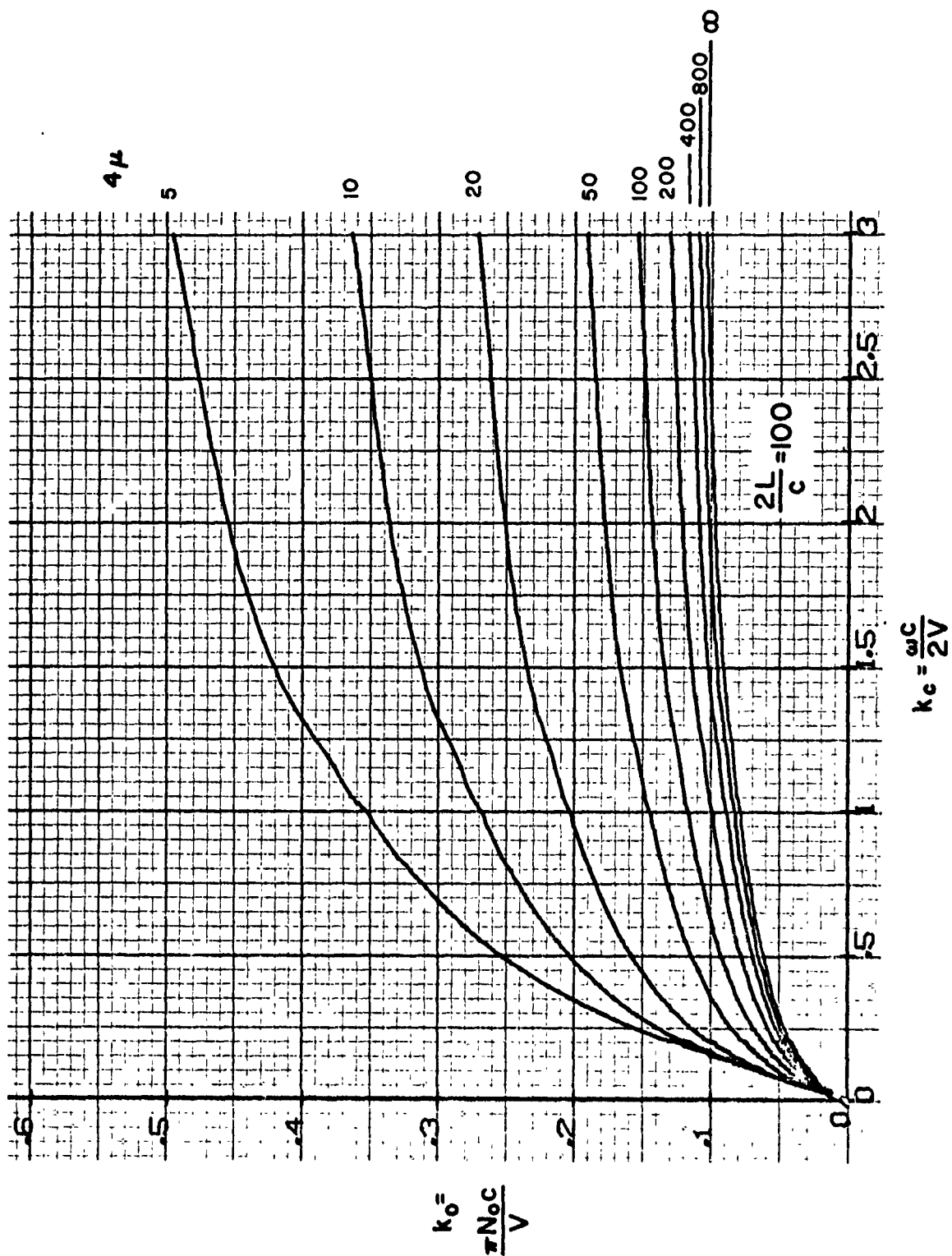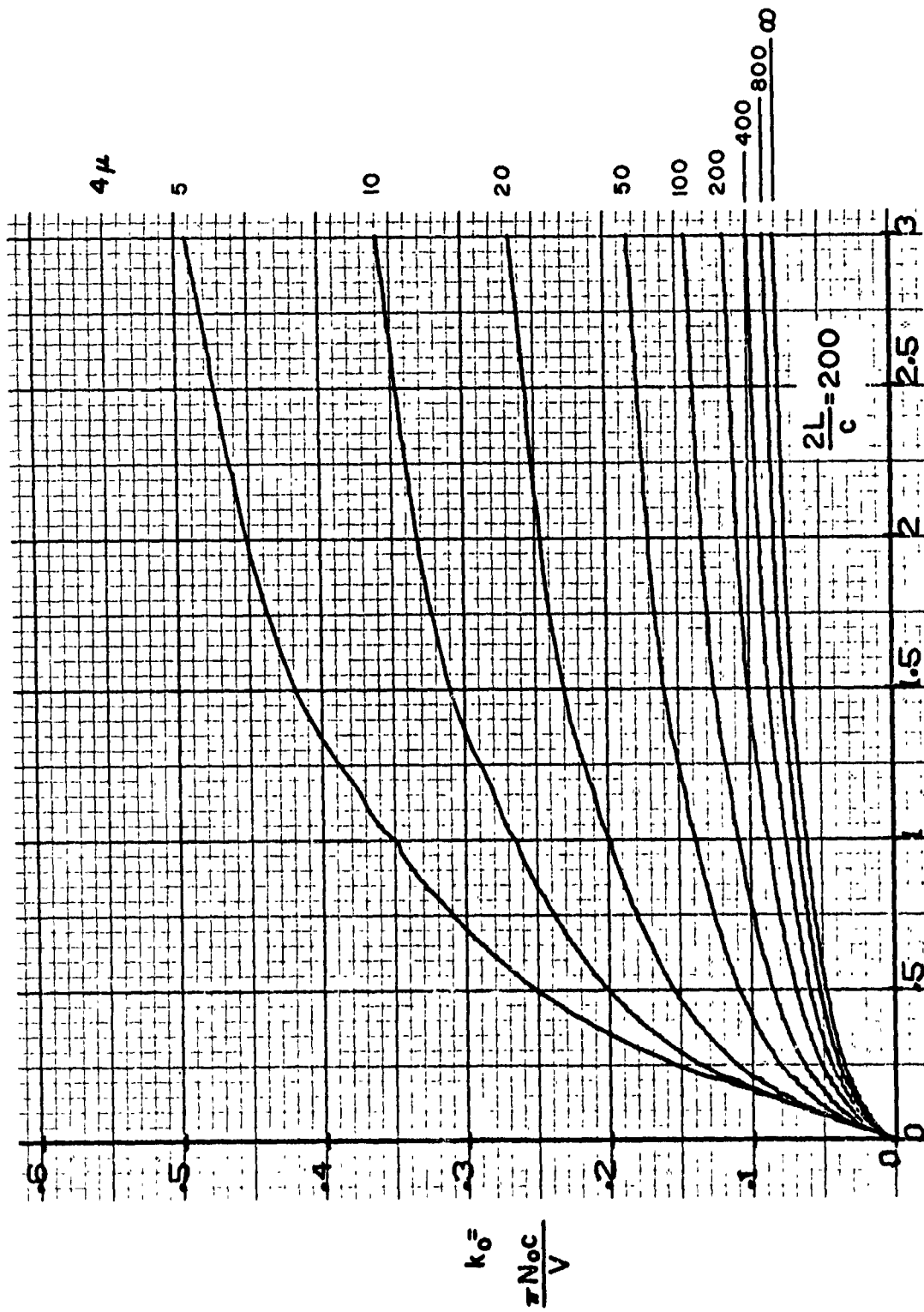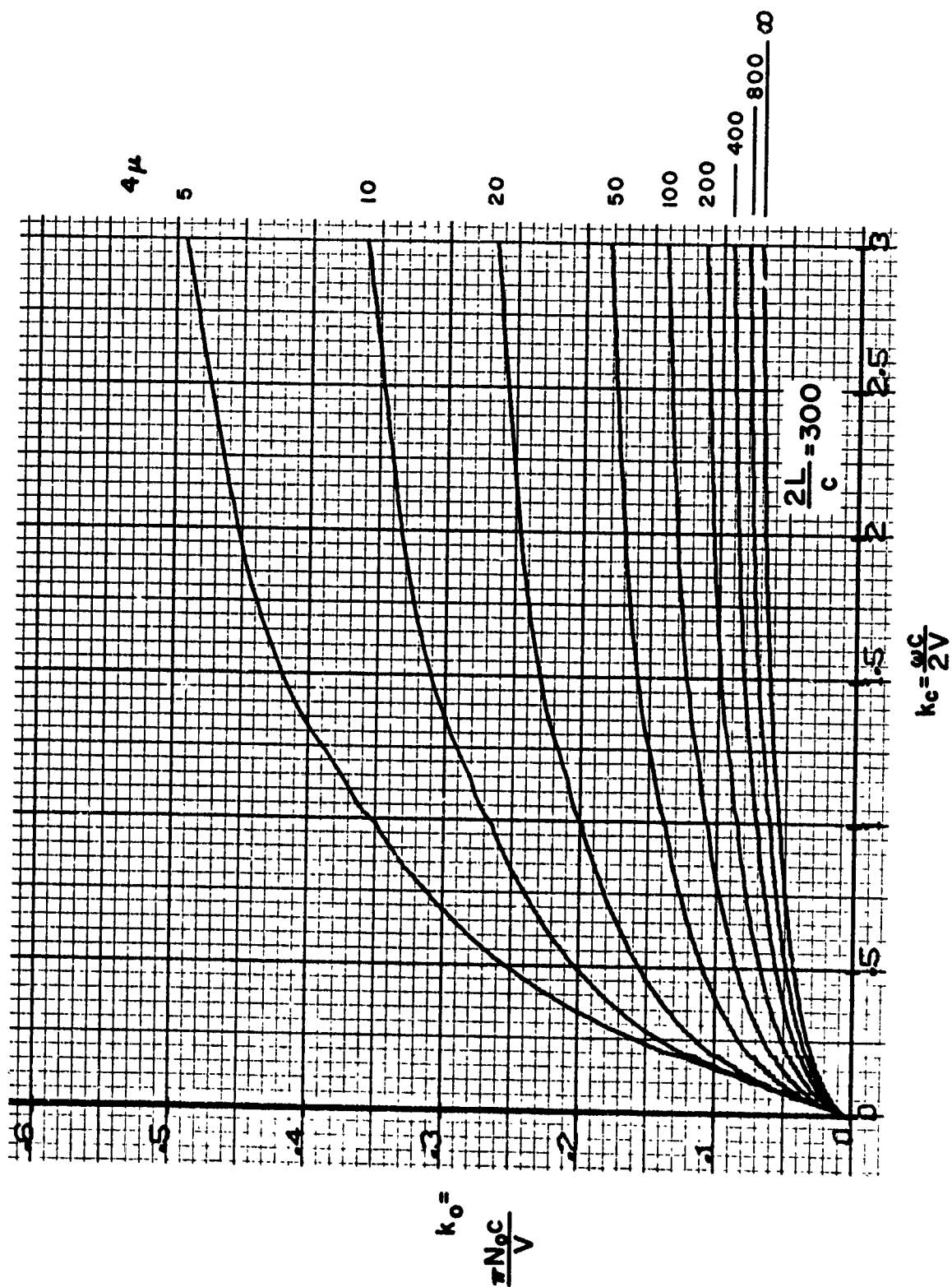
Figure 15 . (Concluded)

45
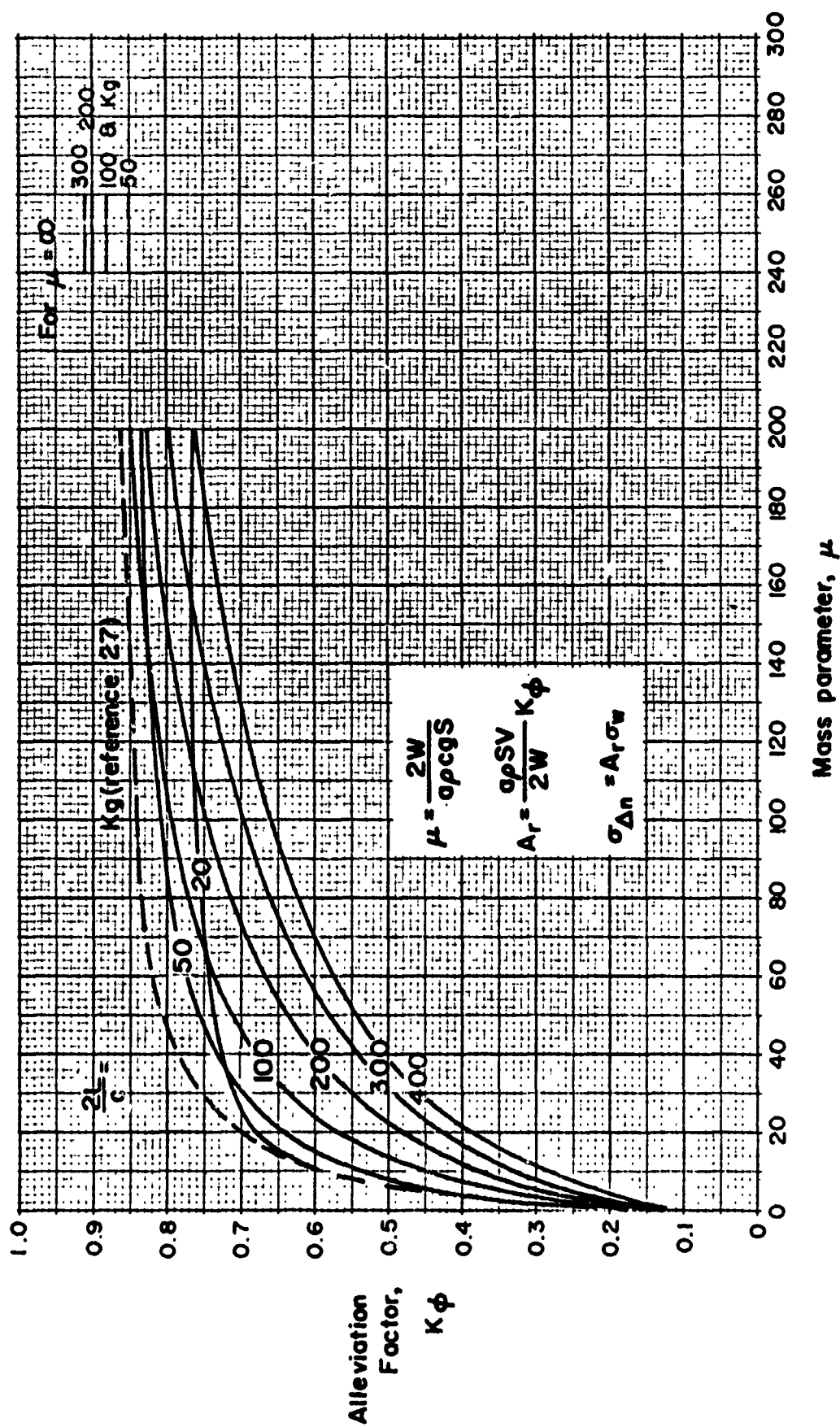
Figure 16. Gust-Alleviation Factor K_ϕ
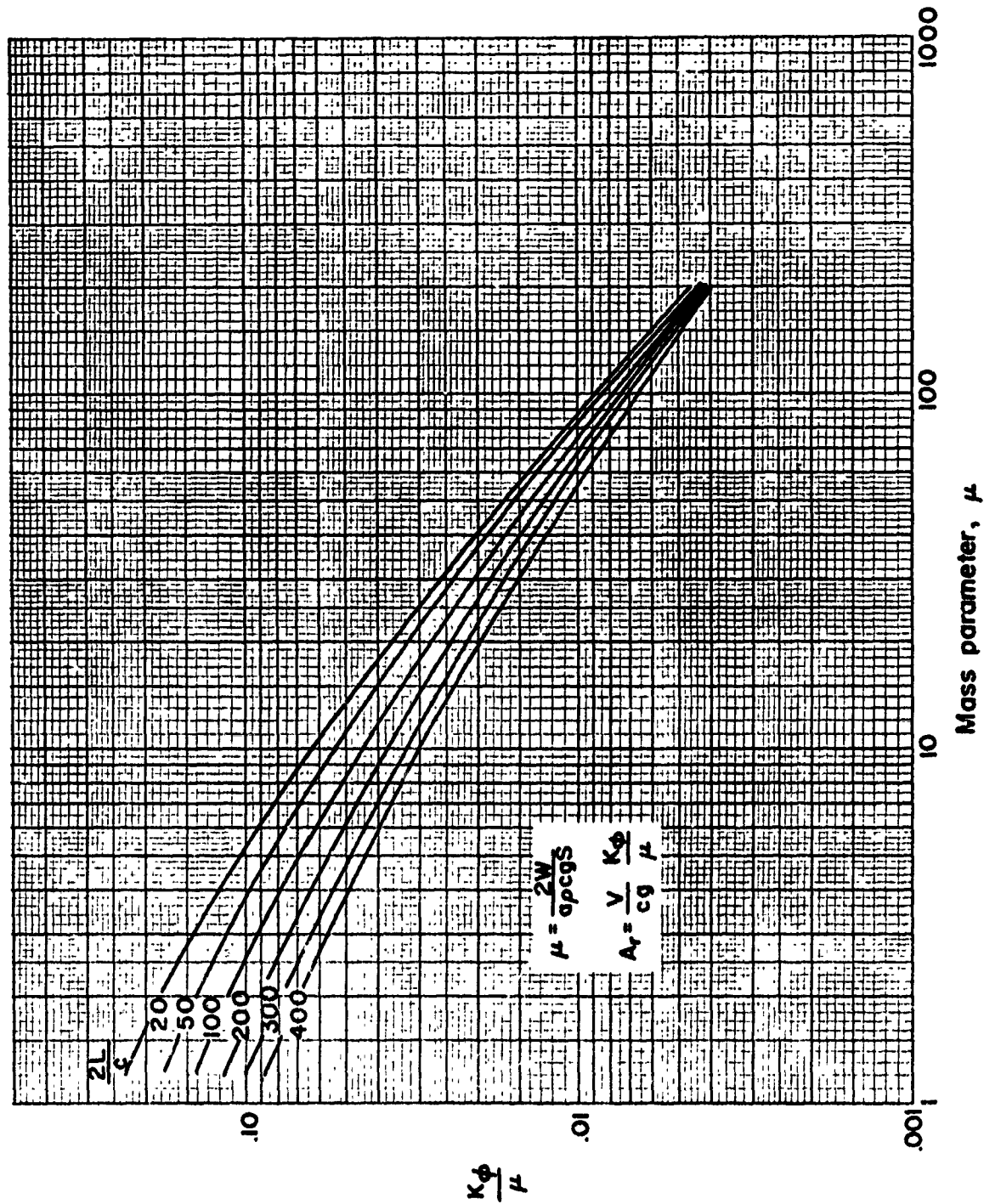
Figure 17. Variation of $\frac{K_\phi}{\mu}$ with μ

47
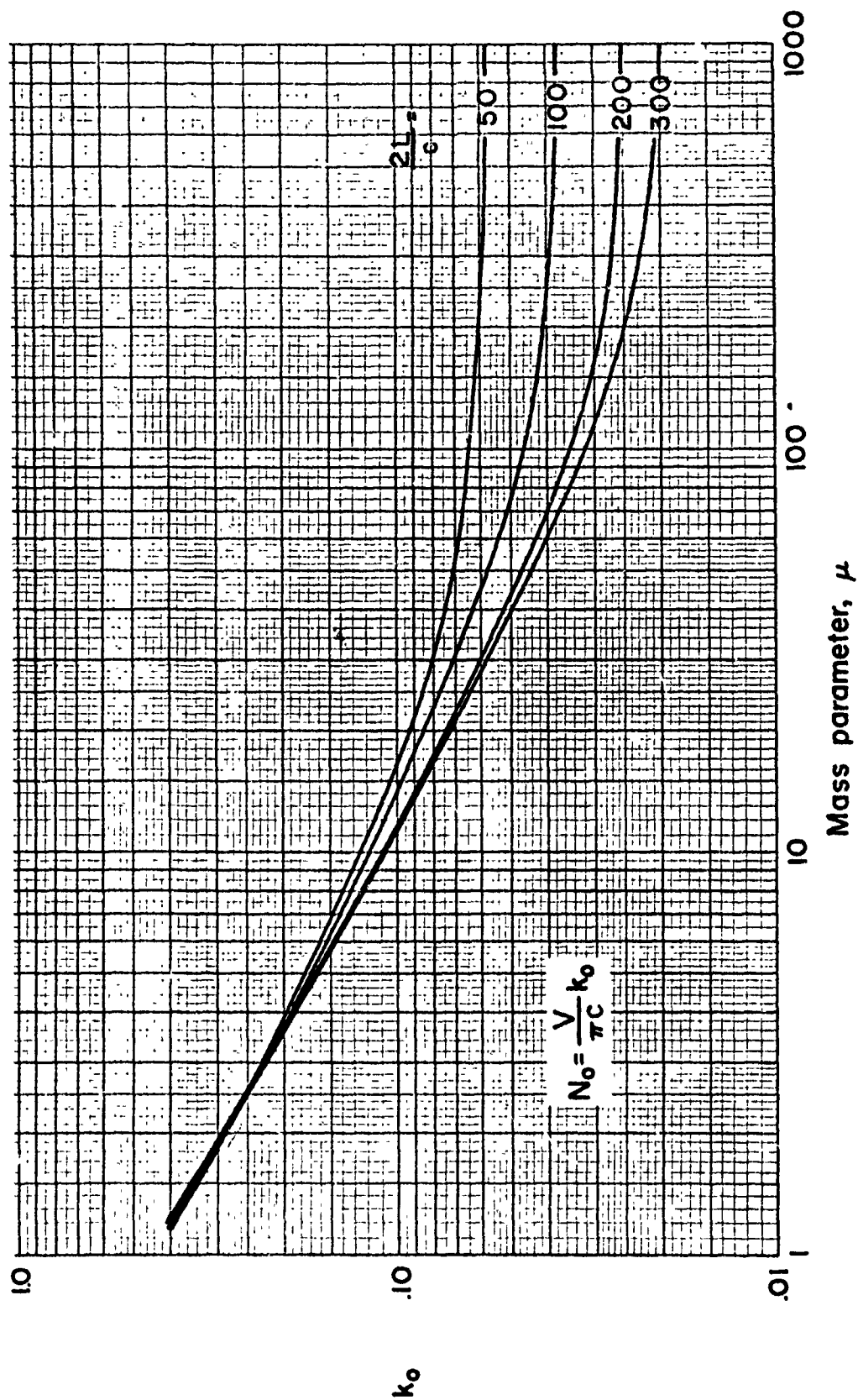
Figure 18. Zero-Crossing Values k_o

48
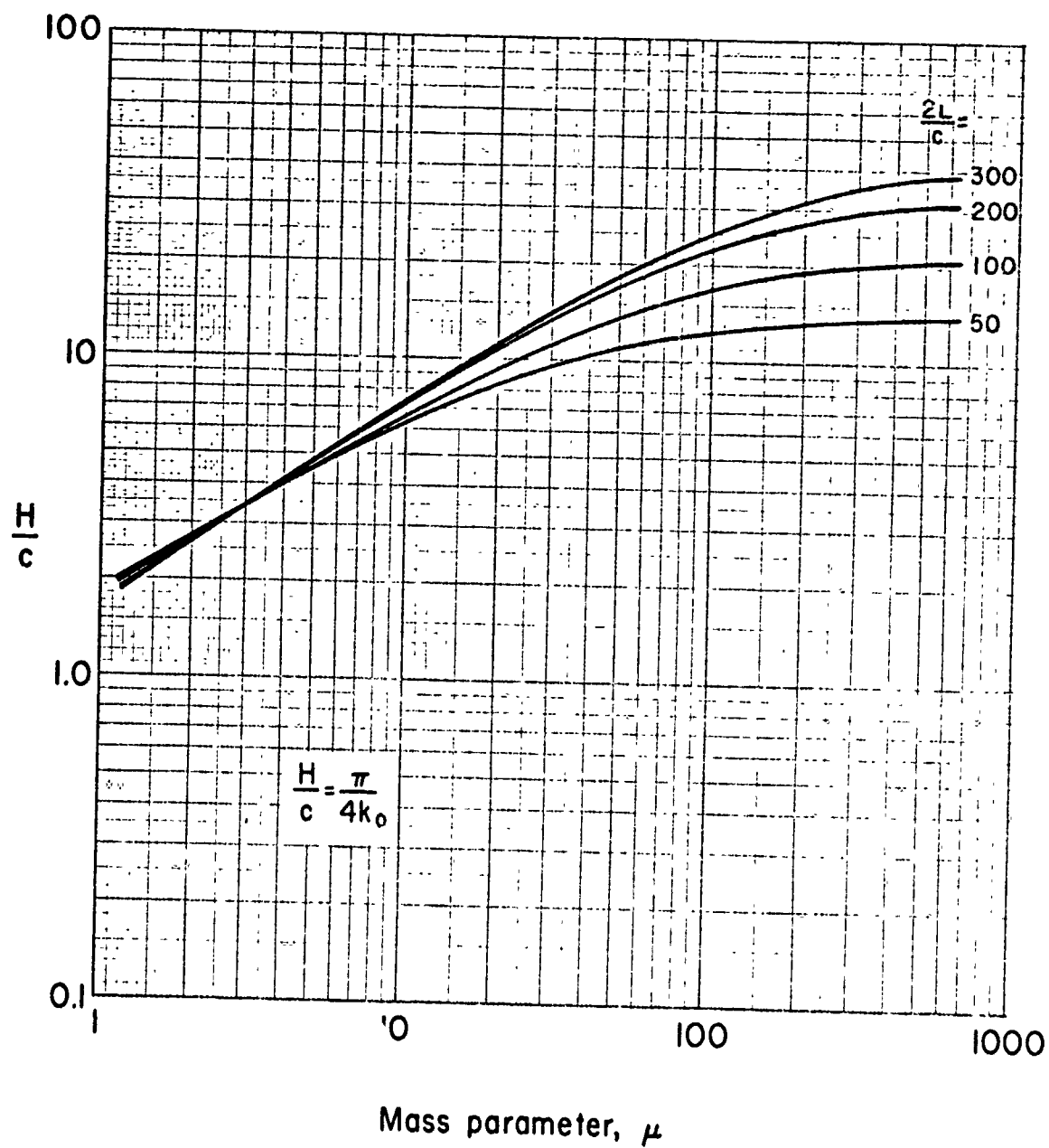
Figure 19. Effective Gust Gradient Distances

SECTION VII

OUTLINE OF DESIGN PROCEDURES

Nature of procedures.- This section outlines the gust design
procedures that are recommended. To keep the coverage as brief
as possible, very little exposition is given in justifying the
numbers given, or in justifying the procedures - although reasons
should be reasonably clear for the most part. To this end, the
procedures are given mainly in step-by-step fashion. In general,
the response is referred to by the variable x, signifying any
response quantity of concern, such as acceleration, a bending
moment, or a stress. It should be kept in mind that the response
values established are incremental values due to gust encounter,
and that these must be superimposed on the 1-g level flight
values to obtain the total response. Note also that in this
section the response refers to an individual or specific load
variable at a particular point on the aircraft structure. The
means for handling the situation of combined loads or stresses
is shown later in Section XI.

A flow chart showing the basic sequence that is involved in
applying the design procedures is shown in figure 20. Study of
this chart may help in understanding the procedural aspects that
follow. Essentially, the procedure is as follows. It is assumed
that the aircraft components have been sized or that the load
values have been established in accordance with some prescribed
maneuver load factor. Loads or stresses due to a 1-g level flight
condition are in turn established for each of several flight
conditions that are likely. A preliminary check for gust en-
counter is then made by fairly simple procedures, based on the
rigid-body results of the previous section and the 1-g flight
loads. If the design fails this preliminary check, evaluation
proceeds into a phase of intermediate detail. This second phase
still makes use of the rigid-body results of the previous section,
but considers the various possible flight conditions in combina-
tion. Should the design fail this phase, design proceeds to a
more detailed study phase where explicit evaluation is made of
some of the frequency response functions. This is the only phase
where detailed evaluation of frequency response functions is re-
quired; the necessity of having to enter this phase will usually
be remote. Note the use of the level flight load values x_{1-g} in
the preliminary and intermediate phases is a key notion;
essentially, the sizing of structural members in a direct fashion,
rather than by an iterative technique, is implied.

The design borders and conditions presented in this section
are based to a large extent on

   a) discrete-gust design values
   b) $\frac{X}{A}$ and N_o values as obtained from airplane computation
       studies, references 6-8, and the related analysis given
       in reference 2

51

c) limit load exceedance values given in reference 16

d) results given in reference 28

e) implications obtained by carefully comparing and inter-
preting the results of past gust studies.

To derive procedures in specific detail, the following equations
for load exceedance were adopted as a base for establishing the
main results of this section

$$N = PN_o e^{-\frac{x}{\sigma_x}} \tag{25}$$

$$n = PTN_o e^{-\frac{x}{\sigma_x}} \tag{26}$$

These equations are assumed to apply in the limit load region of
response. From equation (25) the following interesting alternate
forms may be derived

$$N_h = 3600 PN_o e^{-\frac{x}{\sigma_x}} = \frac{3600}{\pi} \frac{PVk_o}{c} e^{-\frac{x}{\sigma_x}} \tag{27}$$

$$N_m = 5280 \frac{PN_o}{V} e^{-\frac{x}{\sigma_x}} = \frac{5280}{\pi} \frac{Pk_o}{c} e^{-\frac{x}{\sigma_x}} \tag{28}$$

$$N_c = \frac{1}{\pi} Pk_o e^{-\frac{x}{\sigma_x}} \tag{29}$$

where N_h denotes the number of upward crossings per hour of
travel, N_m denotes the number of upward crossings per mile of
travel, and N_c denotes the number of upward crossings per chord
of travel. For various reasons, not discussed here, representation
of load exceedance based on N_h is preferred. It is interesting
to note, however, that of the several forms, the equation for N_c
seems to be the most "natural" form, in the sense that it is the
only form which is completely nondimensional, and because it in-
volves the least number of parameters.

In addition to equations (25) and (26), the basic gust de-
sign condition assumed in this development is that the number of
limit load exceedances shall be 10 or less in 30,000 hours of
flight. The choice of 10 limit load exceedances implies 5 for
positive loads, 5 for negative loads. Based on these values, the
limit load exceedance rate in number per second for satisfactory
gust design is given by

52

$$N \leq \frac{5}{30,000 \times 3600} = 4.62 \times 10^{-8} \qquad (30)$$

With this expression, and the fact that $\sigma_x = A\sigma_w$, equation (25) may be written

$$4.62 \times 10^{-8} \geq PN_o e^{-\frac{x}{A\sigma_w}} \qquad (31)$$

This equation forms the basis of the design procedures.

For the preliminary design phase, equation (31) is applied to specific flight conditions and altitudes. Design is judged satisfactory if this equation is satisfied by the values of $\frac{x}{A}$ and N_o at each of these chosen flight conditions. This application implies the specification of the values of P and σ_w . Recommended values of P and σ_w considered appropriate for design, which were arrived at after much deliberation and reasoning, are shown in figures 21 and 22. With these P and σ_w values, equation (31) yields the N_o vs. $\frac{x}{A}$ preliminary design borders shown in figure 23. The use of this figure implies the following concept. Consider that the airplane is to be flown wholly at a given altitude for the entire lifetime expected of the aircraft. If the design appears satisfactory for all such altitudes, then certainly the design should be adequate regardless of what combinations of altitudes are experienced. Detailed use of figure 23 will be outlined subsequently.

For the intermediate and detailed design phases, equation (31) is also used, but care is taken to combine the results from various flight conditions in a systematic manner. Details of the processes will also be outlined subsequently.

It is of interest to note that reference 16 indicates the number of limit load exceedance per mile of flight of $N_m = 10^{-6}$. This value, and the chosen values of $n = 10$, $T = 30,000$ hrs, implies an average flight speed given by the relation

$$n = \frac{VT}{5280} N_m$$

$$10 = \frac{30,000 \times 3600}{5280} 10^{-6} V$$

This relation yields $V = 488$ fps , which appears representative of operational practice. The values of $n = 10$, $T = 30,000$ hrs, and $N_m = 10^{-6}$ thus appear consistent.

Other values considered representative of a sound gust design condition, and which are implied by the chosen design numbers are as follows. Suppose $\frac{x}{A}$ is taken as 54; at sea level where $\sigma_w = 6$ (figure 21), this yields $\frac{x}{\sigma_x} = \frac{x}{A\sigma_w} = 9$. From figure 23, for $h = 0$ and $\frac{x}{A} = 54$, N_o is found to be $N_o = .75$ cps. This N_o value, and the value of $V = 488$, yield $k_o = \frac{\omega_o c}{2V}$ as follows: $k_o = .0966$ for $c = 20$, $k_o = .0724$ for $c = 15$. These k_o values are also quite representative of practical situations. Thus, a summary of the various numbers chosen or derived in this section leads to the following combination which is considered representative of a sound gust design situation

$$n = 5$$
$$T = 30,000 \text{ hrs}$$
$$N_m = 10^{-6}$$
$$V = 488 \text{ fps}$$
$$P = .0005$$
$$\frac{x}{\sigma_x} = 9$$
$$N_o = .75 \text{ cps}$$

These numbers are self-consistent and satisfy equations (25) through (28).

Preliminary design considerations.- A preliminary - and perhaps final - design check proceeds as follows.

1. List various possible conditions of flight, involving altitude, speed, weight and weight distribution, as depicted in the following sketch
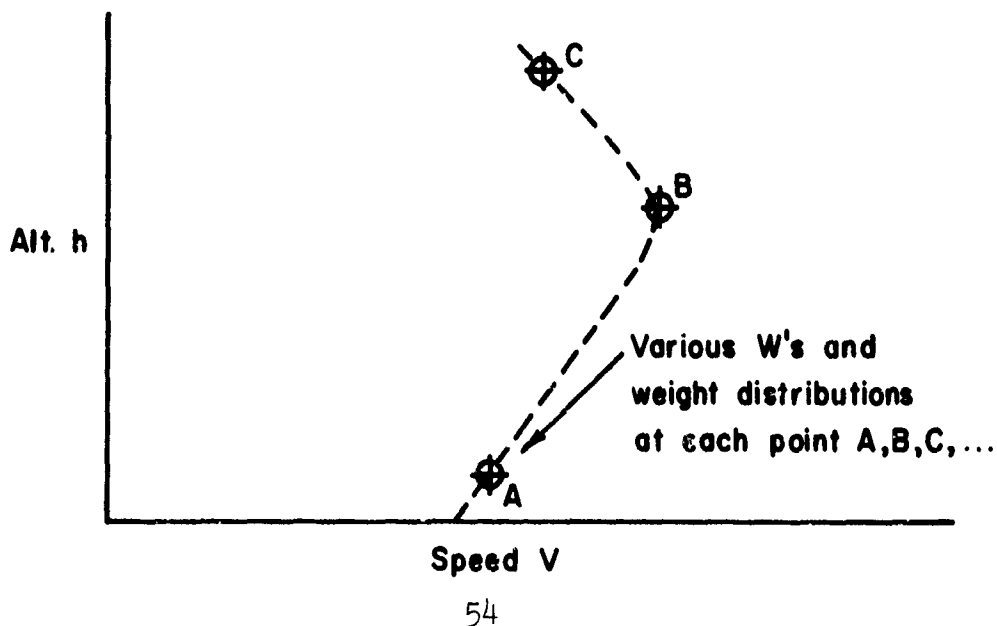
2. Select points throughout the structure that are
   suspected of being critical locations.

3. Establish values of the level flight load or stresses,
   x_{1-g} , at these locations for the various flight
   conditions.

4. Establish the values of A_r for each of the chosen
   flight conditions by equation (23) or (24), using
   the values of K_ϕ or $\dfrac{K_\phi}{\mu}$, as given in figures 16
   and 17. With these A_r's establish Δn values by
   the expression

$$\Delta n = A_r 9\sigma_w \qquad (32)$$

   where σ_w is taken from figure 21. These Δn values
   are very similar to the values that would be established
   by the discrete-gust design approach. The main purpose
   of this step is to isolate those flight conditions which
   are most likely to produce the largest gust loads. Thus
   if Δn is found to exceed the value of the design
   maneuver acceleration value minus one, such as the
   $\Delta n_T = 1.5$ factor often used in the past, then the flight
   condition yielding this Δn will probably also be found
   critical in the subsequent steps. If all Δn's are less
   than the maneuver acceleration minus one value, gust de-
   sign is probably not a problem.

5. With the x_{1-g} values of step 3 and the A_r's of step 4
   determine the values of A by the relation

$$A = A_r x_{1-g} \qquad (33)$$

   For aircraft with large flexible swept wings, the slope
   of the lift curve used in step 4 should be that for the
   flexible airplane, both in determining μ and A_r, so
   that the load effects due to wing bending are approxi-
   mately taken into account. Note the intent of consider-
   ing various flight conditions is to find the condition
   which leads to the largest value of A at each altitude
   for the particular response quantity of concern. Note
   also, that there is no explicit determination of the
   frequency response function or output spectra in this
   preliminary check sequence; results for the rigid-body
   case of Section VI are used directly, much as in the
   discrete-gust design technique.

6. For each flight condition estimate the value of N_o
   using figure 18.

7. For each structural point being checked and each altitude, take the largest values of A found, multiply by 1.1 and divide the resulting value into $x_L - x_{1-g}$, where x_L is the limit load value for the response quantity; specifically, the ratio $\dfrac{x_L - x_{1-g}}{1.1A}$ is found. With equation (33) this ratio becomes the effective $\dfrac{x}{A}$ value as follows

$$\frac{x}{A} = \frac{\dfrac{x_L}{x_{1-g}} - 1}{1.1A_r} \tag{34}$$

Note, the factor 1.1 is introduced as a means for approximately taking into account the amplification effects due to flexibility. The factor is a rough average value; if judgment or some previous results indicates that a different factor may be in order, the number may be adjusted upward or downward accordingly.

8. Enter figure 23 with the N_o and $\dfrac{x}{A}$ values established in steps 6 and 7 and compare each point with the appropriate altitude curve. Decide action according to the following three rules:

Rule (a):   If the point lies well to the right of the curve, the design may be considered satisfactory from a strength point of view, and no further check need be made.

Rule (b):   If the point lies to the left of the curve, the design is probably unsatisfactory, and needs more detailed study, as outlined in detailed design phase.

Rule (c):   If the point lies close to the curve, on either side, the design may or may not be satisfactory, and also needs more detailed study.

9. If either rule (b) or (c) of step 8 is encountered, proceed to the detailed design consideration.

It should be noted that the underlying thought behind rule (a) is that if the airplane is considered to be flown continually in the condition that leads to the most severe loads at a given point, and the structure is shown to be adequate for this situation, then certainly the structure should be satisfactory for all other flight conditions.

56

Detailed design considerations.- Procedures for examining the design in a more detailed sense than offered by the preliminary design considerations are listed here. The procedures have some aspects of a mission consideration but are somewhat easier because explicit evaluation of load exceedance curves is avoided. Three procedures are given, each of different complexity and detail. The first is a composite approach based upon c-g acceleration values. The second is in terms of limit load exceedance rates but is based on the rigid-body results. These two are of intermediate detail. The third is also in terms of limit load exceedance rates but involves detailed evaluation of the frequency response functions. All three make use of equations (25) and (30).

Composite approach based on c-g acceleration:

This approach may be used if rule (b) or (c) of step 8 of the preliminary design procedure applies. It is not a basic design method, but rather serves as a check as to whether a more detailed design treatment appears necessary. It is given because it is quite simple to apply, and because it does not require the use of the x_{1-g} load values.

1. Lay out the most probable mission (or missions) of the airplane, as depicted in figure 24. Usually missions with a cruise altitude of about 30,000 ft will lead to the most severe gust load conditions (unless of course the mission is a low altitude one at very high speeds).

2. Establish the values of A_r and N_o for each segment of the mission; use either equation (23) or (24) and figure 16 or 17 and 18; also establish the value of σ_x for each segment by the relation

$$\sigma_x = A_r \sigma_w \qquad (35)$$

where σ_w is taken from figure 21.

3. Determine composite values of the parameters σ_x and PN_o through means of the following equations:

$$T = T_1 + T_2 + T_3 + \ldots \qquad (36)$$

$$PT = P_1 T_1 + P_2 T_2 + P_3 T_3 + \ldots \qquad (37)$$

$$\sigma_x^2 = \frac{1}{PT} (P_1 T_1 \sigma_{x_1}^2 + P_2 T_2 \sigma_{x_2}^2 + P_3 T_3 \sigma_{x_3}^2 + \ldots) \qquad (38)$$

$$PN_o = \frac{1}{T} (P_1 T_1 N_{o_1} + P_2 T_2 N_{o_2} + P_3 T_3 N_{o_3} + \ldots) \qquad (39)$$

where the subscripts denote the segments and where the P values are given by figure 22. These equations

57

represent simply the overall parameters that are
obtained when all the segments are considered in
combination.

4. From equation (38) establish the effective value of
$\dfrac{x}{\sigma_x}$ by the relation

$$\frac{x}{\sigma_x} = \frac{\Delta n_L}{1.1\sigma_x}$$

where Δn_L is the design maneuver load factor minus
one. Enter figure 25 with this ratio and the value of
PN_o of equation (39).

5. If the point lies well to the right of the curve, the
design may be considered satisfactory; if the point
lies near or to the left of the curve, more detailed
examination is needed as in the following two pro-
cedures. The point shown in figure 25 applies to an
example case that is treated later.

Approach based on rate of limit load exceedances:

This approach is also used if rule (b) or (c) of step 8
in the preliminary design section applies, or if the check
given by the preceding composite approach failed. The approach
is based on the rigid-body results of Section VI, and uses the
x_{1-g} values.

1. Proceed as in steps 1 and 2 of the preceding composite
approach, but also establish the x_{1-g} values. From
the A_r and x_{1-g} values obtain the σ_x value for
each segment by the relation

$$\sigma_x = A_r x_{1-g}\, \sigma_w \tag{40}$$

where σ_w is taken from figure 21 at the appropriate
altitude.

2. Determine the rate of limit load exceedances by the
equation

$$N = P_1 \frac{T_1}{T} N_{o_1} e^{-\alpha_1} + P_2 \frac{T_2}{T} N_{o_2} e^{-\alpha_2} + \ldots \tag{41}$$

where

$$\alpha_n = \frac{1}{1.1\sigma_{x_n}}\left[x_L - (x_{1-g})_n\right]$$

$$= \frac{1}{1.1 A_{r_n} \sigma_{w_n}}\left[\frac{x_L}{(x_{1-g})_n} - 1\right]$$

58

and where the subscripts correspond to the respective segments.

3. If the value of N as obtained in step 2 is significantly lower than the 4.62×10^{-8} value given by equation (30), the design may be considered satisfactory. If the value of N is near this value more detailed consideration is needed as in the detailed approach given next. If N is above the value of 4.62×10^{-8}, the design is probably unsatisfactory and should be also examined in more detail.

Approach based on rate of limit load exceedances (Detailed evaluation):

If the design has failed all previous three approaches (the preliminary check, the composite approach, and the rate of limit load exceedances approach), then detailed design consideration should be given according to the following:

1. Proceed as in the previous approach dealing with rate of load exceedances, except establish the values of A and N_O in accordance with equations (15) and (16). The previous approach using the rigid-body results will identify those segments which contribute most significantly to the N value. Usually one or two segments will contribute N values which far overshadow the values of N that are due to the other segments. Detailed evaluation of A and N_O need only be made for these more critical segments; results of the preceding section may be used for the segments which contribute in a minor way to N. Note: this is the first place in the procedures outlined so far where it is necessary to evaluate explicitly some of the frequency response functions, and in turn the associated values of A and N_O; the intent, however, is to keep the number of such evaluations to a minimum. For the A values that are evaluated explicitly, it is not necessary to use the x_{1-g} values, since the correct units will inherently be included.

2. Evaluate N by means of equation (41). Note: for the segments for which A and N_O have been evaluated in detail, use

$$n = \frac{x_L - x_{1-g}}{A_n \sigma_{w_n}}$$

That is, the factor 1.1 is not included due to the fact that amplification effects due to flexibility will be inherently present in the A_n values.

3. If the value of N as obtained in step 2 is equal to or less than 4.62×10^{-8}, the design may be judged adequate. If N is greater than this value, strengthening of the structure would be indicated.

Design using a comparison approach.- Another design approach that may be used involves the concept of comparing the design under consideration with a previous design which has "proven" itself through years of successful operation. This comparison approach would seem to be particularly attractive if the new design is similar in configuration to a previous model, or represents a stretched version. The comparison approach is accomplished through use of figure 26, which is derivable directly from equation (26). The parameters that are used to enter this figure are evaluated in accordance with the composite values, equations (36) - (39). If the point established by entering the figure with the computed ratio values falls in the "safe" region, then the new design may be considered satisfactory; if the point falls on the "unsafe" side, then more detailed study of the new design is indicated. Note that even though the concept of comparing one aircraft to another is involved, this approach also serves well even for the same airplane, using the idea of comparing in a relative sense one point of the structure with another point of the same structure. In this case, the PT and σ values would simply cancel. The approach is thus useful in establishing which point of the structure seems to be the most critical in relation to other points.

Examples.- Some examples are given to close out this section to illustrate the gust design procedures.

Example 1:

Consider an airplane with characteristics as follows:

$$b = 140 \text{ ft}$$
$$c_m = 20 \text{ ft}$$
$$S = 2800 \text{ ft}^2$$
$$a = 4.88$$
$$W_E = 128,000 \text{ lbs} \quad \text{(Empty wt)}$$
$$W_P = 32,000 \quad \text{(Payload wt)}$$
$$W_F = 140,000 \quad \text{(Fuel wt)}$$
$$W_G = 300,000 \quad \text{(Gross wt)}$$
$$\Delta n_L = 1.5 \quad \text{(Maneuver load factor} = 2.5)$$

Design considerations for wing-root bending moment will be illustrated.

For the preliminary design check, three flight conditions are considered, as listed in the following table:

	h,ft	W,lbs	V,fps	$(B.M.)_{1-g}$,ft-lbs
(1)	0	300,000	422	2.02×10^6
(2)	30,000	300,000	800	2.02×10^6
(3)	30,000	180,000	, 800	1.90×10^6

where B.M. denotes wing-root bending moment. Condition (1) also applies to maneuver load design and, therefore, with a maneuver load factor of 2.5, the maneuver design bending moment is

$$x_L = 2.5 \times 2.02 \times 10^6 = 5.05 \times 10^6 \text{ ft-lbs}$$

The various values of μ, $\dfrac{K_\phi}{\mu}$, A_r that apply to each of these flight conditions, together with the values of Δn as given by equation (32), the $\dfrac{x}{A}$ values as given by equation (34), and the N_o values as determined from figure 18, are listed in the following table:

	μ	$\dfrac{K_\phi}{\mu}$	A_r	σ_w	Δn	$\dfrac{x}{A}$	N_o
(1)	28.6	.0225	.0147	6.0	.794	92.7	.517
(2)	76.6	.0103	.0125	9.6	1.08	109.2	.725
(3)	46.0	.0158	.0196	9.6	1.69	76.8	.828

where a value of $\dfrac{2L}{c} = \dfrac{1500}{20} = 75$ was used. The first point to notice is the $\Delta n = 1.69$ load factor for flight condition (3); this value is in excess of the $\Delta n_L = 1.5$ value. Flight conditions which approach condition (3), which corresponds to a lightly loaded airplane (14 percent fuel) at high altitude at high speed, may thus be suspected as possible critical gust loads producers.

A plot of the $\dfrac{x}{A}$ and N_o values and the appropriate design borders of figure 23 are shown in figure 27. Conditions (1) and (2) are quite "safe" but condition (3) is noted to appear as "unsafe." More detailed examination is thus indicated; this examination is indicated in the following section.

Detailed design check:

The mission chosen for study is shown in figure 28; a take-off gross weight of 300,000 lbs, involving a full payload and full fuel condition, is considered. Near the top of figure 28 are listed the operational parameters, and the 1-g root-bending moment. Next, values of σ_w and P as obtained from

61

figures 21 and 22 are listed. The pertinent response parameters (ρ, μ ... N_O) that are evaluated by the various equations and charts of this report are then given.

The composite values of σ_x and PN_O as obtained from equations (38) and (39) (using σ_x as obtained from equation (35)) are as follows:

$$\sigma_x^2 = \frac{.0005}{.15}\left[15(.087)^2 + 15(.106)^2 + 120(.1324)^2 + 120(.1535)^2\right.$$
$$\left. + 15(.187)^2 + 15(.118)^2\right]$$

$$= \frac{1}{300}(.11 + .17 + 2.1 + 2.84 + .53 + .27)$$

$$= .0198$$

$$\sigma_x = .141$$

$$PN_O = \frac{.0005}{300}(15 \times .48 + 15 \times .60 + 120 \times .75 + 120 \times .78$$
$$+ 15 \times .87 + 15 \times .55)$$

$$= .000368$$

The values of .15 and 300 appearing in these equations are the PT and T values as evaluated in figure 28. The value of $\frac{x}{\sigma_x}$ is thus found to be

$$\frac{x}{\sigma_x} = \frac{1.5}{1.1\sigma_x} = 9.7$$

This value and the value of PN_O plot as shown in figure 25; since the point is to the right of the design border, the design would appear to be safe.

A more definitive check is afforded by the approach in terms of rate of limit load exceedances. For this example equation (41) is found to be

$$N = \frac{.0005}{300}\left(15 \times .48\ e^{-15.7} + 15 \times .60\ e^{-12.86} + 120 \times .75\ e^{-10.57}\right.$$
$$\left. + 120 \times .78\ e^{-9.42} + 15 \times .87\ e^{-7.86} + 15 \times .55\ e^{-12.54}\right)$$

$$= \frac{.0005}{300 \times 8100}(.01 + .19 + 18.7 + 61.5 + 41 + .24)$$

$$= 2.51 \times 10^{-8}$$

62

The α_n values (the exponential values of e) in this equation are found from the σ_x values given by equation 40, the $(B.M.)_{1-g}$ values, and the x_L value of 5.05×10^6 ft-lbs. The value of 8100 appearing in the evaluation is the result of removing a factor e^{-9} from all the exponential terms in parentheses, so as to simplify the evaluation of each term. The value for N that is found is noted to be well below the design value of 4.62×10^{-8} given by equation (30). The design is therefore judged safe. It is to be noted that the equation for N shows that the 4th and 5th segments are the largest contributors to the load exceedance rate. If N were found to be larger than the value of 4.62×10^{-8}, then evaluation would proceed by evaluating the frequency response function for bending moment, and the A and N_O values, for only the 4th and 5th segments. This observation thus brings out the fact that the design procedures given herein are intended to keep the amount of detailed work to a minimum.

Example 2:

In this example let all the conditions be the same as in example 1, but with changes in segments 4 and 5 as follows. Assume that previous work with the airplane design indicated that the 1.1 factor chosen for flexible body amplification effects was too small. Thus specific evaluation of the frequency response functions and the A and N_O values appeared necessary. Suppose that these evaluations were made and that values of $\alpha_4 = 8.63$ and $\alpha_5 = 7.2$ were found as a result (contrasted to $\alpha_4 = 9.42$ and $\alpha_5 = 7.86$ of example 1). These more refined α values indicate, in effect, that the amplification effects due to flexibility were indeed greater, as suspected; specifically a factor of around 1.2 instead of 1.1 is indicated. With these α_4 and α_5 values, and all other values as in example 1, the equation for N becomes

$$N = \frac{.0005}{300 \times 8100} (.01 + .19 + 18.7 + 135 + 79 + .24)$$

$$= 4.8 \times 10^{-8}$$

This value is greater than the design value of 4.62×10^{-8} given by equation (30). The value is only 4% greater and thus the design appears to be only slightly inadequate. If strict adherence to the design number is maintained, however, some strengthening of the structure due to gust encounter effects is indicated.
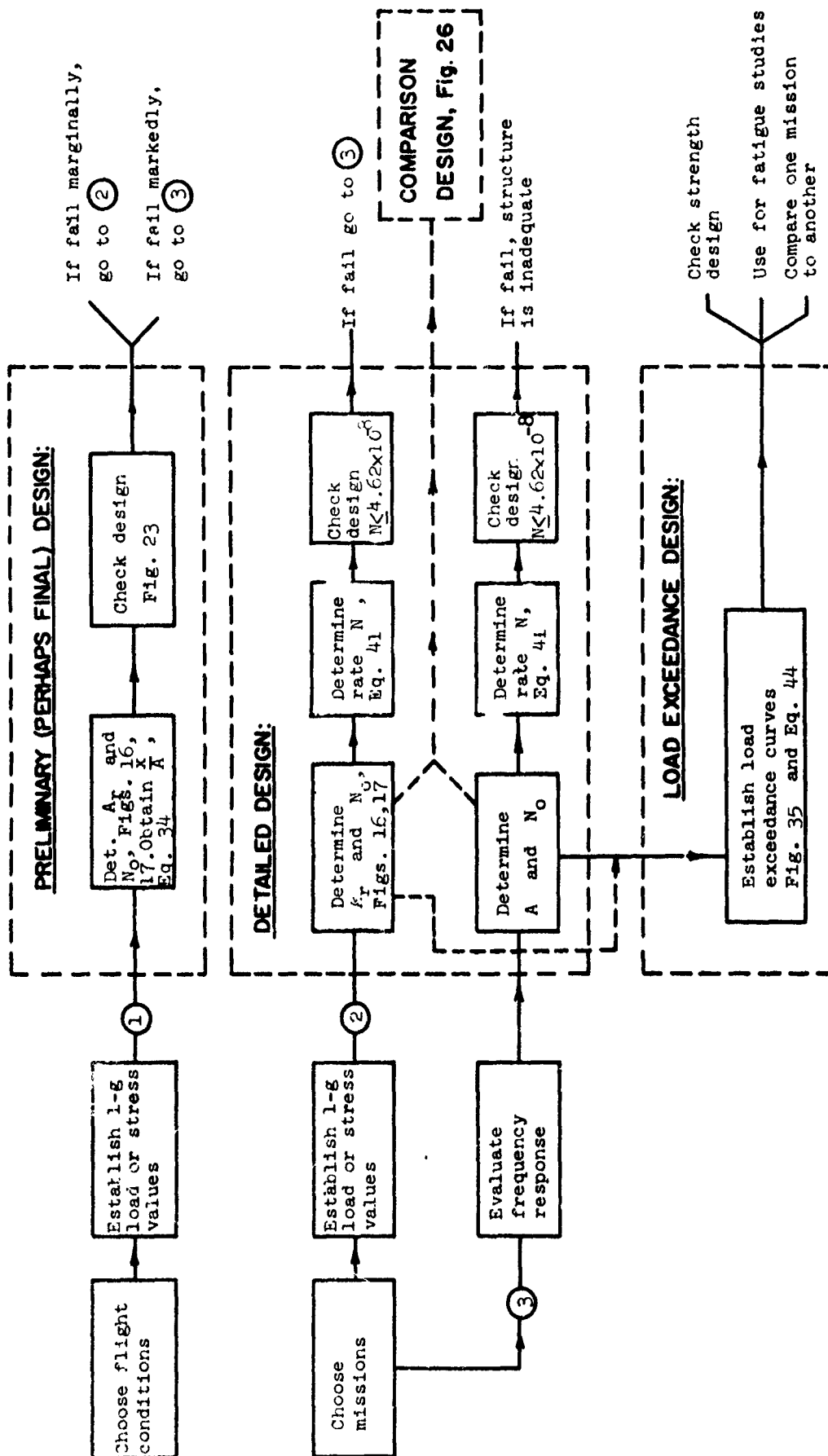
Figure 20. Sequence of Gust Design Procedure
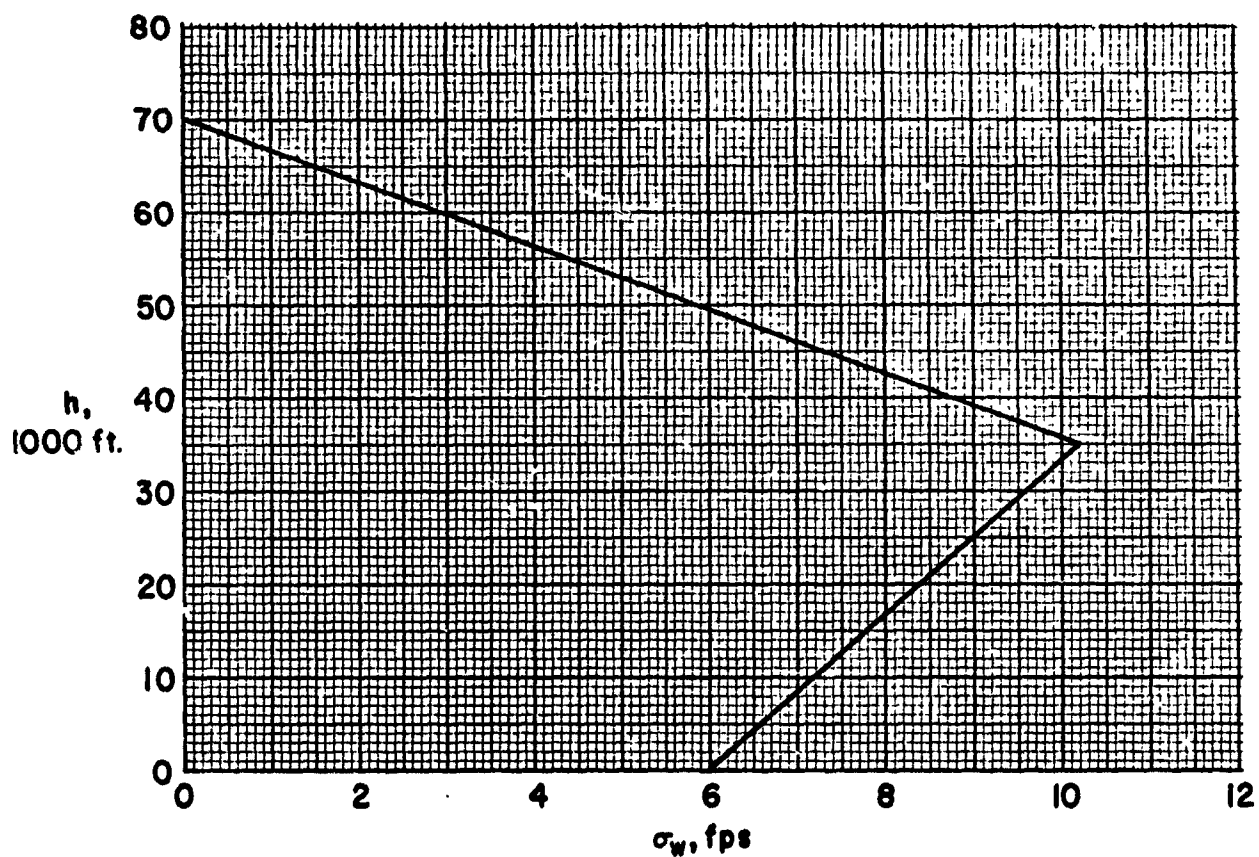
Figure 21. Recommended σ_w Values for Composite Approaches
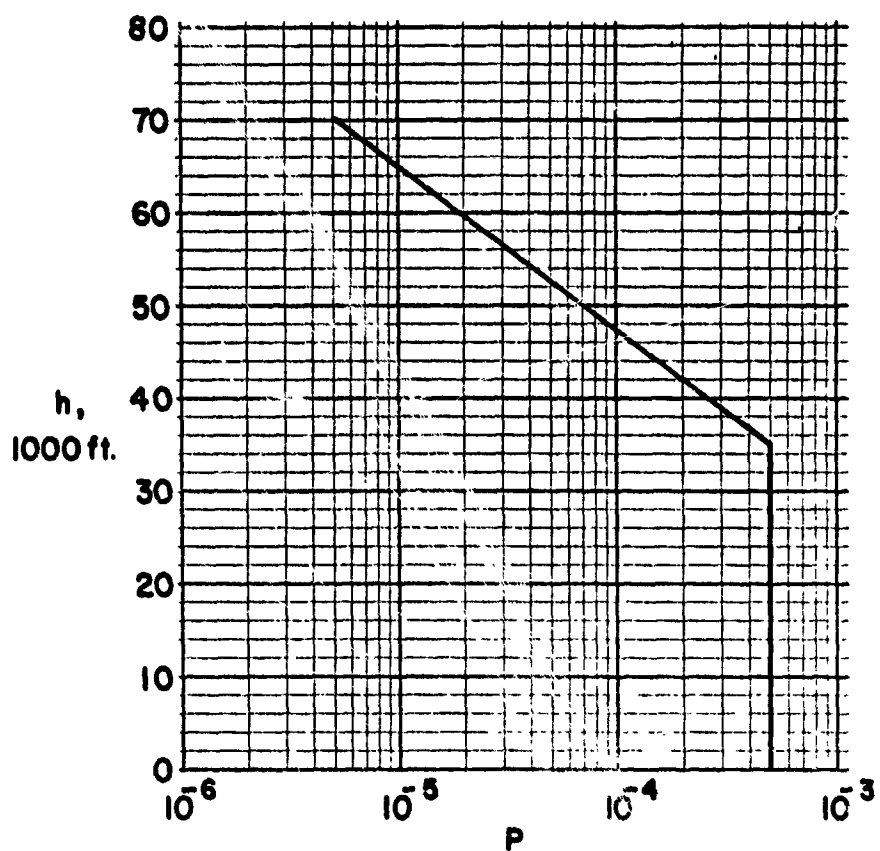
Figure 22. Recommended P Values for Composite Approaches
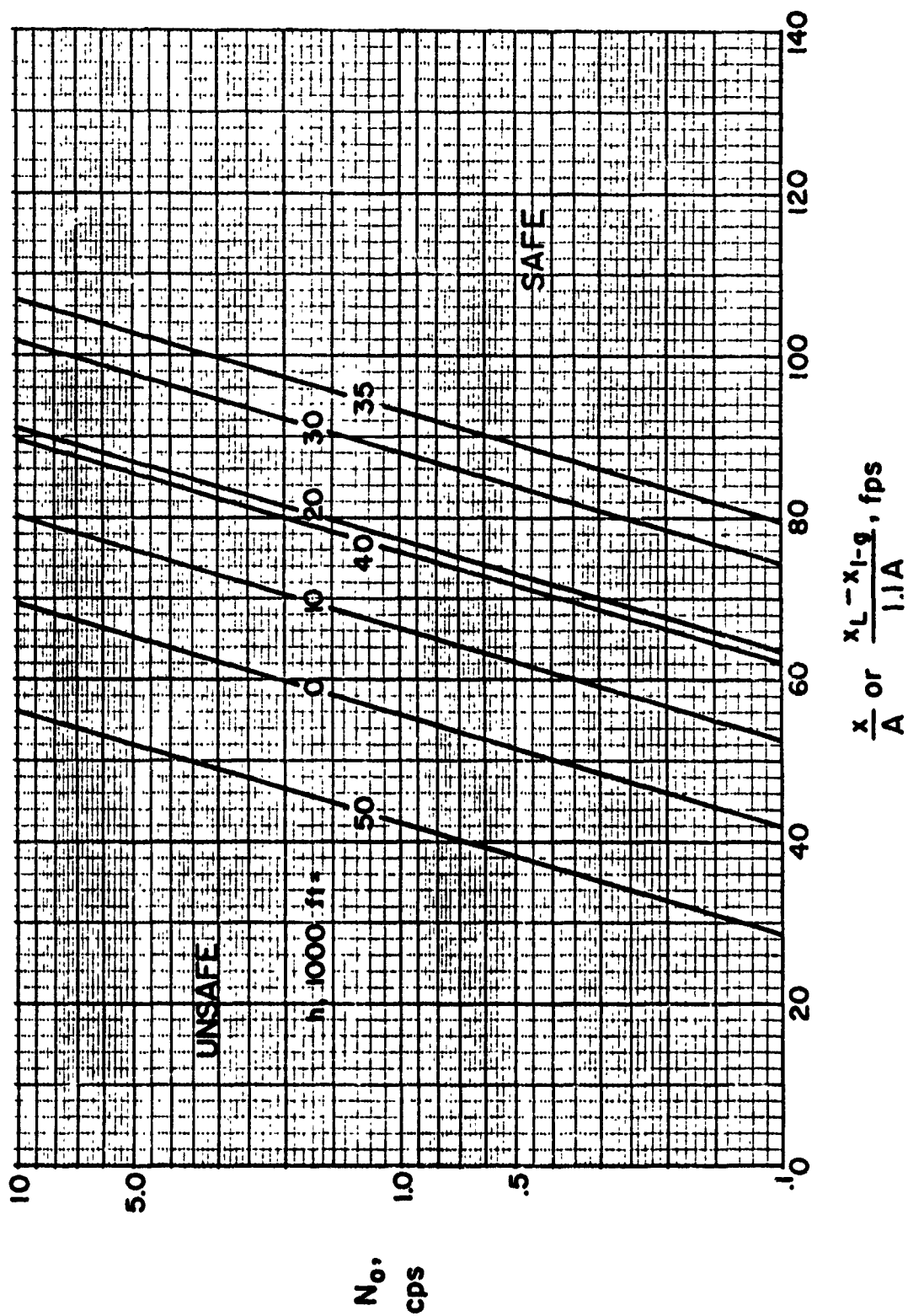
Figure 23. N_0 vs. $\frac{x}{A}$ Design Approach

66
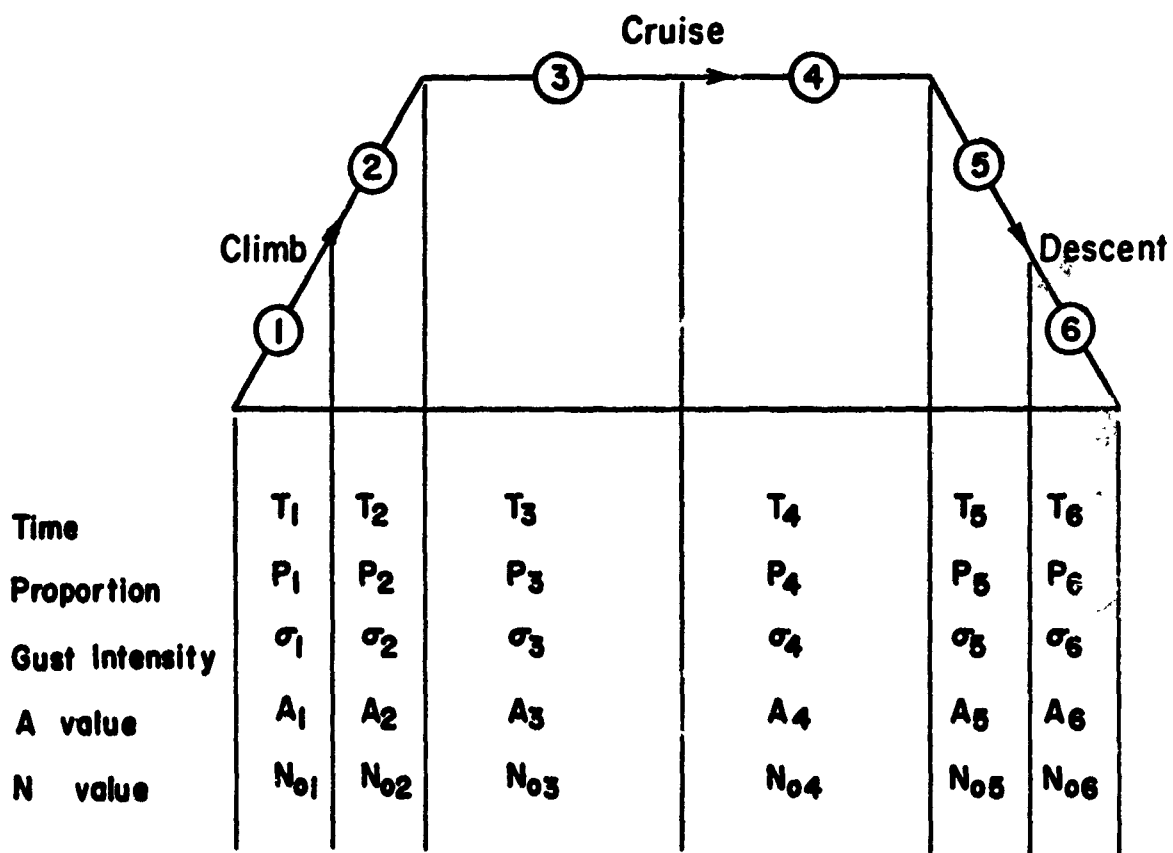
Figure 24. Illustrative Mission Profile
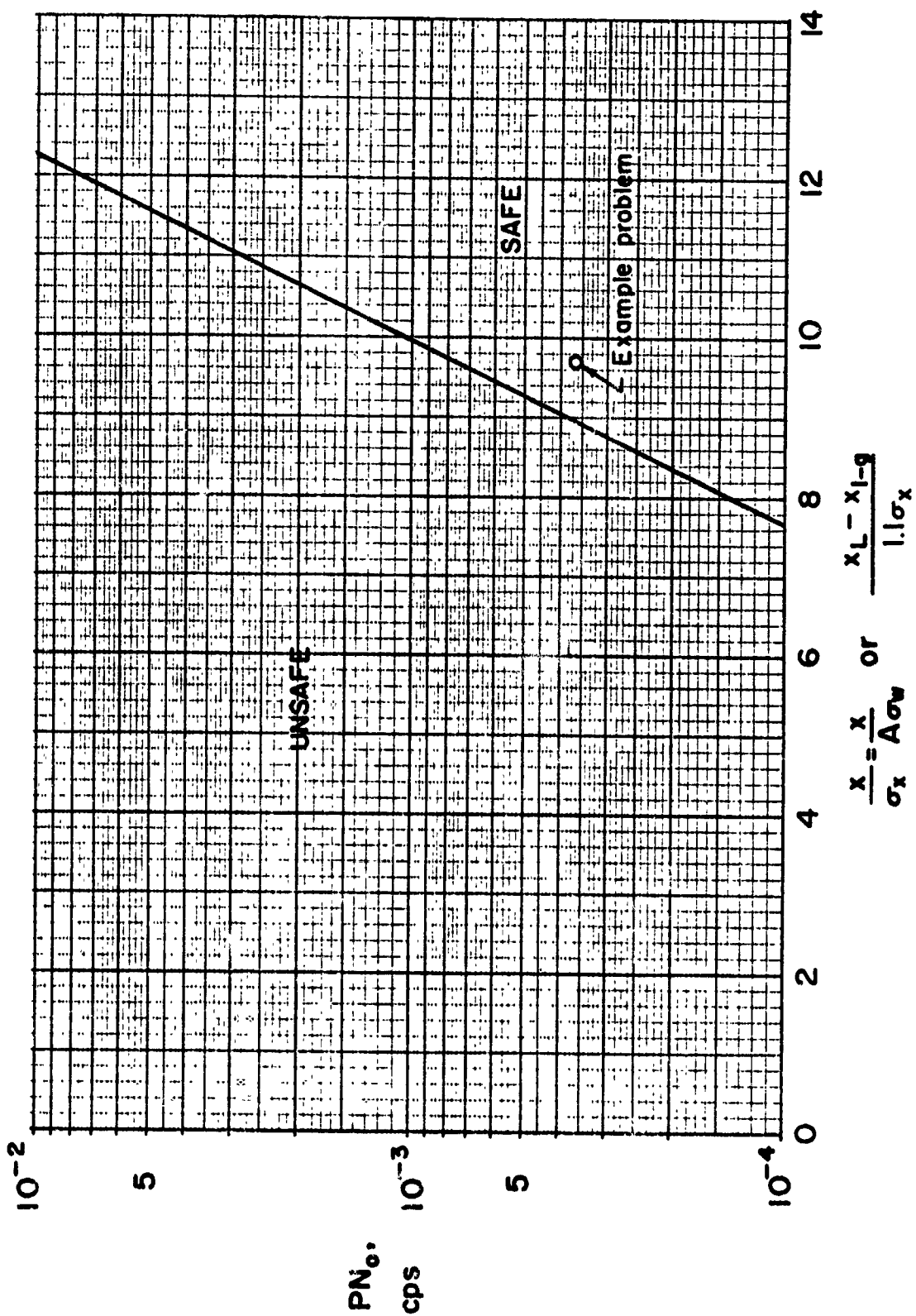
Figure 25. Design Chart Using Composite Values of σ_x and PN_o
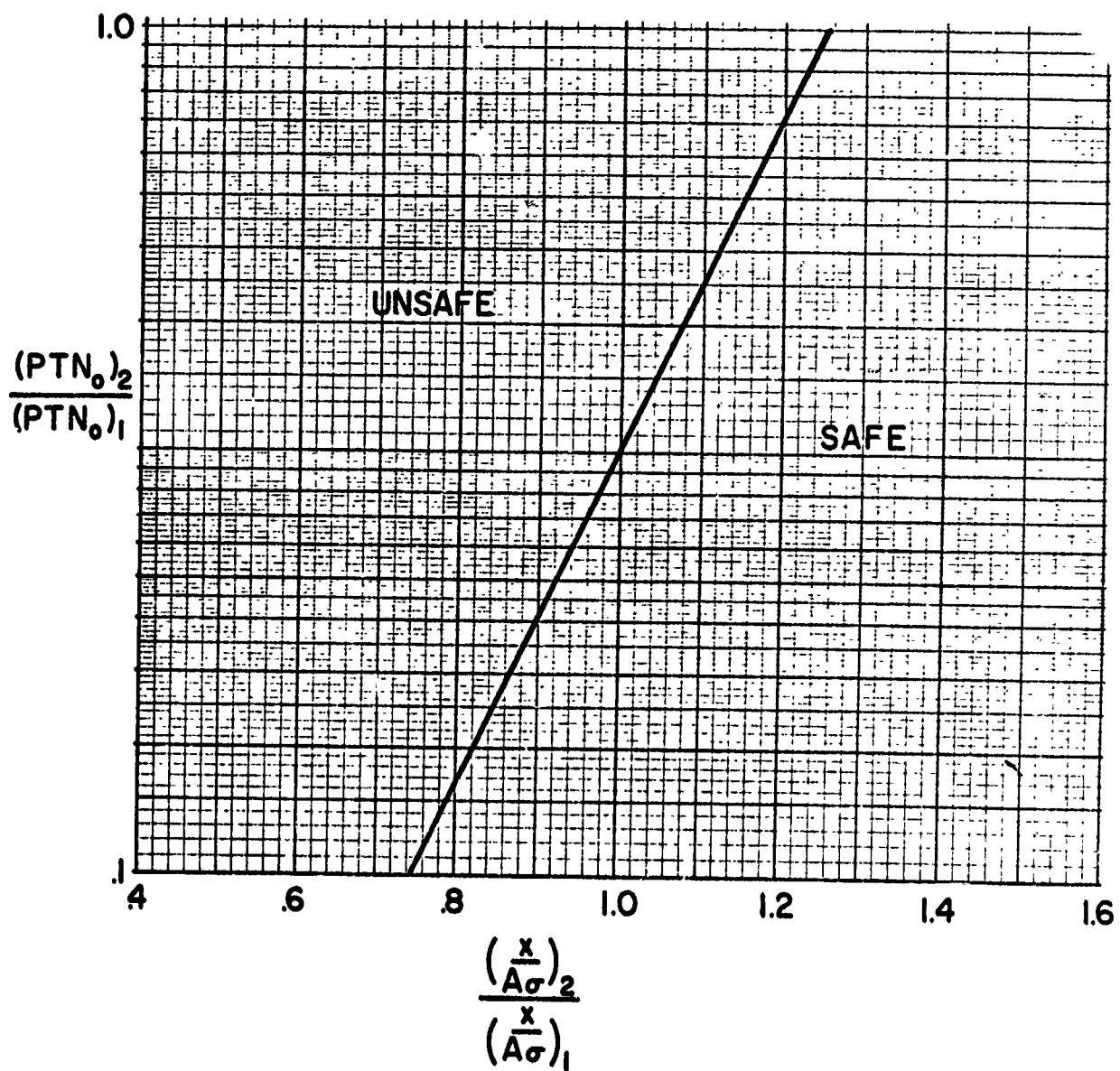
Figure 26. Design by Comparison

69
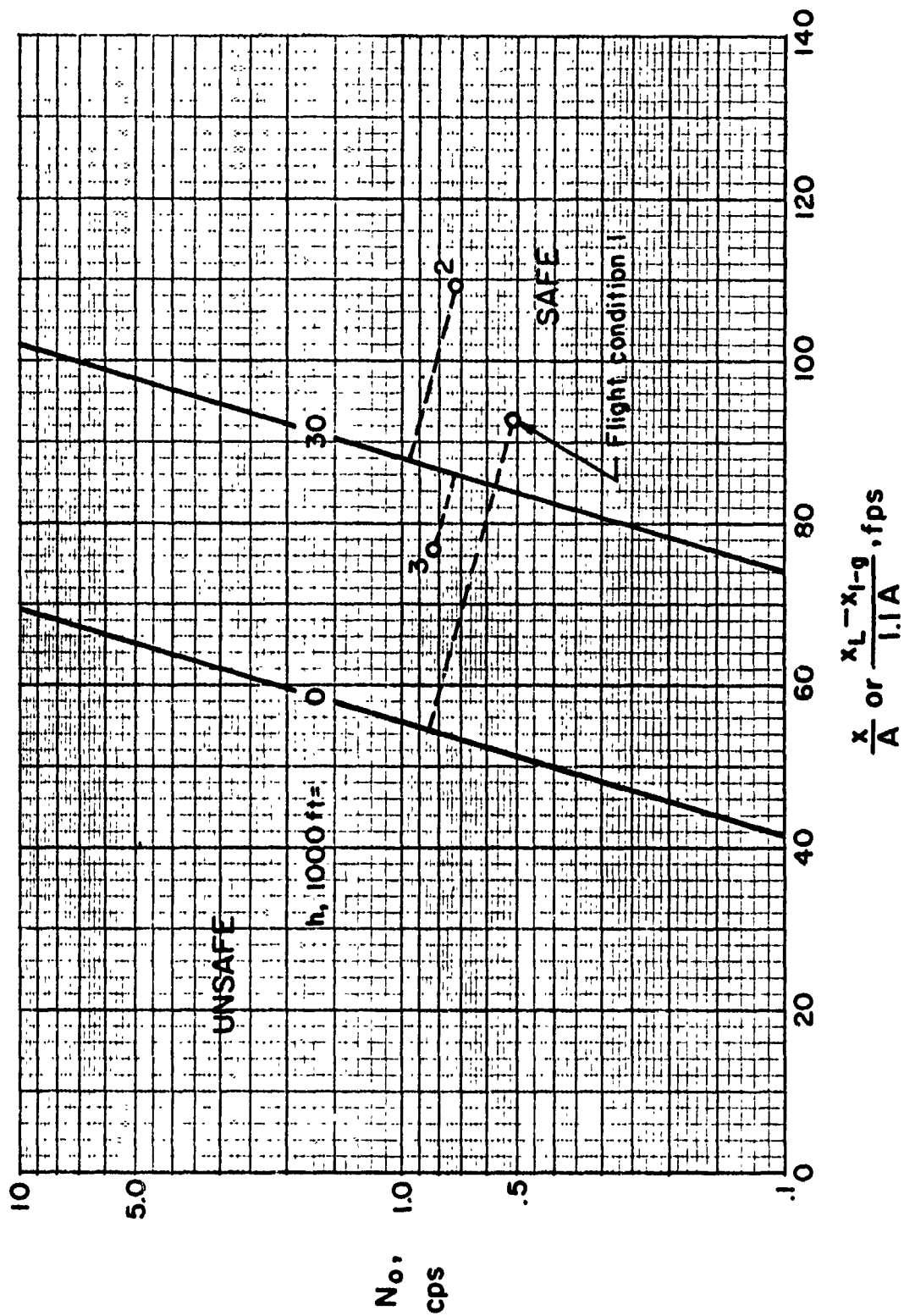
Figure 27. Preliminary Design Results for Example Problem

Segment	1	2	3	4	5	6	
T	15	15	120	120	15	15	min
W	297.5	292.5	270	230	207.5	202.5	× 1000 lbs
V	420	600	800	800	800	420	fps
$(B.M.)_{1-g}$	2.02	2.02	1.99	1.95	1.93	1.92	× 10^6 ft-lbs
σ_w(fig. 21)	6.9	8.7	9.6	9.6	8.7	6.9	
P(fig. 22)	.0005	.0005	.0005	.0005	.0005	.0005	
ρ	.0019	.00116	.00889	.00889	.00116	.0019	
μ	35.5	57.2	69	58.7	40.6	24.2	
$\dfrac{K_\phi}{\mu}$	.0193	.0131	.0111	.0129	.0173	.0262	
A_r	.0126	.0122	.0138	.0160	.0215	.0171	
σ_x(eq. 35)	.087	.106	.1324	.1535	.187	.118	
σ_x(eq. 40)	.1756	.214	.264	.299	.361	.227	× 10^6 ft-lbs
k_o	.072	.063	.059	.061	.068	.082	
N_o	.48	.60	.75	.78	.87	.55	

$$T = 15 + 15 + 120 + 120 + 15 + 15 = 300$$

$$PT = .0005 \times 300 = .15$$

Figure 28. Mission Characteristics of Example Problem

71

LOAD EXCEEDANCE CURVES

The means for establishing overall load exceedance curves based on mission considerations are outlined in this section. These exceedance curves may be desired for possible use in structural fatigue studies of the airplane, or they can be of value in comparing how the load exceedance curve of one mission compares relatively with that of another. Three cases differing slightly in detailed makeup, but all of which should yield essentially the same load exceedance curves, are described. Specifically, the cases have been tailored so that the exceedance curves would pass through control points which are indicated by equation (25); these control points are given in the following listing:

h, 1000 ft	P	σ_w, fps	$\dfrac{x}{A}$	$\dfrac{N}{N_0} \times 10^8$
0	.0005	6	54	6.17
5	.0005	6.6	59.3	6.17
10	.0005	7.2	64.8	6.17
20	.0005	8.4	75.6	6.17
30	.0005	9.6	86.4	6.17
35	.0005	10.2	91.8	6.17
40	.000257	8.7	78.3	3.17
50	.0000714	5.8	52.2	.882

Basically, a constant value of $\dfrac{x}{\sigma_x} = 9$ was chosen for all the control points.

Case (a).- Suggested generalized load exceedance curves for this case are given by the following equation

$$\frac{N}{PN_0} = .993\, e^{-a_1 \frac{x}{A\sigma_w}} + .007\, e^{-a_2 \frac{x}{A\sigma_w}} \tag{42}$$

where

$$a_1 = \sqrt{.993 + .007\alpha^2}$$

$$a_2 = \frac{a_1}{\alpha}$$

This equation represents a modified and simplified form of Cases k and ℓ presented in reference 2. It is seen to be a function

73

of just three environmental parameters, a proportion of time P, an intensity σ_w, and a shape parameter α, each a function of altitude only. Recommended values of these three parameters are given in figure 29. Basic nondimensional exceedance curves derived from equation (42) using the values of α given in figure 29 are shown in figure 34. The values of α were established so that, using the P and σ_w values shown in figure 29, the exceedance curves would pass through the control points listed at the beginning of this section. The use also of the values of P and σ_w given in figure 33 allows the curves of figure 30 to be converted into the convenient working form shown in figure 31. Steps for establishing the expected load exceedance curve are as follows:

1. Lay out the mission, as in figure 24, and establish the A and N_0 value for each segment through use of equations (15 and (16).

2. Determine the composite exceedance curve through either of the following equivalent expressions

$$ n = P_1 T_1 N_{0_1} f_1\!\left(\frac{x}{A_1 \sigma_w}\right) + P_2 T_2 N_{0_2} f_2\!\left(\frac{x}{A_2 \sigma_w}\right) + \cdots \tag{43} $$

$$ n = T_1 N_{0_1} g_1\!\left(\frac{x}{A_1}\right) + T_2 N_{0_2} g_2\!\left(\frac{x}{A_2}\right) + \cdots \tag{44} $$

where f_1 refers to the curves of figure 30 an altitude appropriate to the segment i, while g_i refers to figure 31. Illustrative load exceedance curves that result from this procedure, and the means for making a design check, if desired, are shown in figure 32. For example, in reference to this figure, if mission A is taken as the design mission, and if the design requirement is stipulated that the number of positive limit load exceedances must not exceed 5 in 30,000 hours of flight, then the curve for mission A for 30,000 hours must be such that it falls on or below the design limit point designated by P, on the figure.

Case (b).- Although not essential, generalized exceedance curves may be constructed through use of the concept of dividing turbulence encounter into two parts, one associated with mild to intermittent intensity levels, a second with severe levels. Because of the popularity of this concept in the past, curves based on this concept are also included here. The specific equation for this case is

$$ \frac{N}{N_\Theta} = P_1 e^{-\frac{x}{A\sigma_1}} + P_2 e^{-\frac{x}{A\sigma_2}} \tag{45} $$

74

The P and σ values that are recommended are given in figures 33 and 34. From these values, the generalized curves of figures 35 and 36 follow, where for figure 35

$$P = P_1 + P_2 \tag{46}$$

$$\sigma_w^2 = \frac{P_1}{P} \sigma_1^2 + \frac{P_2}{P} \sigma_2^2 \tag{47}$$

Again, the generalized exceedance curves are such that they pass through the control points listed at the beginning of this section. The values of P and σ_w as found from equations (46) and (47) are very similar to the values of P and σ_w given in figure 29. Thus, the P and σ_w values of Case (a), figure 29, serve also for use with the generalized curves for this case given in figure 35. Note that the curves of figures 35 and 36 agree substantially with the curves of figures 30 and 31. Expected load exceedance curves for a specified mission are found for this case in the same manner as outlined in Case (a). It is to be noted that the σ_2 and P_2 values of this case are simply the σ_w and P values given in Section VII on design procedures.

Case (c).- This case is included to show that certain properties of generalized exceedance curves are still not known, and further that there is a sensitive relationship between the shape of the curves and turbulence intensity values. Each portion of the curves of figure 35 is derived on the basis that the r.m.s. values of turbulence intensity are distributed according to an equation of the form

$$p(\sigma) = \frac{1}{\sigma_x} \sqrt{\frac{2}{\pi}} \, e^{-\frac{1}{2} \frac{\sigma^2}{\sigma_x^2}}$$

This equation leads to an exceedance curve of the form $e^{-\frac{x}{\sigma_x}}$, illustrated by curve a in figure 37; the curve was readily accepted and became popular mainly because of the ease of handling the simple exponential form. There is evidence, however, that the $p(\sigma)$ distribution may be more in the form of a Rayleigh-type distribution given by

$$p(\sigma) = 2 \, \frac{\sigma}{\sigma_x^2} \, e^{-\frac{\sigma^2}{\sigma_x^2}}$$

This distribution leads to exceedance curve b of figure 37, see Case h, figure 1, of reference 2; the equation for the curve is

$$\frac{N}{PN_0} = \sqrt{2} \, \frac{x}{\sigma_x} \, K_1\left(\sqrt{2} \, \frac{x}{\sigma_x}\right) \tag{48}$$

75

It is noted that experimental data often exhibit the convex shape noted in the b curve for low values of the abscissa, thus adding substance to the thought that the $p(\sigma)$ distribution leading to b might be more realistic. With the use of equation (48) an equation analogous to equation (42) may be written as follows

$$\frac{N}{PN_0} = .993\sqrt{2}\ a_1 \frac{x}{A\sigma_w} K_1\!\left(\sqrt{2}\ a_1 \frac{x}{A\sigma_w}\right) + .007\sqrt{2}\ a_2 \frac{x}{A\sigma_w} K_1\!\left(\sqrt{2}\ a_2 \frac{x}{A\sigma_w}\right)$$

$$(43)$$

where also

$$a_1 = \sqrt{.993 + 007\alpha^2}$$

$$a_2 = \frac{a_1}{\alpha}$$

Exceedance curves given by equation (49) and the values of α from figure 29 are shown in figure 38. These curves may be used in the same manner as for Cases (a) and (b) but they call for the use of different σ values, specifically those recommended in figure 39. The P values remain the same as given in figure 29. With the σ value of figure 39 and the P values of figure 29, curves quite similar to those shown in figures 31 and 36 result. Thus, the difference in shape of the curves of figure 38 relative to the curves of figures 30 and 35 is compensated for, to a large extent, by the increased σ values.

Stationary aspects.- Some comments relative to the stationary properties of gust encounter are given to close this section. The treatment given in reference 2 indicated that generalized exceedance curves could be derived whether the r.m.s. value of the gusts was stationary or not (see discussion associated with equation (11) in reference 2). It may be of interest to demonstrate the construction of a gust response model that is implied by the generalized exceedance curves, which shows a stationary property with respect to N_0 . Consider gust encounter in terms of the discrete patch concept as depicted by the top sketch in figure 40; in general, the r.m.s. and N_0 values are different in each patch. (The t_i values are assumed to correspond to the $P_i T_i$ values used elsewhere in this report.) Various relations associated with the response shown are

$$t = t_1 + t_2 + t_3$$

$$tN_0 = t_1 N_{0_1} + t_2 N_{0_2} + t_3 N_{0_3}$$

$$\sigma_x^2 = \frac{1}{t}\!\left(t_1 \sigma_1^2 + t_2 \sigma_2^2 + t_3 \sigma_3^2\right)$$

$$(50)$$

76

$$n = t_1 N_{0_1} f_1\left(\frac{x}{\sigma_1}\right) + t_2 N_{0_2} f_2\left(\frac{x}{\sigma_2}\right) + t_3 N_{0_3} f_3\left(\frac{x}{\sigma_3}\right) \qquad (51)$$

If the equation for n is multiplied by x and integrated, in accordance with equation (14) of reference 2, then the following result for σ_x is indicated

$$\sigma_x^2 = \frac{1}{tN_0}\left(t_1 N_{0_1} \sigma_1^2 + t_2 N_{0_2} \sigma_2^2 + t_3 N_{0_3} \sigma_3^2\right) \qquad (52)$$

This result appears to contradict the value given by equation (50). Equation (52), however, has a meaningful interpretation. Assume the time scale of each patch is expanded or contracted so that the N_0 value for each patch is the same, specifically N_0. The change is easily made by the transformation

$$t_1' = \frac{N_{0_1}}{N_0} t_1$$

The transformed system is depicted by the bottom sketch of figure 40. It is noted that the transformation does not change the r.m.s. value of each patch, nor does it change the peak count of the record. The mean square value of the new system, however, is changed and is precisely that given by equation (52). It is thus seen that the construction of exceedance curves in the format given by equations (43) or (51) and use of a mean square definition given by equation (14) of reference 2 effectively converts the response record into one which is stationary with respect to N_0. Generally, there will be little difference between the r.m.s. values given by equations (50) and (52). Equation (50) rather than equation (52) was therefore adopted as the basis for establishing the composite r.m.s. values of Section VII (equation (38)), since it is somewhat easier to evaluate.
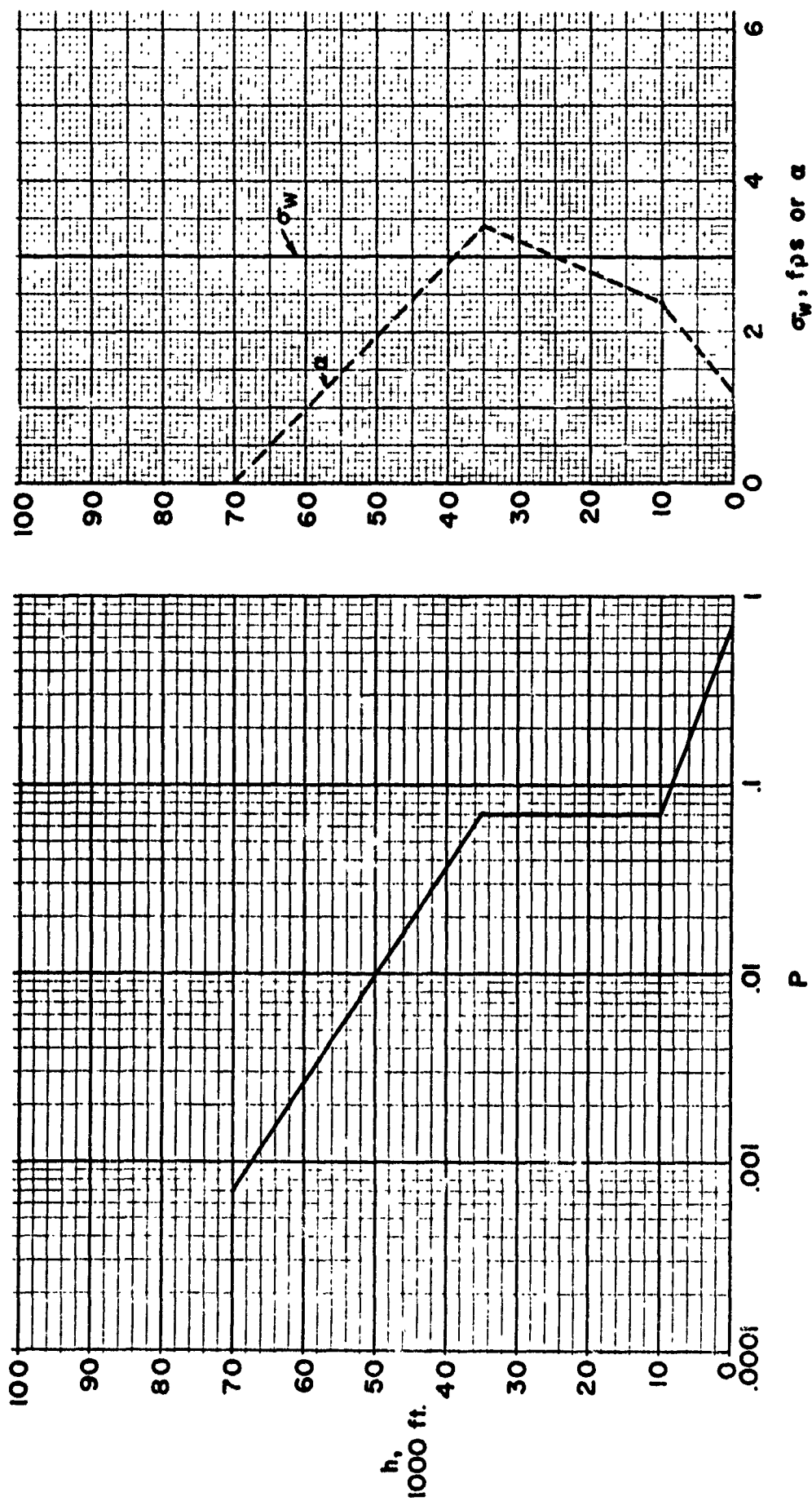
Figure 29.   P , σ_w , and α Values Recommended for Case (a)

Figure 30. Generalized Exceedance Curves for Case (a)

79
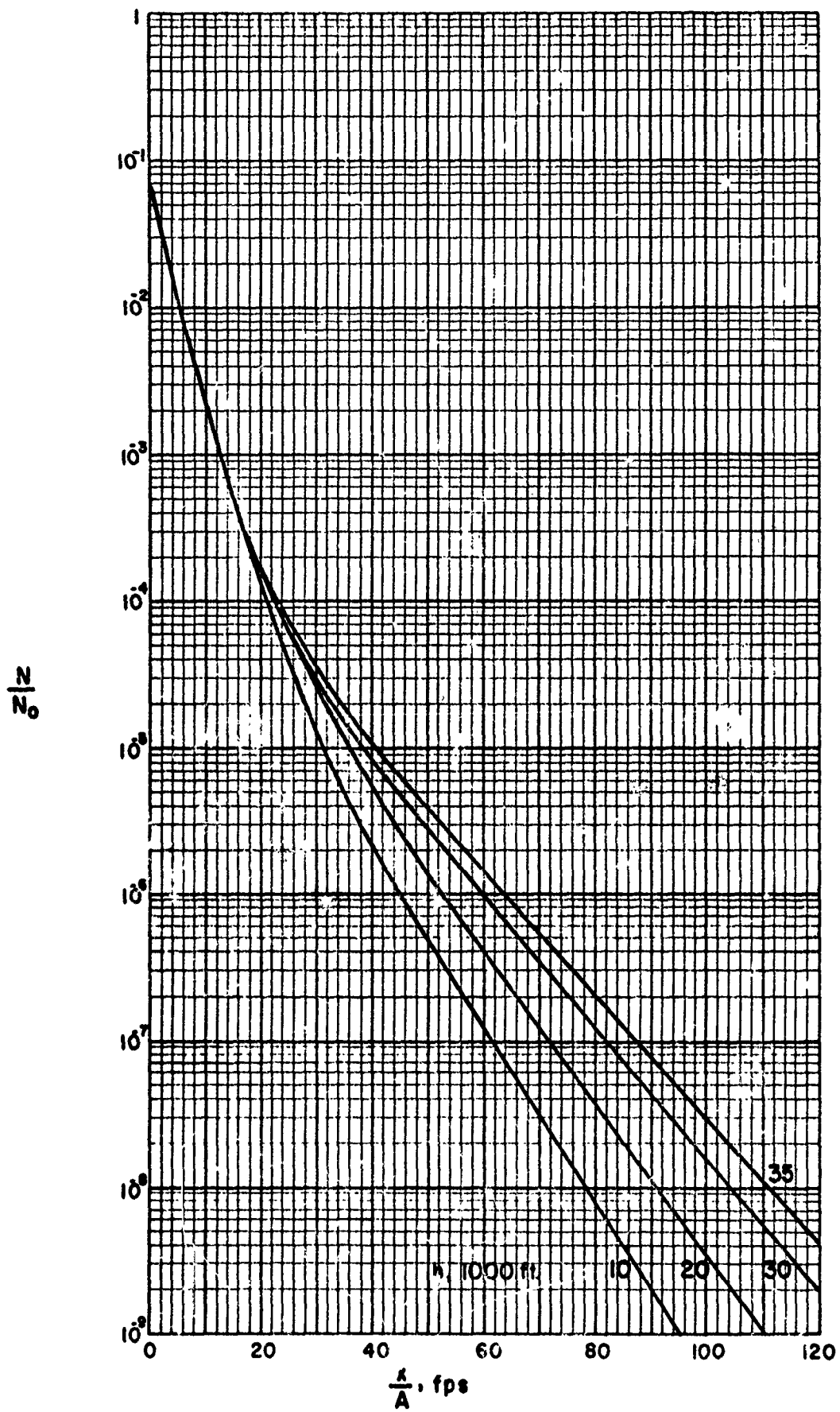
Figure 31. $\frac{N}{N_O}$ vs. $\frac{X}{A}$ Curves for Case (a)   80

Figure 31. (Concluded)   81

Figure 32. Illustrative Load Exceedance Curves Obtained
by Mission Analysis

82
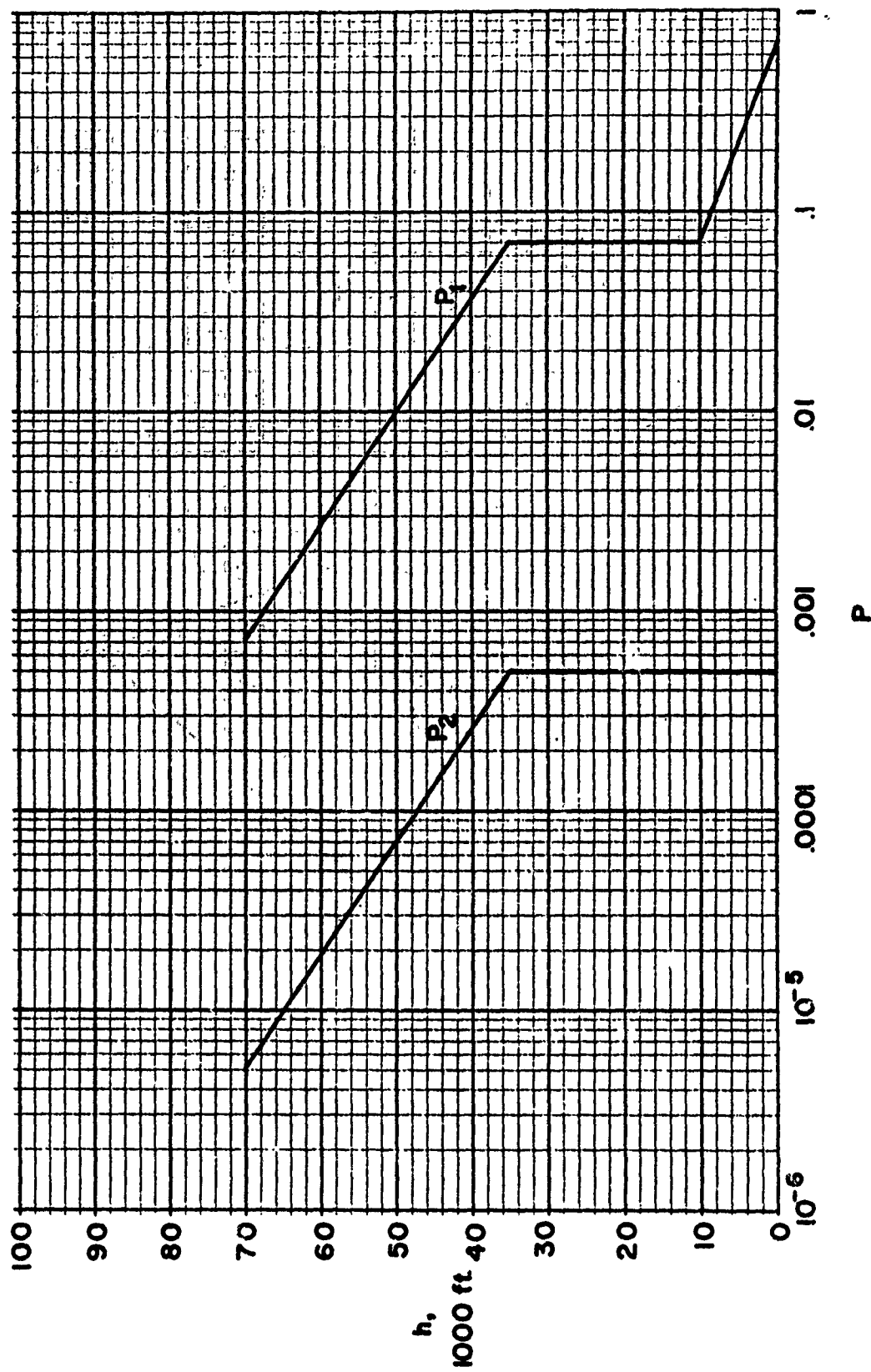
Figure 33.   P   Values for Case (b)

83

Figure 34.   σ   Values for Case (b)
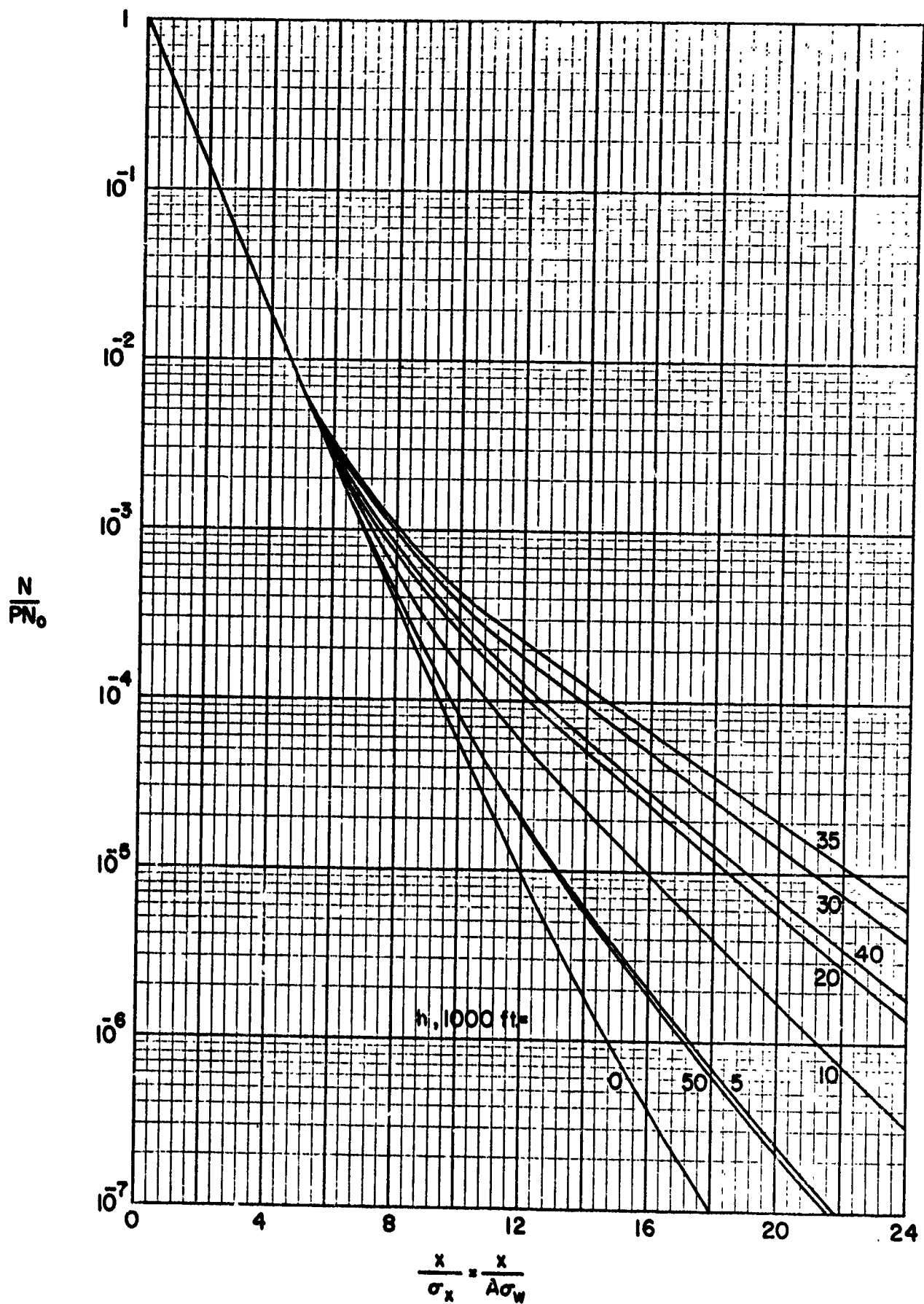
Figure 35. Generalized Exceedance Curves for Case (b)

85

Figure 36. $\frac{N}{N_o}$ vs. $\frac{x}{A}$ Curves for Case (b)

86

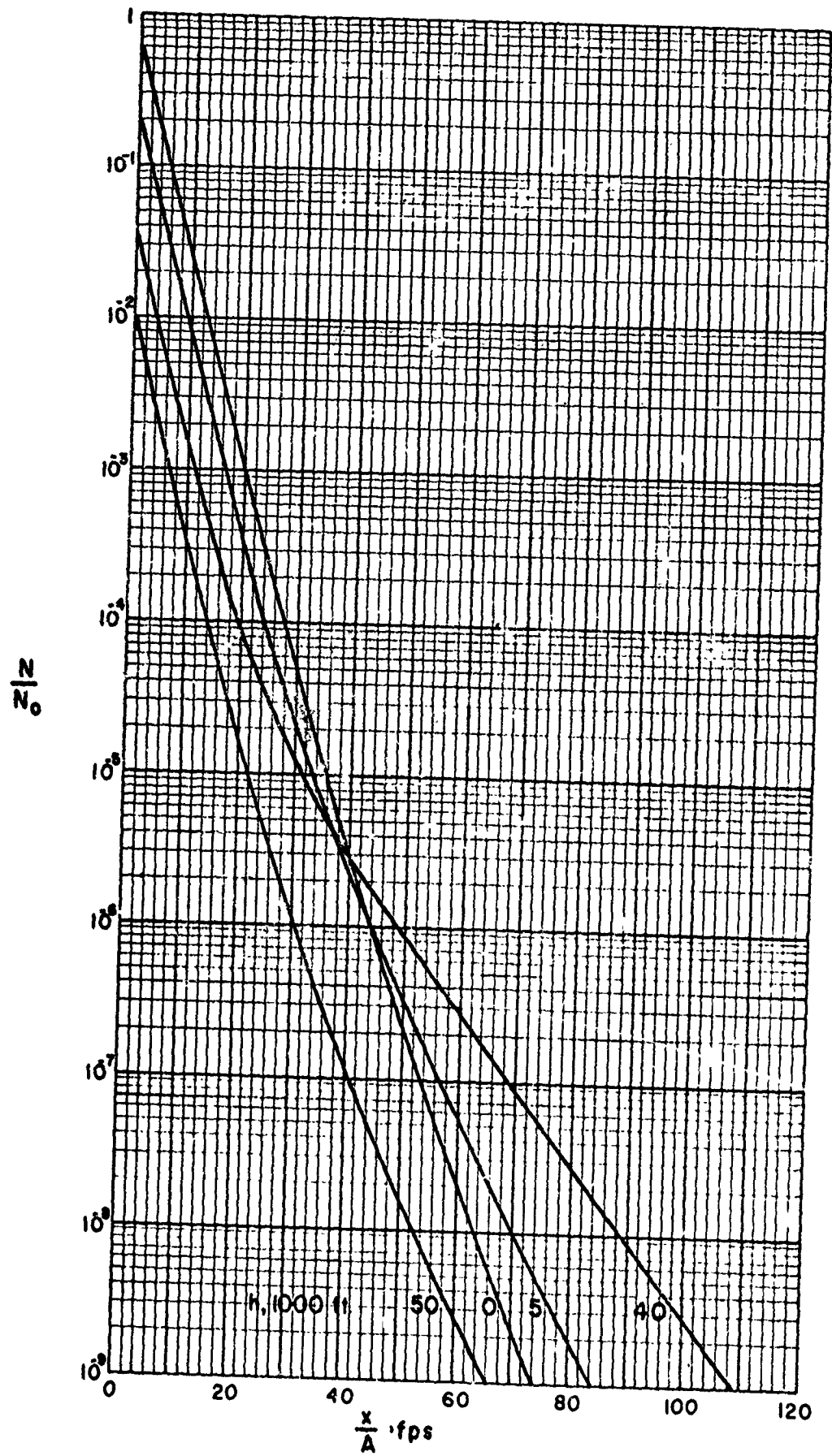Figure 36. (Concluded)
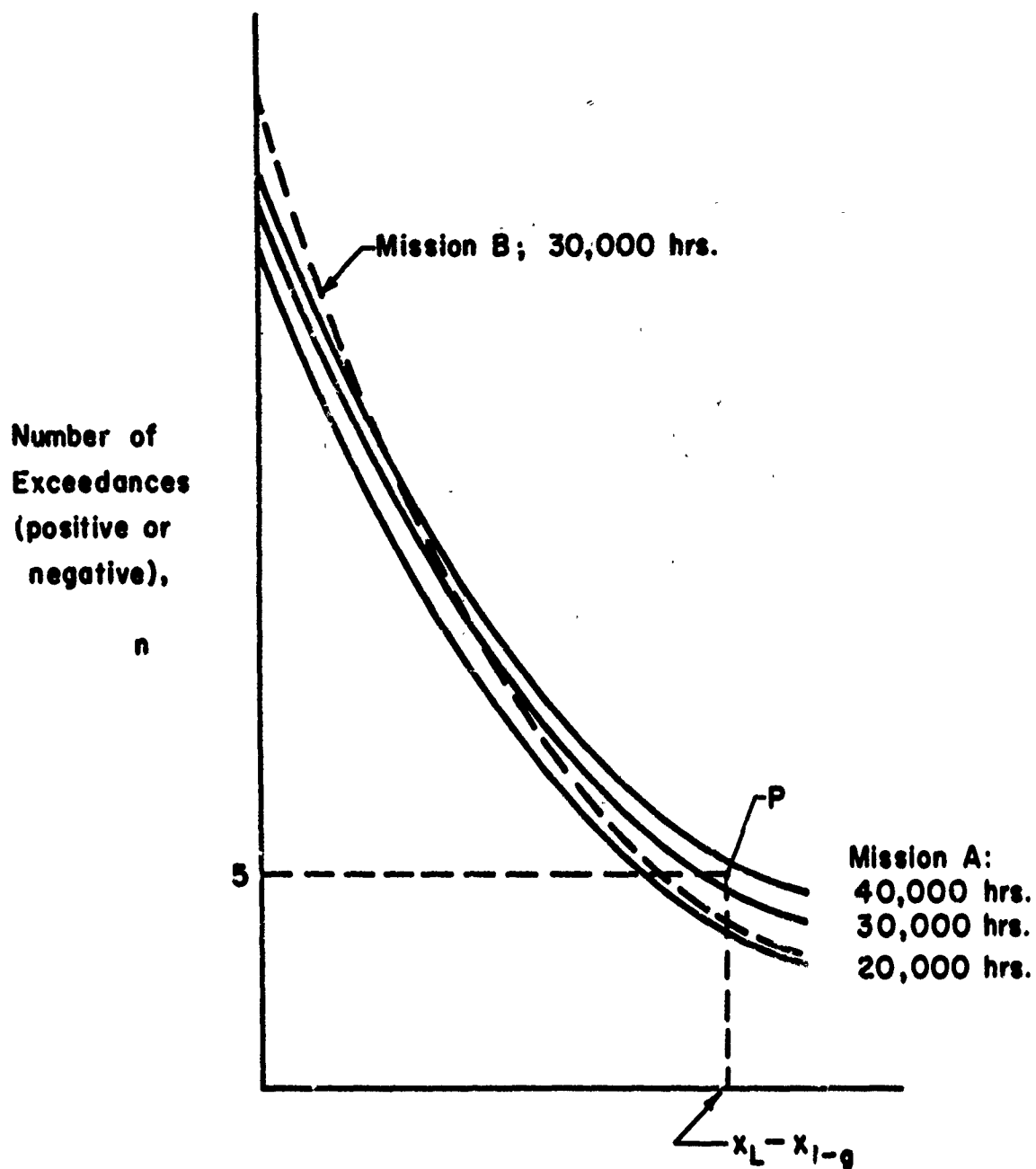
87

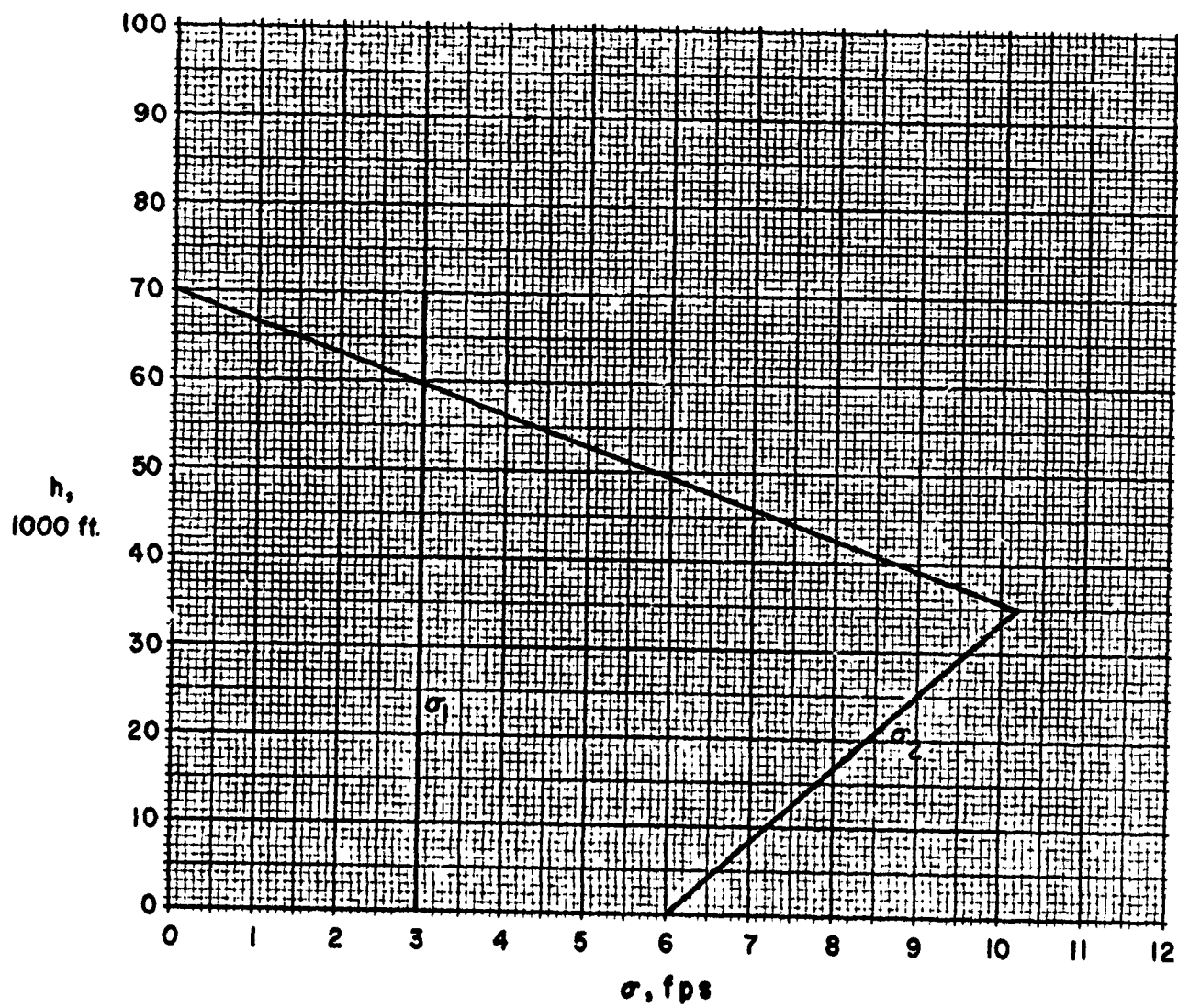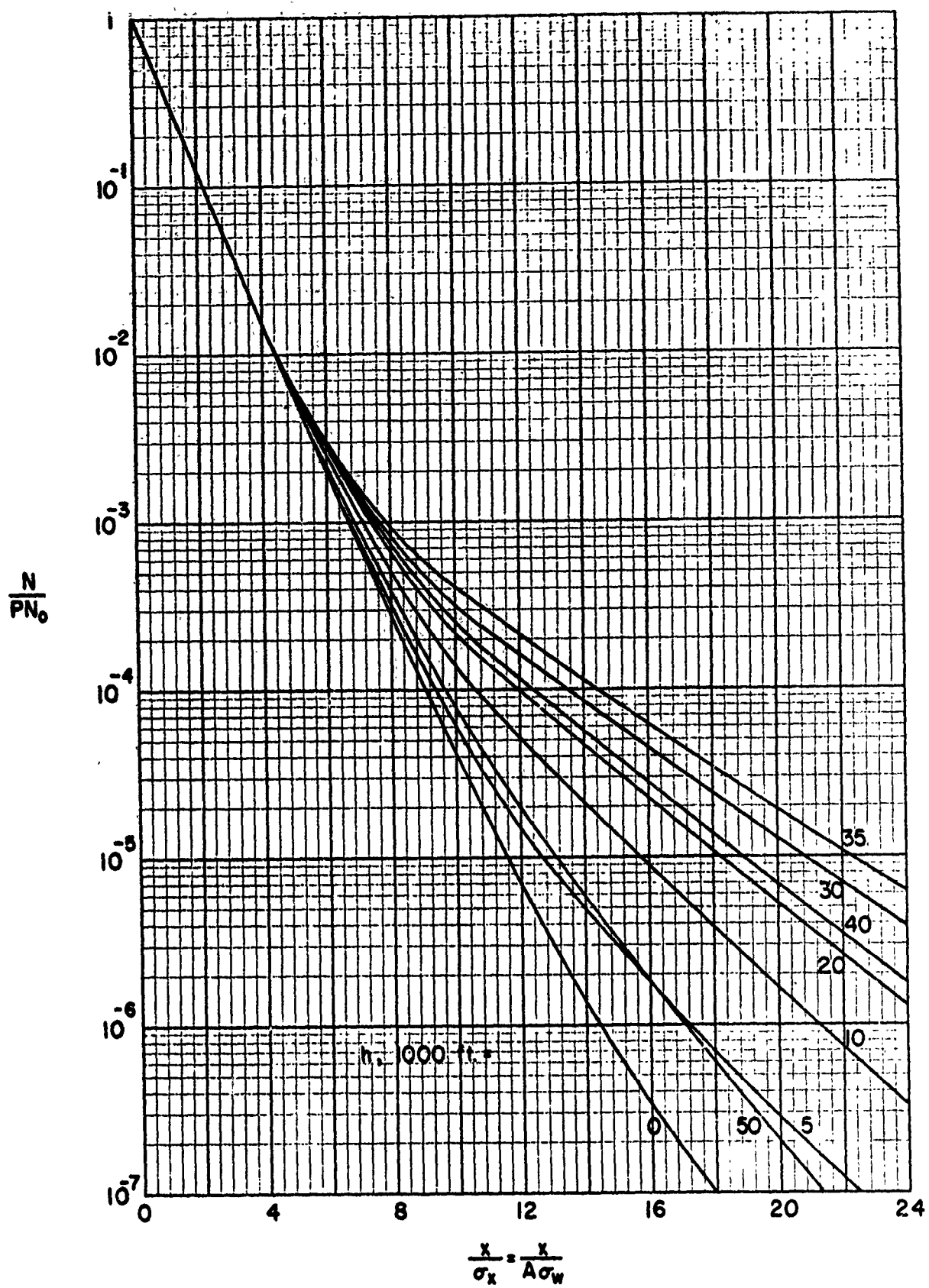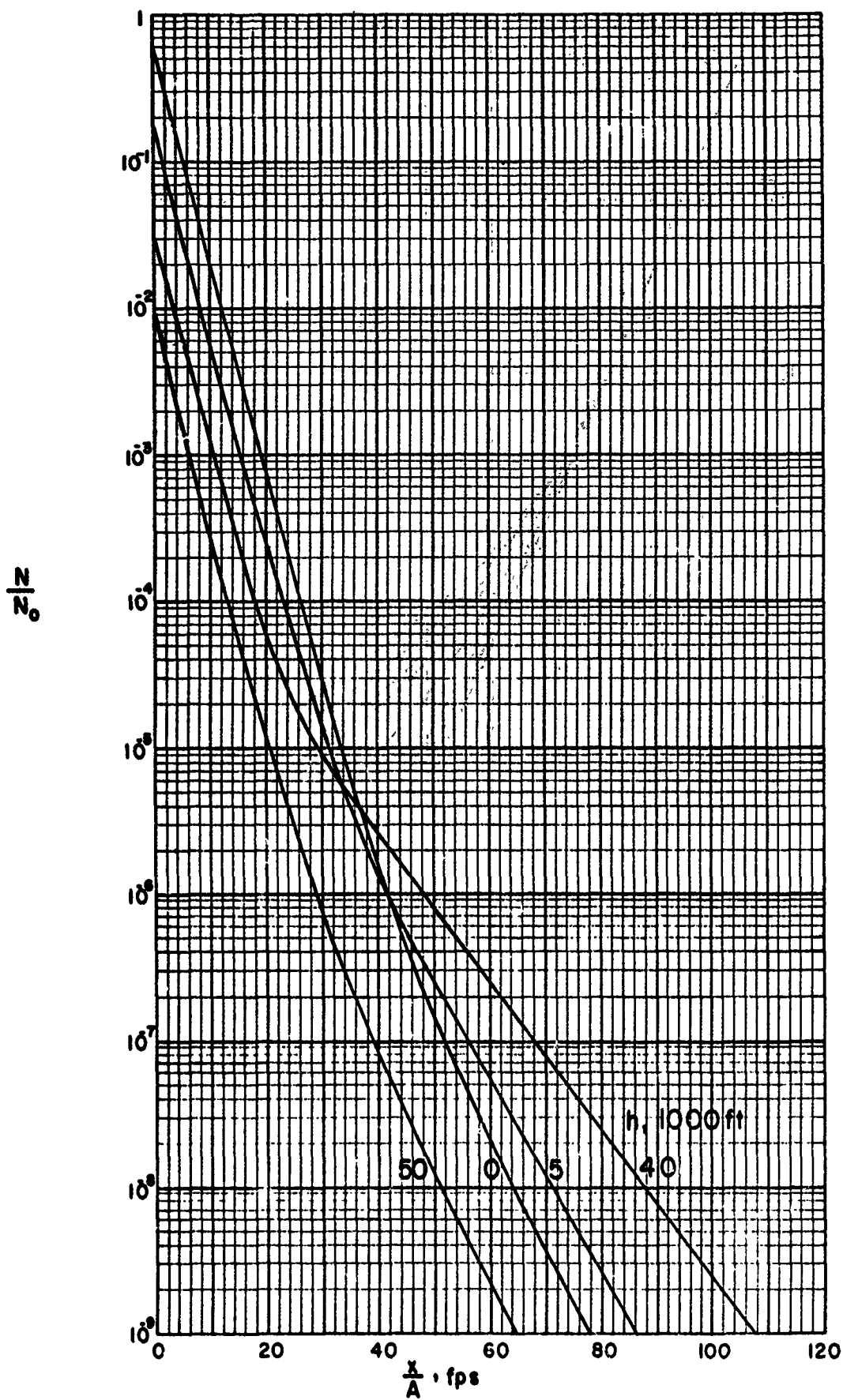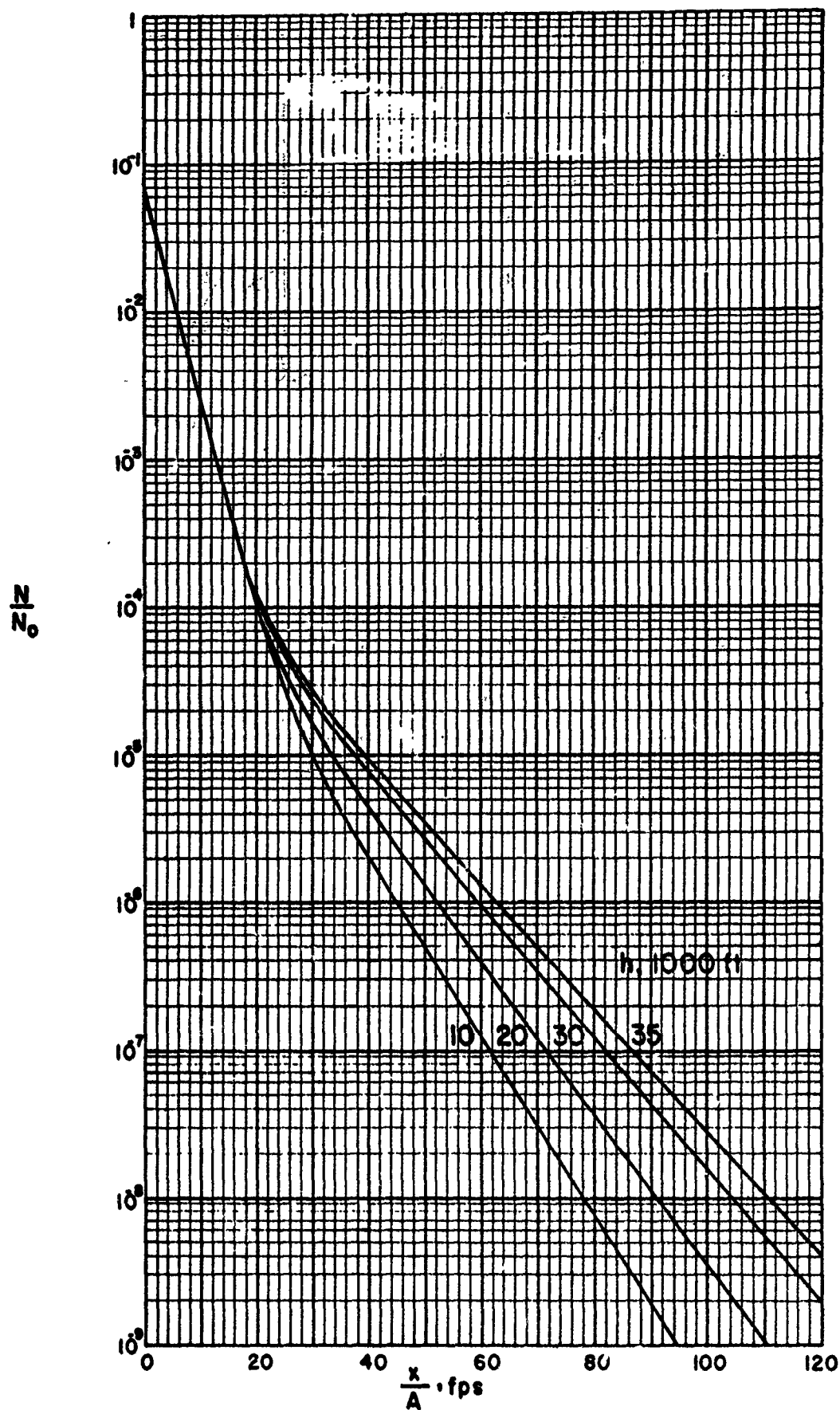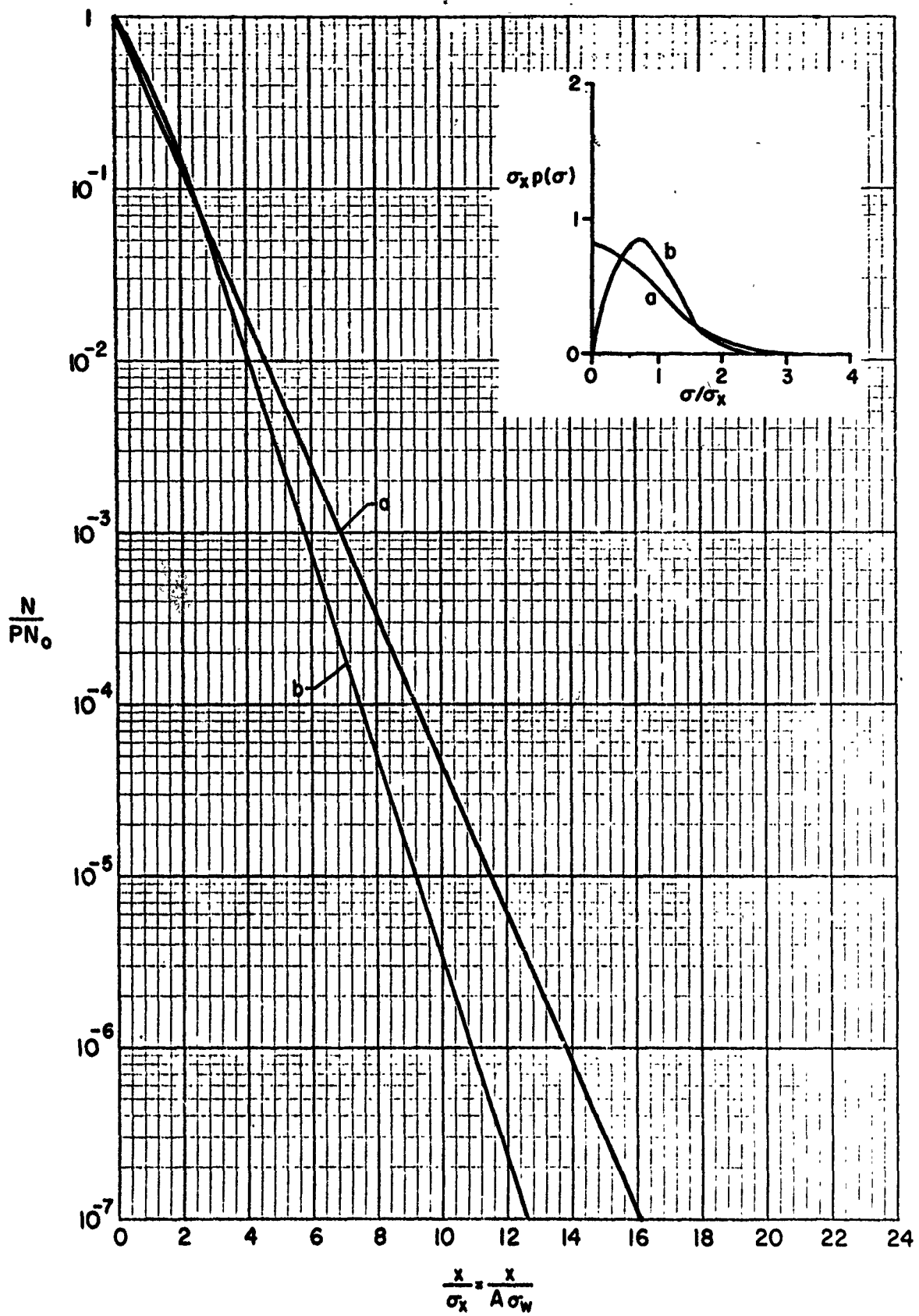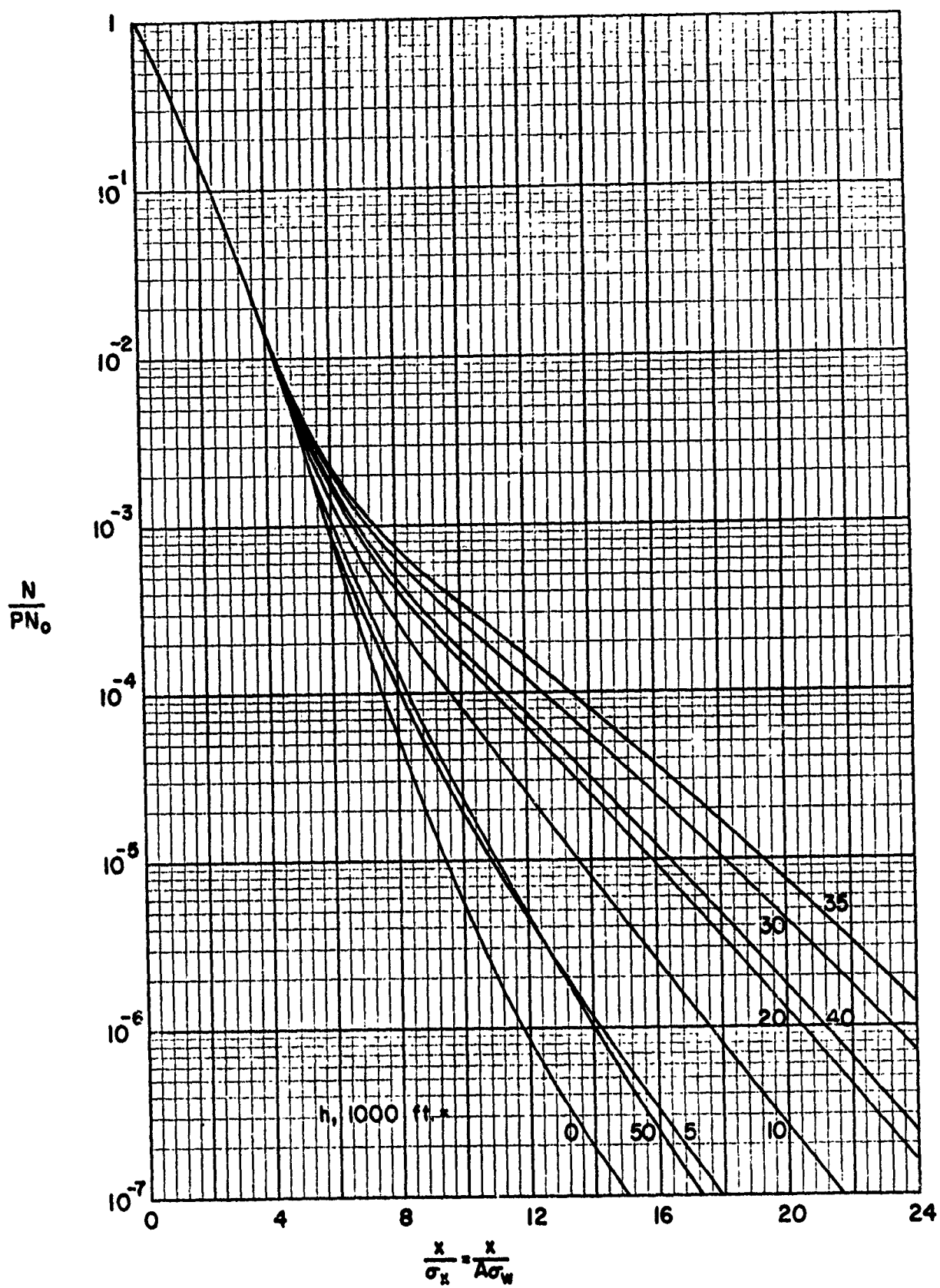Figure 37. Influence of $p(\sigma)$ on Exceedance Curves

88

Figure 38.   Generalized Exceedance Curves for Case (c)

89
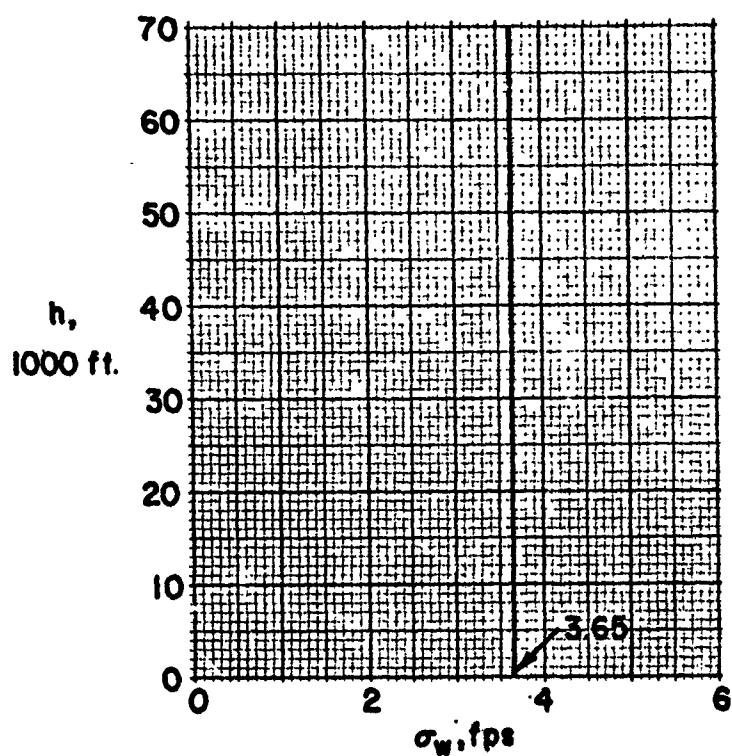
Figure 39. σ_w Values for Case (c)
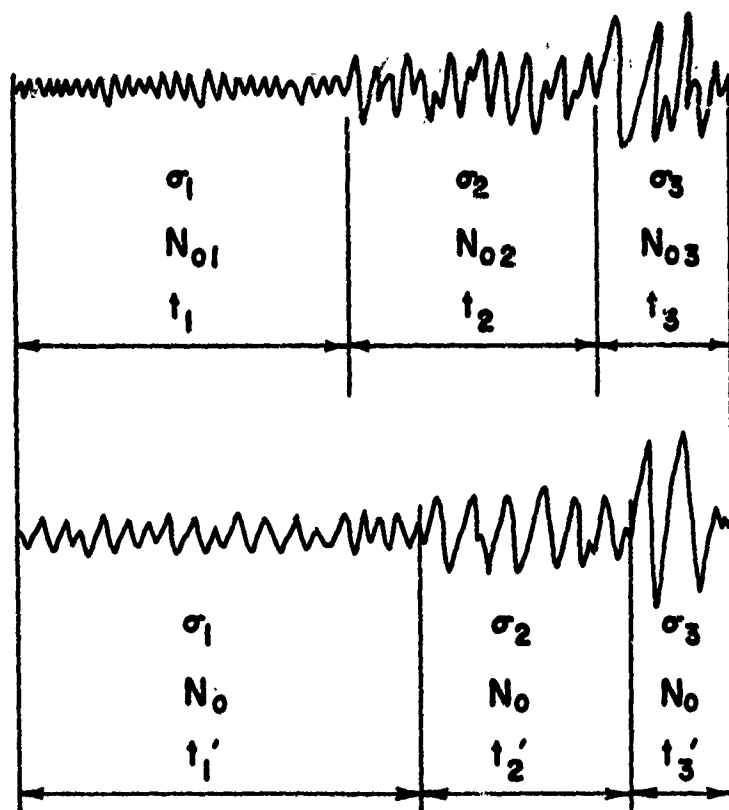
Figure 40.   Record Conversion to Stationary N_o

SECTION IX

SPECTRAL VS. DISCRETE-GUST DESIGN

The concern of some is that while spectral approaches to the gust problem may be appropriate in many respects, they may not be so in certain respects relative to the discrete-gust design method. One concern is that the spectral approaches are more involved computationally; another is that the spectral approach may not include the consideration of the severe isolated-type gust that seemingly is encountered on occasions. The purpose of this section is to show that the spectral approaches of this manual effectively obviate both of these concerns. Indeed, particular note should be taken of the fact that the preliminary procedure recommended herein is quite equivalent to the discrete-gust method; it is just as simple, has the same basic steps, but at the same time includes in better fashion inherent dynamic-behavior effects of the airplane.

It should be noted that in the discrete-gust approach, the choice of the 1-cosine gust has really no sound basis. A sine gust, a triangular gust, or even a rectangular gust would serve as well. Thus, the representation of gust encounter by a single type gust is quite an arbitrary matter. It would seem that the question of "gust shape" in the discrete-gust approach poses just as great a problem as is involved in deciding whether the gusts should be random or of discrete shape.

For most gust encounter there is little doubt that the process is continuous and random. Spectral analyses are thus appropriate. It may be asked, however, whether the spectral approach includes the effects of large isolated gusts, assuming they do exist. The intent of the analysis leading to equation (11), reference 2 is to take into account such possibilities. Thus, if the function g used in this equation is chosen properly and contains the information relative to the large gusts, then these gusts should be reflected in the peak count curve. Further, gust intensity values out to infinity are usually considered (for mathematical convenience) in the derivation of the exceedance curves. The tail portion of the exceedance curves, thus, introduces extreme intensities, even though they do not exist in practice. The effect on the exceedance curves of placing a finite upper limit on the gust intensity that can be encountered is shown in the section on ultimate load (Section X).

Some of the thoughts of the preceding paragraph may be illustrated more specifically by the following analysis which is intended to show that the preliminary spectral approach given herein is quite comparable to the discrete approach. The acceleration given by the discrete approach is

$$\Delta n = \frac{a \rho S V}{2W} K_g U_{de}$$

Multiply equation (22) by η to obtain

$$\eta\sigma_{\Delta n} = \frac{a\rho SV}{2W} K_\phi \eta\sigma_w = A\eta\sigma_w$$

Consider now that $\eta\sigma_{\Delta n}$ equals Δn , then these two equations yield

$$\frac{K_g}{K_\phi} U_{de} = \eta\sigma_w$$

A spectral velocity value $\eta\sigma_w$ is thus established that may be considered to assume the same role in the spectral approach as does U_{de} in the discrete-gust approach; that is, the multiplication of $\eta\sigma_w$ by the spectral value of A yields the same acceleration as does the discrete-gust approach. Values of $\eta\sigma_w$, as obtained from this relation and the K_ϕ values of figure 16 are shown in figure 41. using $U_{de} = 50$ fps . This plot yielded part of the information that was used to establish the design values of this manual, such as shown in figures 23 and 25. Specifically, a value of $\eta\sigma_w = 54$ was chosen for design at sea level. Other values of η that are implied herein may be found from this choice by considering the various values for σ_w that are specified in this report for $h = 0$. Note values at $h = 0$ are used so as to place σ_w on comparable terms with U_{de} since σ_w is true, while U_{de} is an equivalent gust velocity. Based on the $\sigma_w = 3$ value given in figure 29, the choice of $\eta\sigma_w = 54$ indicates a value of $\eta = 18$; with reference to the $\sigma_w = 6$ value (h = 0) of figure 21, the value which is critical for design at sea level, a value of $\eta = 9$ is indicated, in agreement with the value of x/σ_x that is included in the combination of numbers listed in the introductory remarks of Section 7.
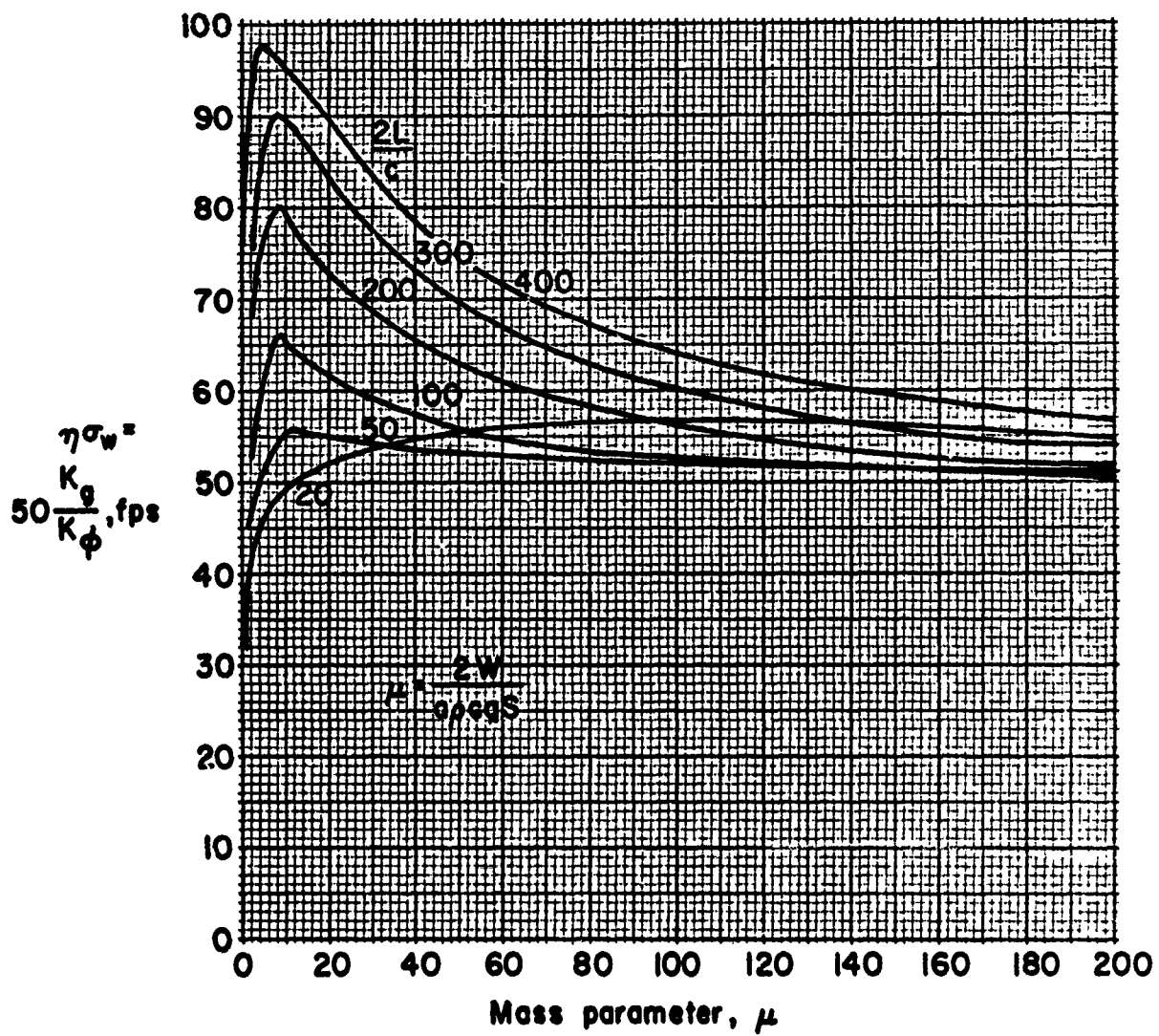
Figure 41.   Spectral "Velocities" Equivalent to the
Discrete-Gust Design Velocity

93

SECTION X

VIEWS ON ULTIMATE LOAD DESIGN

Gust design loads associated with limit load levels are recommended herein; gust design in terms of ultimate loads is not. The main reason is because of the large uncertainty of the load exceedance values in the region of ultimate load levels. With the presently available exceedance curves, there is still some uncertainty in the range of limit load values (x/σ_x = 18 to 30), and the uncertainty becomes ever increasing for load levels that extend out to the ultimate load range (x/σ_x = 27 to 45 , on the assumption that ultimate strength levels are 1.5 limit strength). In fact, data on load exceedance in the ultimate load range are virtually nonexistent.

The marked sensitivity of the load exceedance curves in the region of large load levels can be demonstrated by studying the influence of various finite limits on representative joint-probability distribution functions for gust encounter. Specifically, a study of the effect of using a finite upper limit in equation (11a) of reference 2 is pertinent. Normally, exceedance curves, as established in reference 2, are derived on the assumption that the values of x and $\dot{x}$ in the joint distribution function are unbounded; that is, they extend to infinity. This assumption, of course, is not realistic. Nature, itself, seems to have a self-limiting process on the maximum gust velocity that can develop. If this value is, say, 300 fps , and if the overall r.m.s. value of turbulence encounter is 3 fps , then it would appear that x/σ_x cannot ever be larger than 100 . Other limiting processes also enter. For example, a gust velocity of 100 fps may cause the airplane to stall. Thus, the maximum load-producing velocities may be limited to 100 , indicating a maximum value of $x/\sigma_x \cong 30$.

To study how the tails (or absence of tails) of the joint-distribution curve affect the exceedance curves, equation (11) of reference 2 was used in conjunction with some of the joint distribution curves also given in that reference, with the restriction that the equation applied only within the region defined by

$$\frac{x^2}{\sigma_x^2} + \frac{\dot{x}^2}{\sigma_{\dot{x}}^2} \le R^2$$

Outside of this limit, p was taken as zero. It was found that the exceedance curves so obtained could be approximated with good accuracy by simply subtracting a constant value from the exceedance curves that were derived with an upper limit of infinity. The constant is chosen simply as the value of the unbounded exceedance curve at the abscissa equal to the upper limit bound of x/σ_x = R; the value of the bounded exceedance curve thus approaches zero as the limit R is approached. Some results associated with the exceedance curves of Case (c), figure 30, are shown in figure 42. In the region of large x , it is seen that the exceedance

values are very sensitive to the cutoff value R . It may be observed that the curves for finite R are more realistic than the curves for $R = \infty$, since the concept of a joint-probability distribution, confined to within a finite region, is probably more realistic of nature. There is no way to ascertain, however, which of thé curves, if any, most closely represent realistic behavior. This large uncertainty, then, is one of the reasons why it is felt appropriate to avoid ultimate load design concepts.
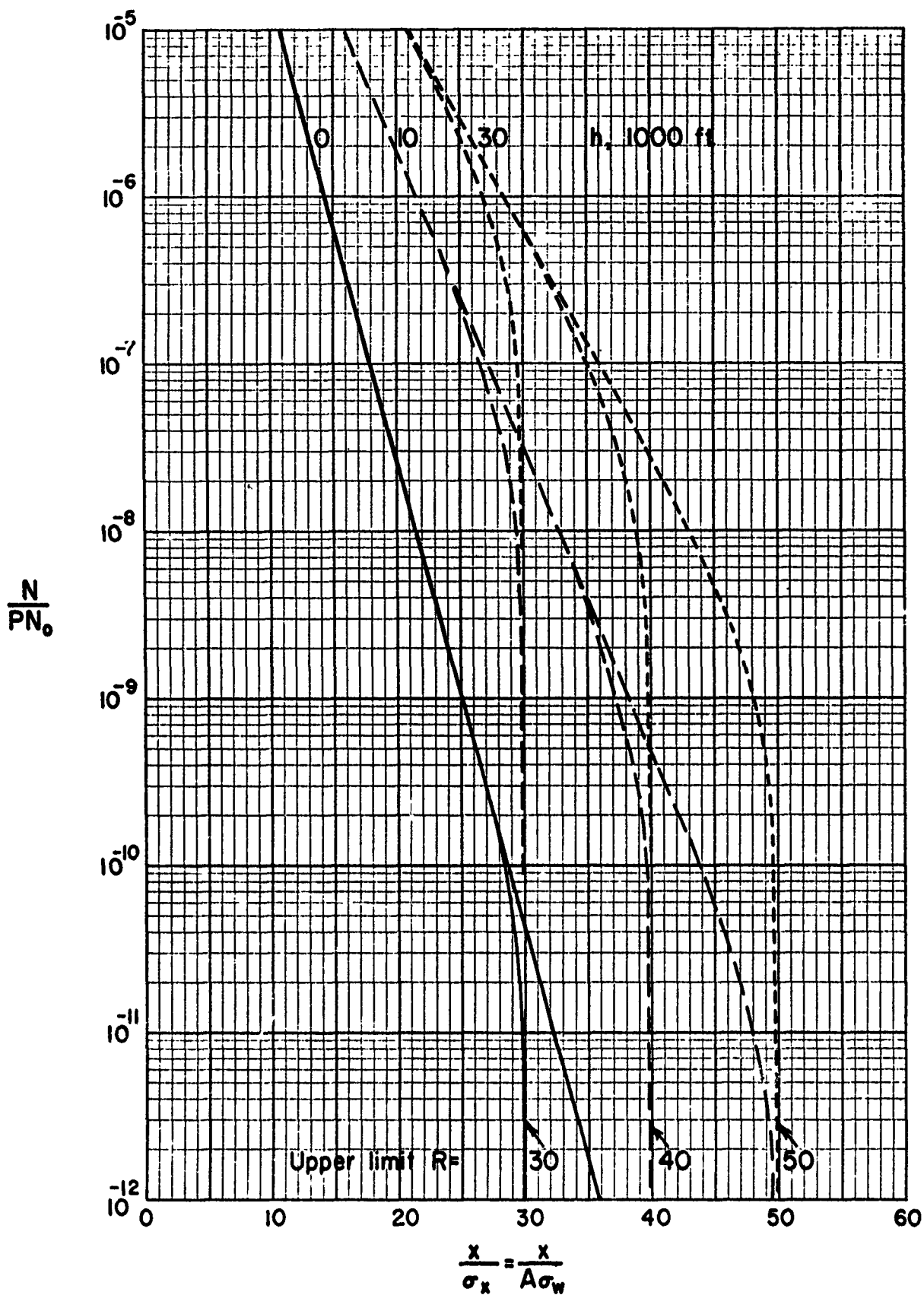
Figure 42. Effect of Bounded Joint Distribution
on Exceedance Curves

97

SECTION XI

STRUCTURAL INTERACTION EFFECTS

Previous sections of this manual have dealt mainly with response quantities that can be treated in an independent or separate manner. Often, however, a structural component is designed by loads or stresses which act in combination. The manner of handling such situations is described in this section. There are two basic combined loads problems; each will be treated separately.

Stresses due to superposition.- Reference 4 indicates the means for handling this case. In summary, the stress at a critical point in the structure may be due to several loads that act simultaneously, for example

$$s = a_1 M(t) + a_2 V(t) + a_3 T(t)$$

where M , V , and T refer to moment, shear, and torque, respectively. The proper way to handle this case is to establish the frequency response function for s , thus

$$H_s(\omega) = a_1 H_M(\omega) + a_2 H_V(\omega) + a_3 H_T(\omega)$$

This frequency response function is used to establish the power spectrum

$$\phi_s(\omega) = |H_s(\omega)|^2 \phi_W(\omega)$$

Treatment thereafter is in the same manner as for an individual stress. By this approach, all phase relationships between the moment, shear, and torque will be taken into account automatically.

Combined stresses by interaction.- A general treatment of combined stresses by interaction is given in reference 5. Only a summary of some of the simplified aspects of the treatment will be given here. If a design check fails to meet the tests that are outlined herein, then recourse should be made to the more detailed procedures given in reference 5.

Consider that a structural element is under the action of two stresses, such as an axial stress and a shear stress, and that the integrity of the element is governed by an interaction curve in terms of these two stresses. The problem is to find the expected number of crossings of the interaction border. Figure 43 illustrates the case.

Steps for making a simplified solution based on using an approximating elliptical interaction curve are as follows:

1. As in the preliminary approach, decide on the critical flight conditions.

2. By equations (8) to (15) compute σ_s , σ_τ , $\sigma_{\dot{s}}$, $\sigma_{\dot{\tau}}$, ρ , and ν ; note, for convenience choose $\sigma_W = 1$.

99

3. By the sequential graphical construction shown in figure 44, establish:

a) σ_{s_m} , σ_{τ_m} and ϕ_0 from σ_s , σ_τ , and ρ; since $\sigma_w = 1$ was used in step 2, then $A_{s_m} = \sigma_{s_m}$ and $A_{\tau_m} = \sigma_{\tau_m}$ (top sketch).

b) $\sigma_{\dot{s}_0}$, $\sigma_{\dot{\tau}_0}$ and ν_0 from $\sigma_{\dot{s}}$, $\sigma_{\dot{\tau}}$, ν , and ϕ_0 of step 3(a) (middle sketch).

c) s_a from σ_{s_m} , σ_{τ_m} , $\sigma_{\dot{s}_0}$, $\sigma_{\dot{\tau}_0}$ and ν_0 of steps 3(a) and 3(b) (bottom sketch).

4. Refer to figure 45. Through origin of s , τ axes, which is located at the 1-g load point, draw s_m and τ_m axes; the direction of rotation from s to s_m is the same as the direction of rotation of diameter A-B in figure 44 to the σ_{s_m} and σ_{τ_m} values. Establish ellipses on the s_m , τ_m axes according to the equation

$$\frac{s_m^2}{z^2 A_{s_m}^2} + \frac{\tau_m^2}{z^2 A_{\tau_m}^2} = 1$$

for various values of z .

5. Choose the largest ellipse which just begins to exceed the boundaries set by the interaction curve and note the value for z for this ellipse.

6. From σ_{s_m} , σ_{τ_m} , of step 1, and from s_a of step 3, determine N_0 by the equation

$$N_0 = \frac{1}{2\pi} \frac{s_a}{\sigma_{s_m} \sigma_{\tau_m}}$$

7. With the value of z established in step 5, the value of N_0 of step 6, the $\sigma_{\cdot}$ and P values of figures 21 and 22, and a chosen time of flight T , establish the number of expected exceedances by the equation

$$n = 1.596 \ PTN_0 \sqrt{\frac{z}{\sigma}} \ \rho^{-\frac{z}{\sigma}}$$

This equation represents the approximation of equation (38), $n = 1/2$, of reference 5, for large z .

100

8. Judge whether the value for n obtained in step
   7 is acceptable; the acceptable value of n depends,
   of course, on the nature of the interaction curve -
   whether it is a strength-type boundary, a buckling
   boundary, or some other form. If n is judged too
   large, proceed to step 9.

9. If n of step 7 is judged to be too large, then
   proceed as follows:

   a) In terms of the elliptic boundary approach
      described in the previous steps, re-evaluate n
      by means of a mission segment consideration
      similar to that given in the section on detailed
      design considerations; that is, use the equation
      in step 7 in a way analogous to that indicated by
      equation (41).

   b) If n as found in (a) is still judged too large,
      then recourse should be made to the detailed
      method of treatment that is outlined in reference
      5, using the given interaction curve, in segmented
      fashion. The use of the elliptic curve approxi-
      mation yields an upper bound; in general, the use
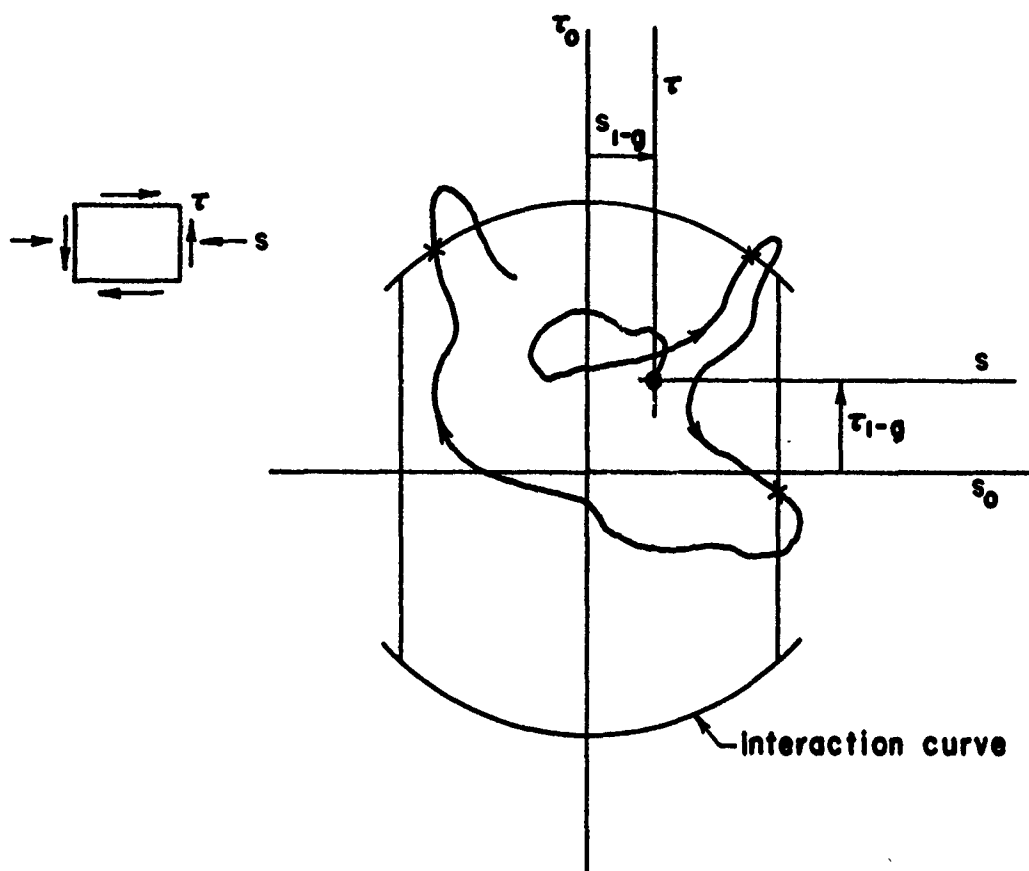   of the actual interaction curve will lead to
      smaller values for n .

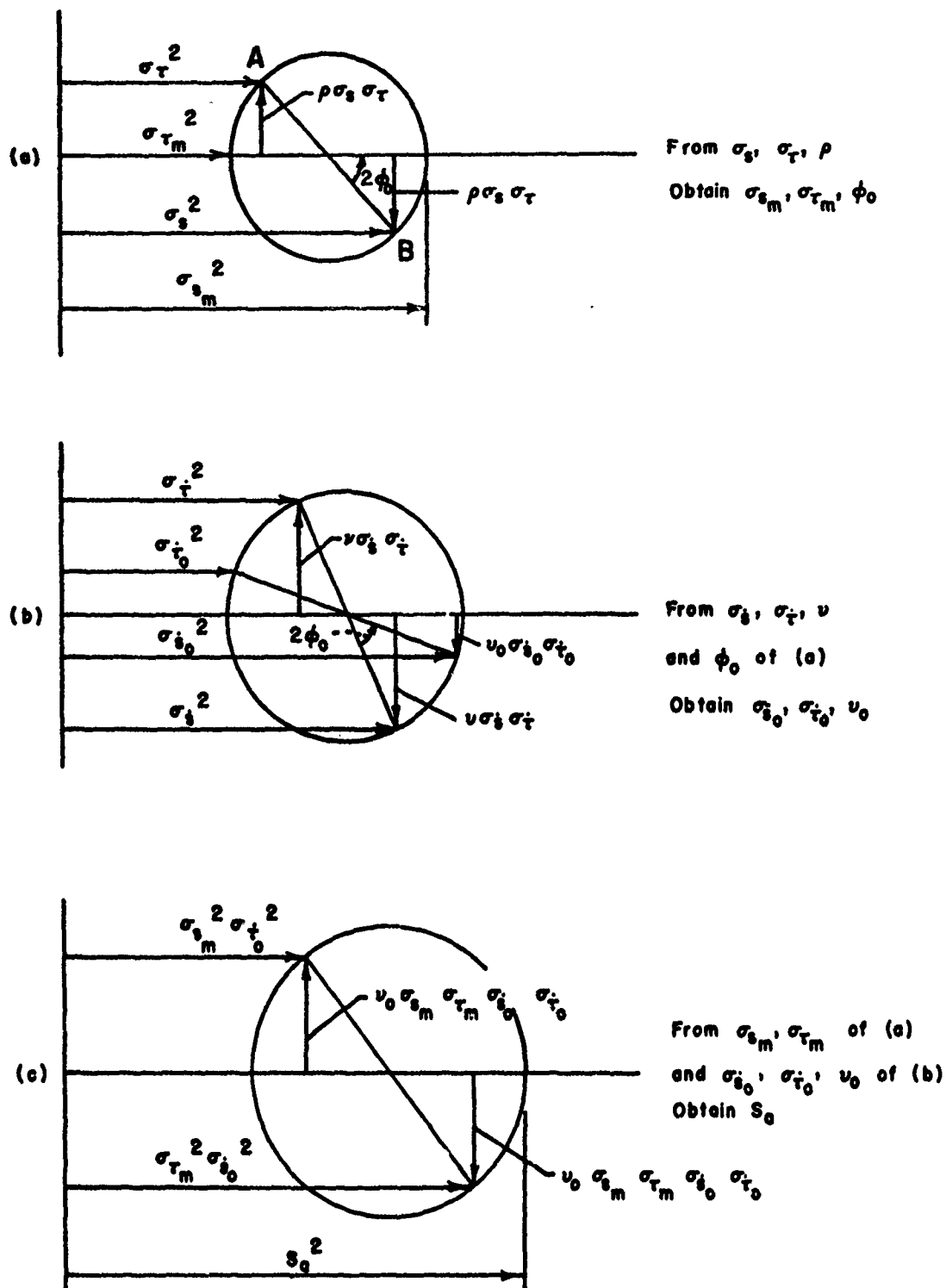Figure 43. Combined Stresses by Interaction

Figure 44. Graphical Construction for σ_{s_m}, σ_{τ_m}, and S_a
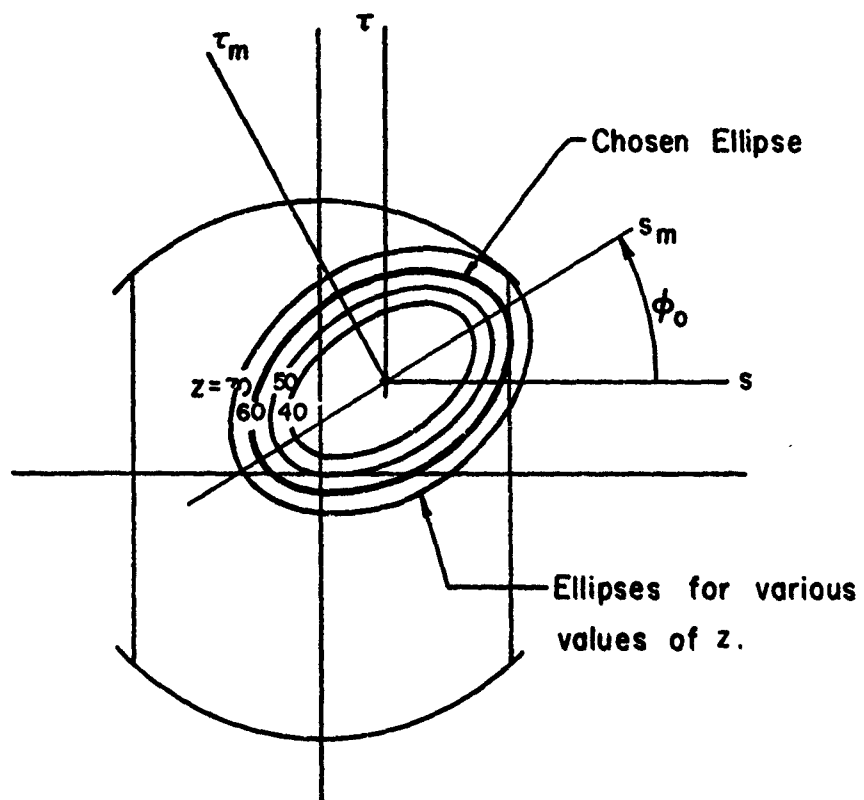
Figure 45. Approximating Elliptical Interaction Boundary

104

SECTION XII

NONUNIFORM SPANWISE GUSTS

This section outlines the means for treating the gust encounter case wherein the gusts are considered random in the spanwise direction, as well as in the direction of flight, as depicted in the following sketch.
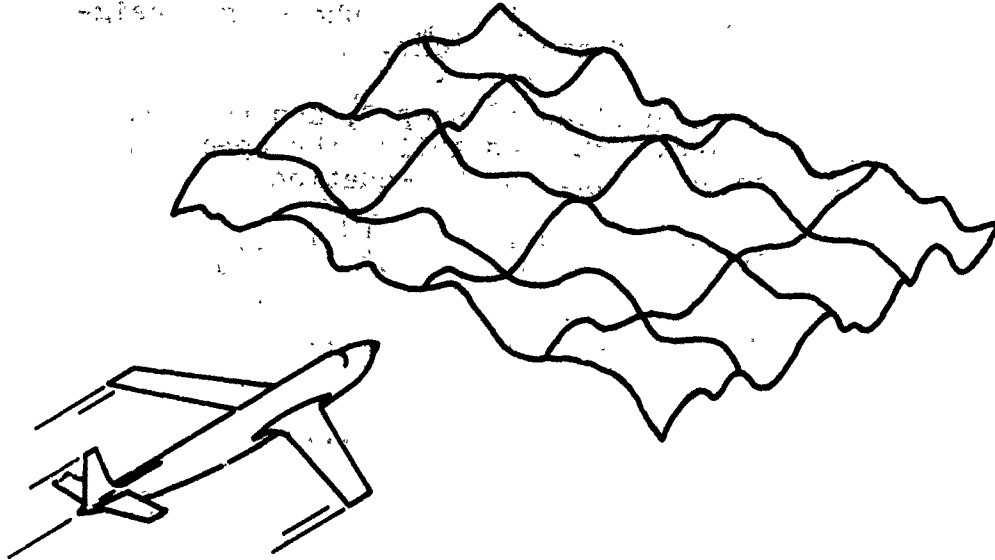
This case may be of significance for large flexible aircraft where the span may become an appreciable fraction of the scale of turbulence. In these circumstances, it is possible for some of the modes, particularly the antisymmetrical and higher frequency modes, to be excited to a much greater extent than they would be in the case of uniform spanwise gusts. The overall response for the completely random gust environment may thus be larger than for the environment which is considered random only in the flight direction.

Detailed consideration of this case is given in reference 29. Essentially, the case is that of a system which is being excited by multiple random inputs rather than by a single one. As such, the cross spectra between the individual inputs must be considered, along with the spectral values of each input. The cross spectra which are of concern here, and which are related to the basic gust input spectrum of this manual, equation (17), have been established by the principal investigator, reference 30 . Some of the basic derived results are shown in figure 46. The means for using these results in gust response calculations is quite straightforward, involving mainly an increase in computational effort. Suggested procedures based on the work of reference 29 are as follows:

1. Divide the wing into equally spaced spanwise segments; from 6 to 10 segments over the span should be adequate for most cases. Suppose the length in the span direction for each segment is designated by ϵ .

2. For each segment, derive the frequency response
    functions for the response variable of concern,
    considering that the sinusoidal gust encounter
    acts only over the segment being treated; this is
    similar to a strip theory-type of treatment, where-
    in each segment is handled separately. Call the
    frequency response function H_m , where m desig-
    nates the number of the segment.

3. With the H_m functions of step 2, and the cross
    spectra of figure 46, establish the spectrum
    for response according to the equation

$$\phi_x = \phi_0 \left[|H_1|^2 + |H_2|^2 + |H_3|^2 + \ldots \right]$$

$$+ \phi_{01}\ 2\ \mathrm{Re}(H_1\bar{H}_2 + H_2\bar{H}_3 + \ldots)$$

$$+ \phi_{02}\ 2\ \mathrm{Re}(H_1\bar{H}_3 + H_2\bar{H}_4 + \ldots)$$

$$+ \ldots$$

$$+ \phi_{0m}\ 2\ \mathrm{Re}(H_1\bar{H}_m + H_2\bar{H}_{m+1} + \ldots)$$

where ϕ_0 is the spectrum for $\xi = 0$ (the same
            as equation (17)

            ϕ_{0m} is the cross spectrum for $\xi = s/L = m\epsilon/L$
and where Re   denotes the real part.

4. With ϕ_x of step 3, establish A and N_0 as
    with any output spectrum.

5. Use the A and N_0 values of step 4 in the same
    manner as used in other sections of the manual.

106
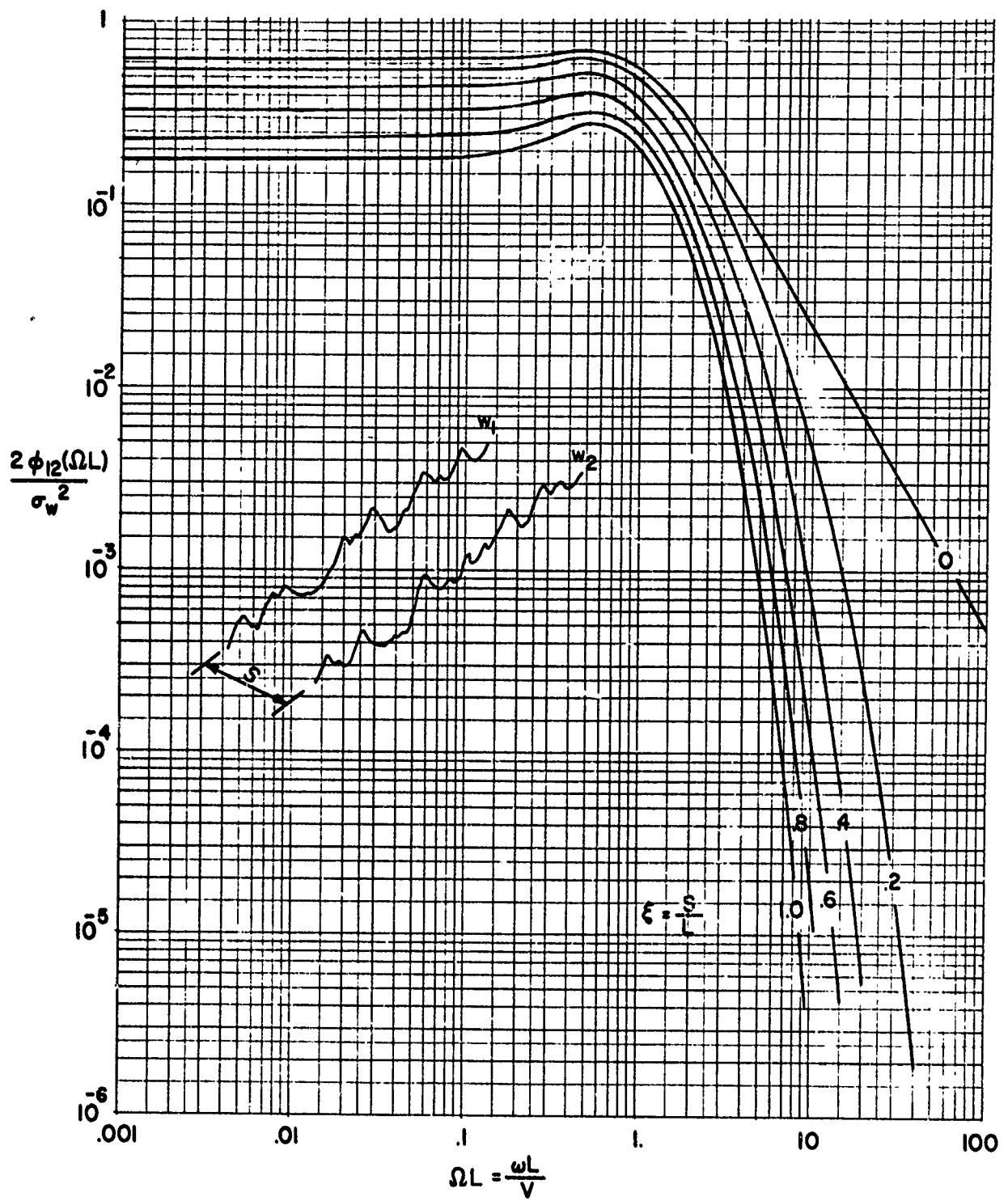
Figure 46. Cross-Spectra for Treatment of Nonuniform Spanwise Gusts

107

APPENDIX A

STANDARD DATA AND CONVERSION CHARTS

This appendix includes data which may be useful in studying various gust response problems. Included are some data on a standard atmosphere, some graphs pertaining to common probability density and probability functions, and several conversion graphs related to frequency and wavelength. Various definitions involved in the conversion charts are the following:

$$f = \frac{\omega}{2\pi} = \frac{V\Omega}{2\pi} = \frac{V}{\lambda} = \frac{Vk}{\pi c}$$

$$\omega = 2\pi f = V\Omega = \frac{2\pi V}{\lambda} = \frac{2Vk}{c}$$

$$\Omega = \frac{2\pi f}{V} = \frac{\omega}{V} = \frac{2\pi}{\lambda} = \frac{2k}{c}$$

$$k = \frac{\pi f c}{V} = \frac{\omega c}{2V} = \frac{\Omega c}{2} = \frac{\pi c}{\lambda}$$

$$L\Omega = \frac{2\pi L f}{V} = \frac{L\omega}{V} = \frac{2\pi L}{\lambda} = \frac{2Lk}{c}$$

$$\lambda = \frac{V}{f} = \frac{2\pi V}{\omega} = \frac{2\pi}{\Omega} = \frac{\pi c}{k}$$

where
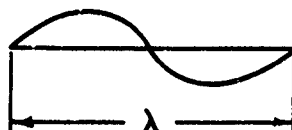
TABLE I - SOME STANDARD ATMOSPHERIC PROPERTIES

h 1000 ft	T $^{\circ}$R	$\rho \times 10^3$ slugs/cu ft	ρ/ρ_0	c ft/sec
0	518.7	2.377	1.000	1117
5	500.9	2.048	.8617	1098
10	483.0	1.755	.7385	1078
15	465.2	1.496	.6292	1058
20	447.4	1.266	.5328	1037
25	429.5	1.065	.4481	1016
30	411.7	.8893	.3741	995.1
35	393.9	.7365	.3099	973.3
36.089	390.0	.7061	.2971	968.5
40	390.0	.5851	.2462	968.5
45	390.0	.4601	.1936	968.5
50	390.0	.3618	.1522	968.5
55	390.0	.2845	.1197	968.5
60	390.0	.2238	.09414	968.5
65	390.0	.1760	.07403	968.5

Note: here T represents temperature
and c speed of sound.
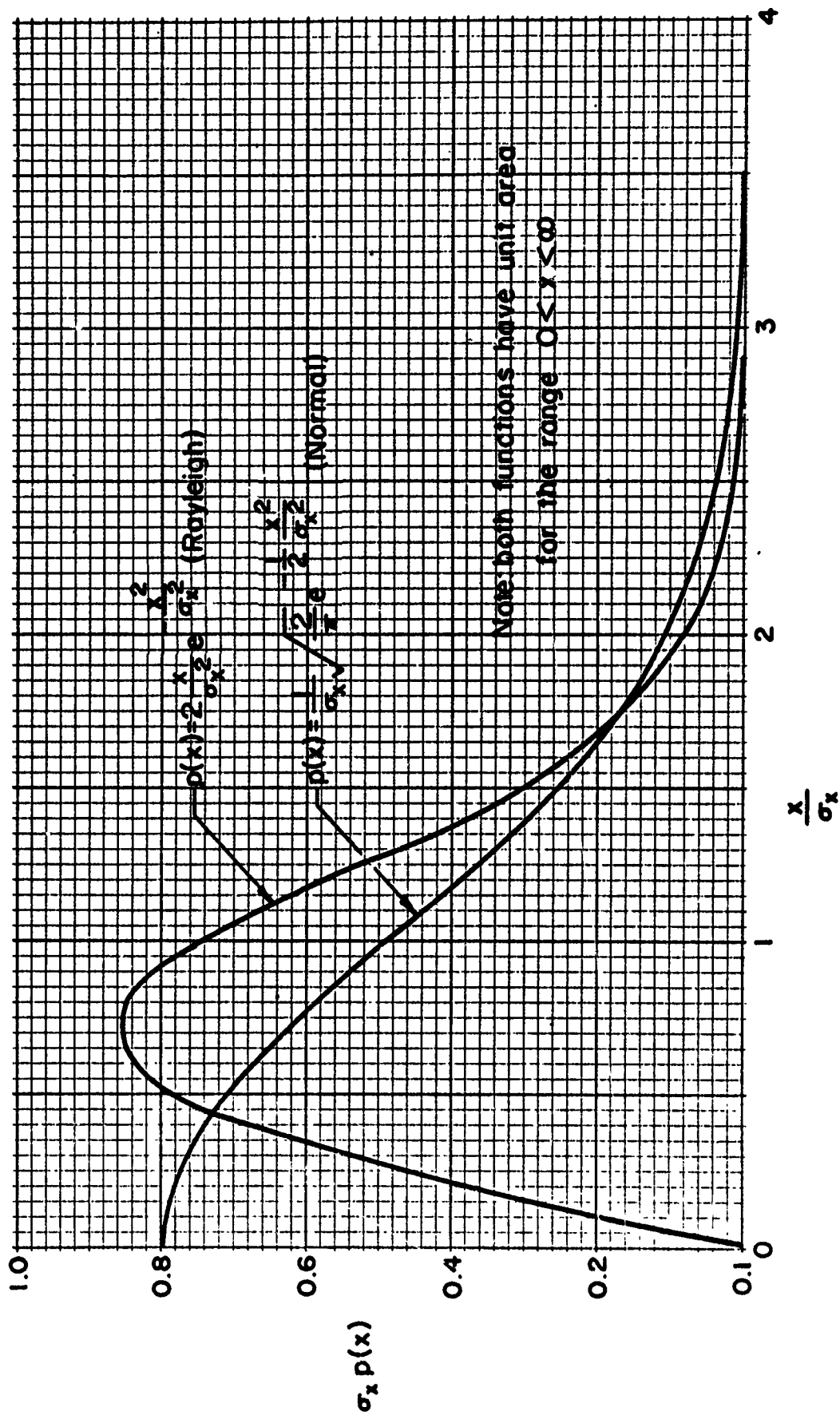
Figure A-1. Probability Density Curves

The figure shows two probability density curves plotted with axes $\sigma_x\, p(x)$ (vertical) versus $\frac{x}{\sigma_x}$ (horizontal).

$$p(x) = 2\frac{x}{\sigma_x^2} e^{-\frac{x^2}{\sigma_x^2}} \quad \text{(Rayleigh)}$$

$$p(x) = \frac{1}{\sigma_x}\sqrt{\frac{2}{\pi}}\, e^{-\frac{1}{2}\frac{x^2}{\sigma_x^2}} \quad \text{(Normal)}$$

Note both functions have unit area for the range $0 < x < \infty$
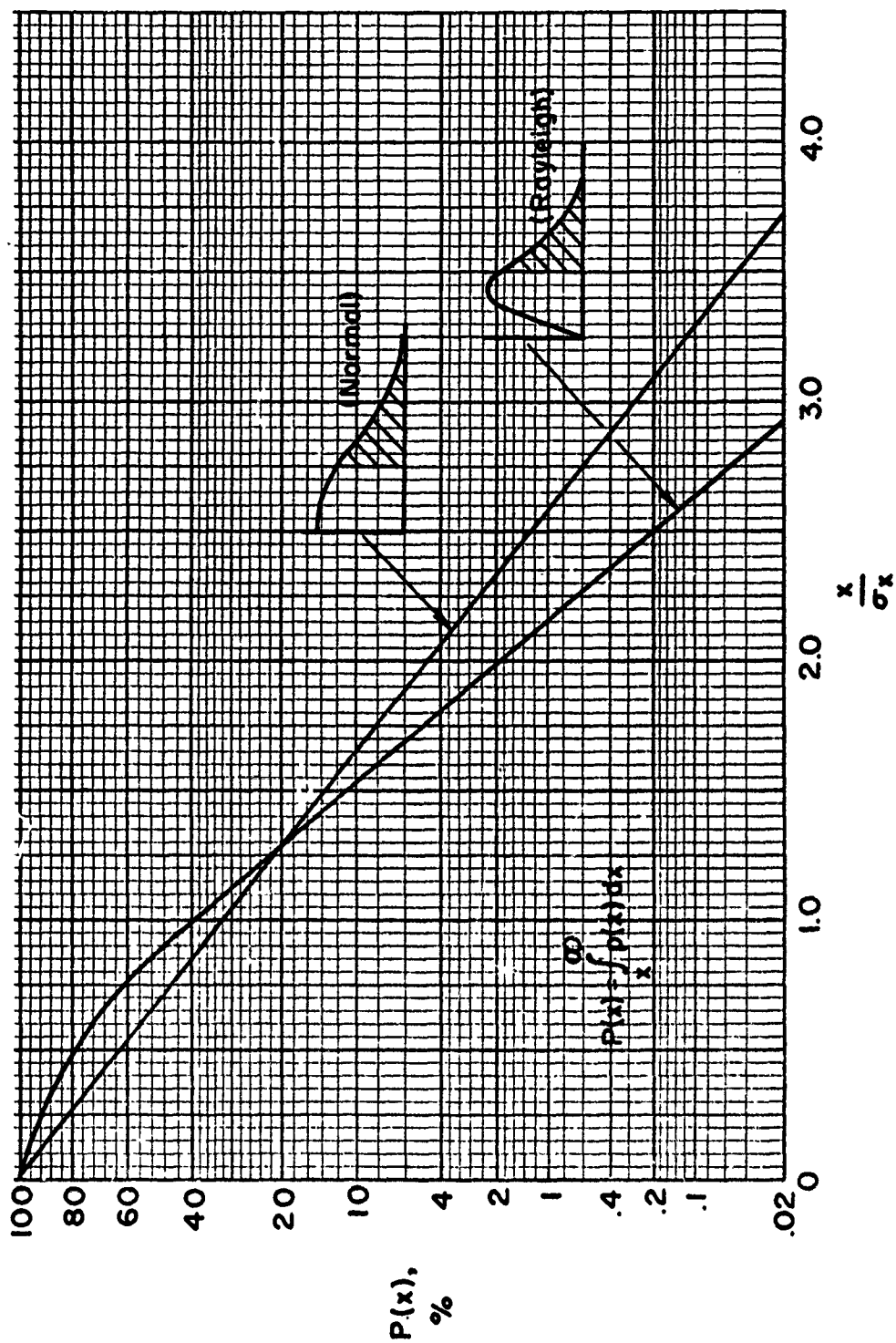
Figure A-2. Probability Values for Curves of Fig. A-1

112

Figure A-3. Nomograph Relating Ω and f

Figure A-4. Nomograph Relating k and f
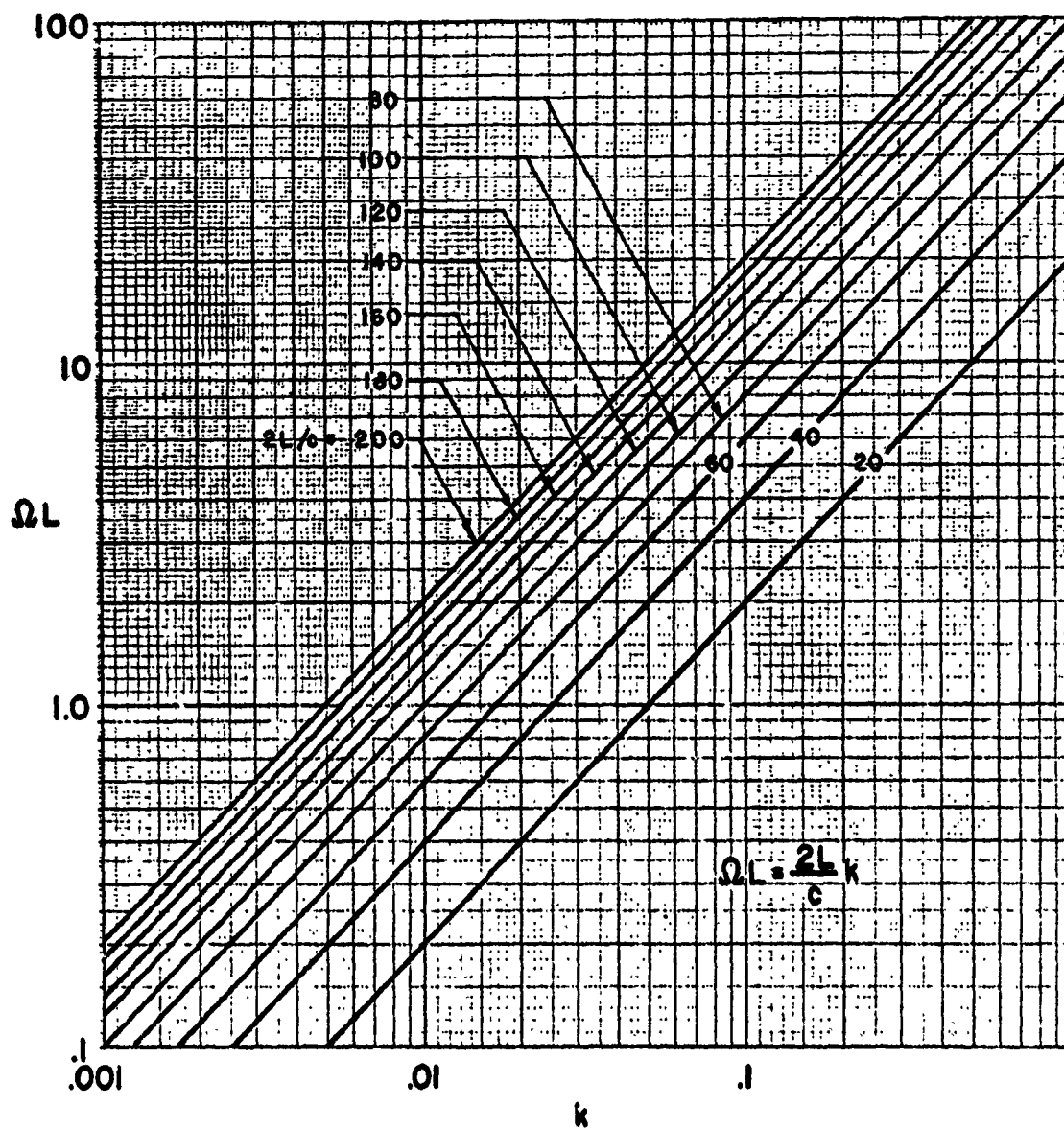
Figure A-5. Nomograph Relating ΩL and k
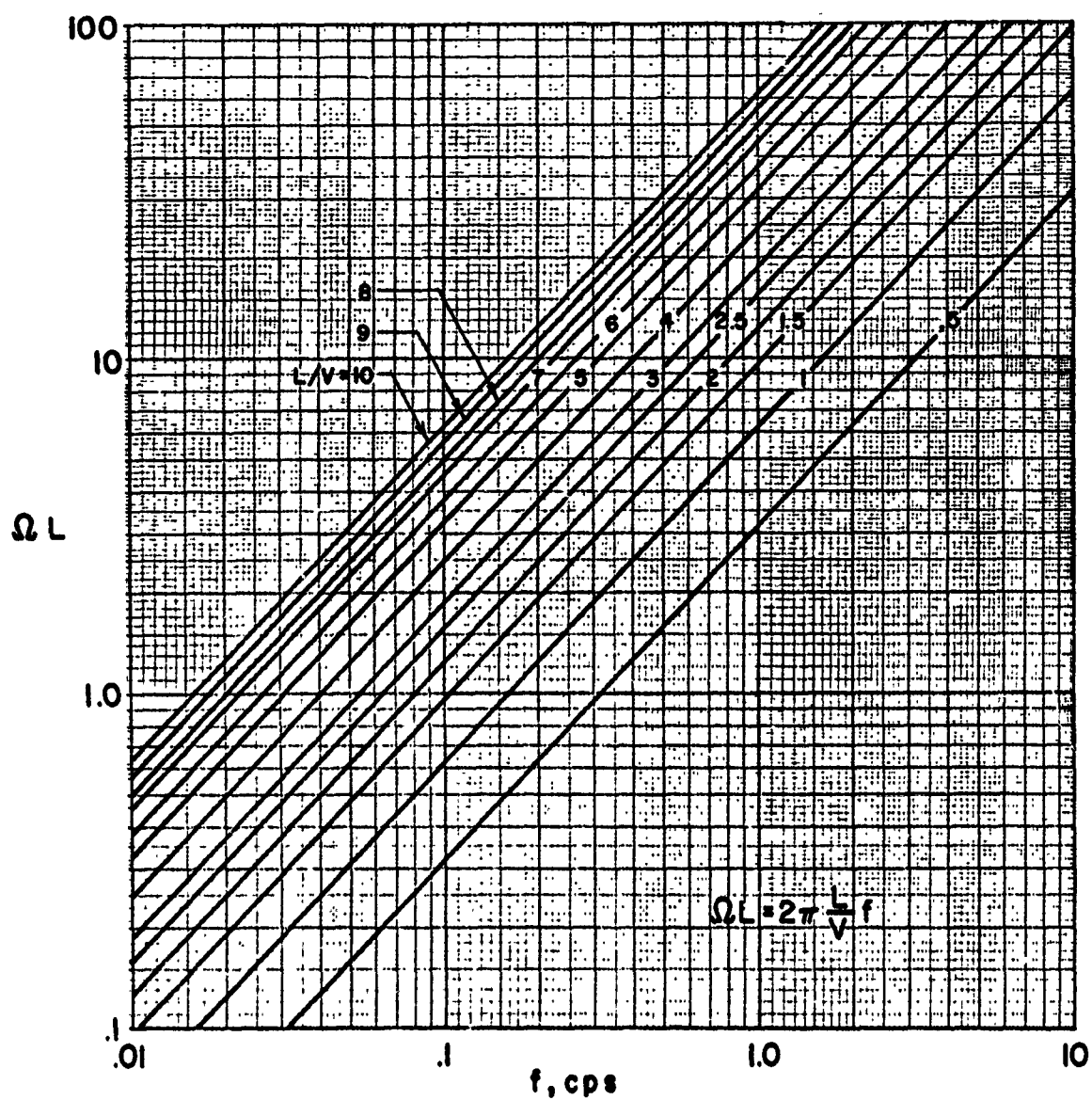
Figure A-6. Nomograph Relating ΩL and f
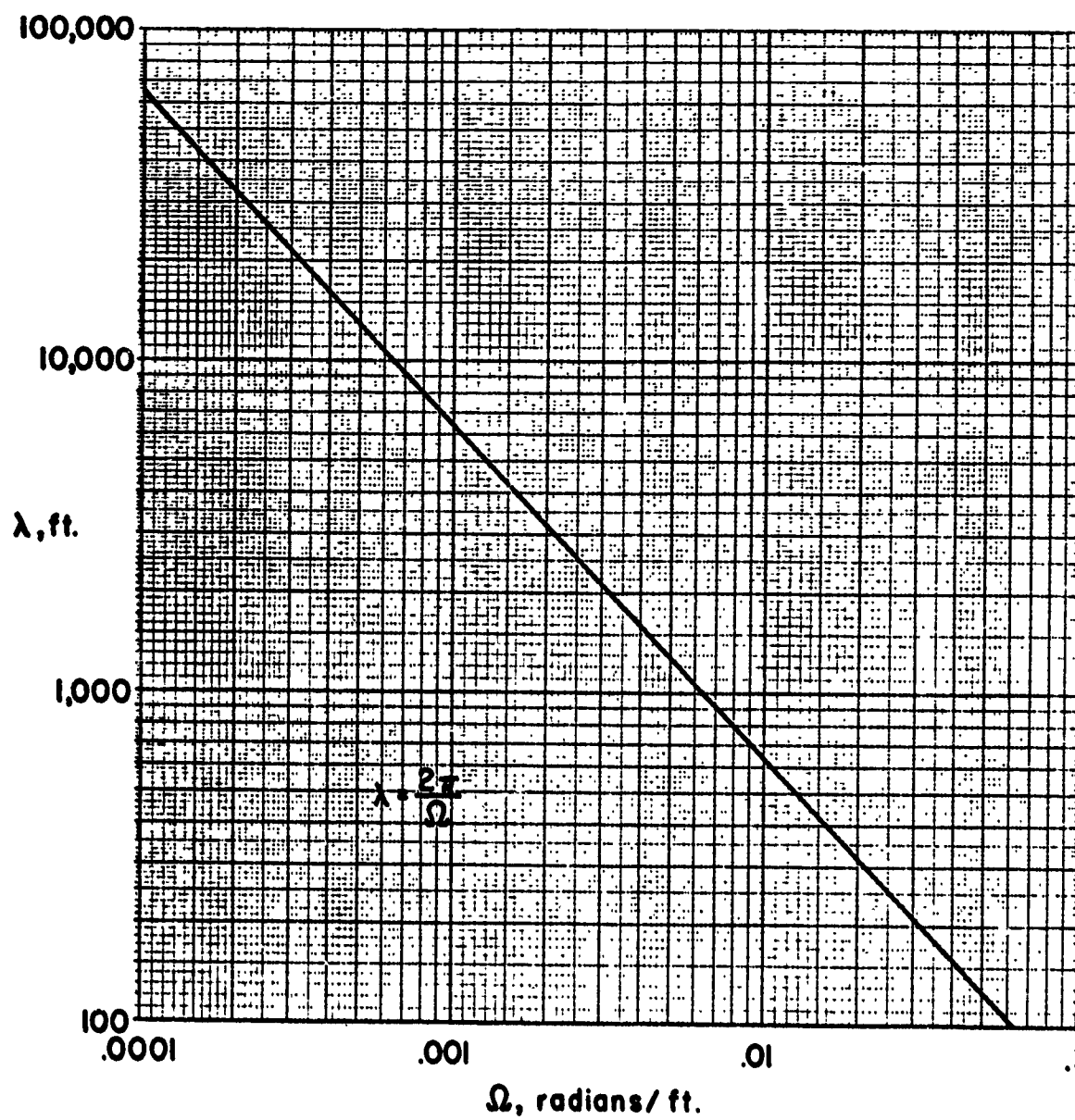
Figure A-7. Nomograph Relating λ and Ω

117
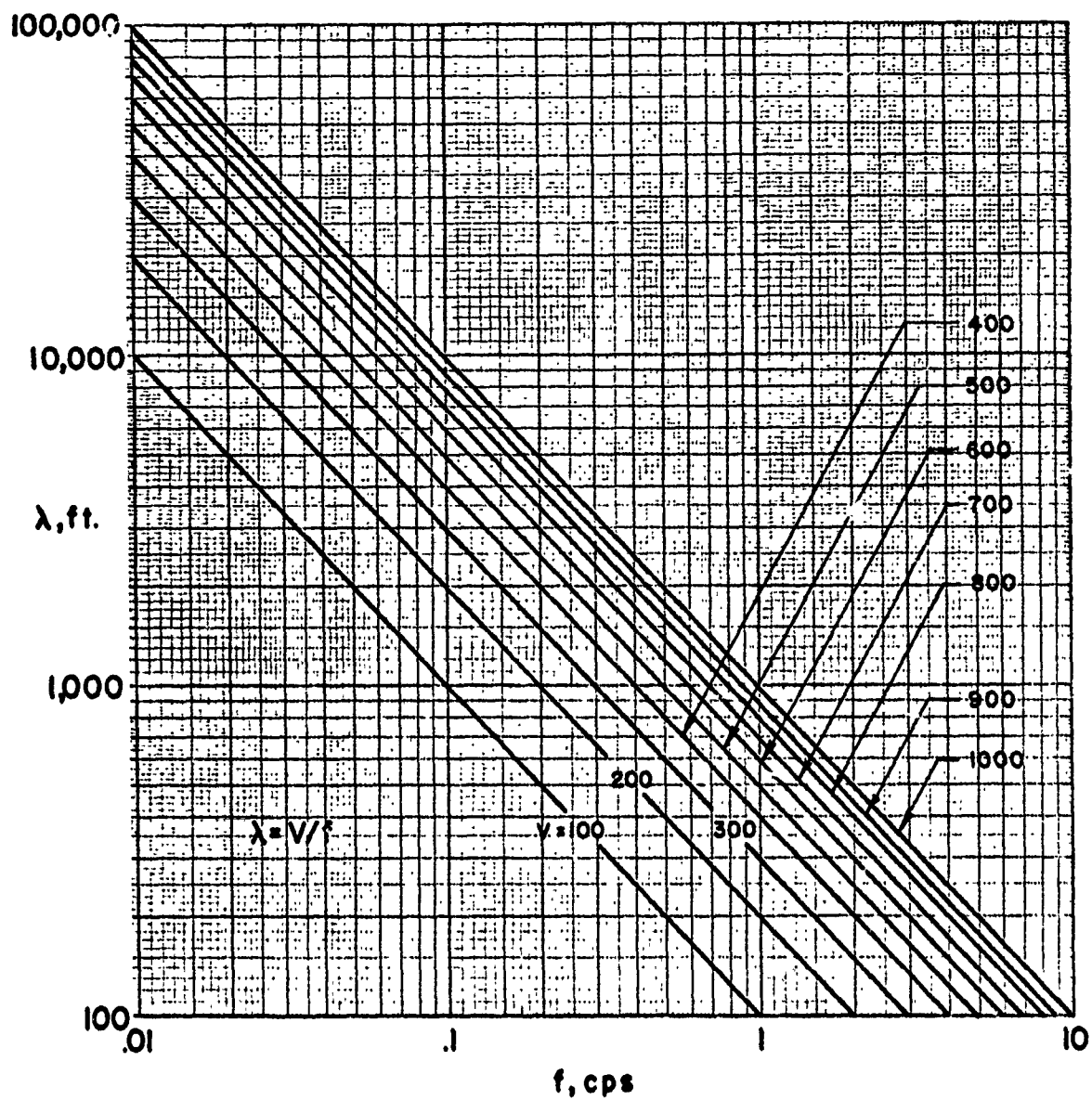
Figure A-8. Nomograph Relating λ and f

118
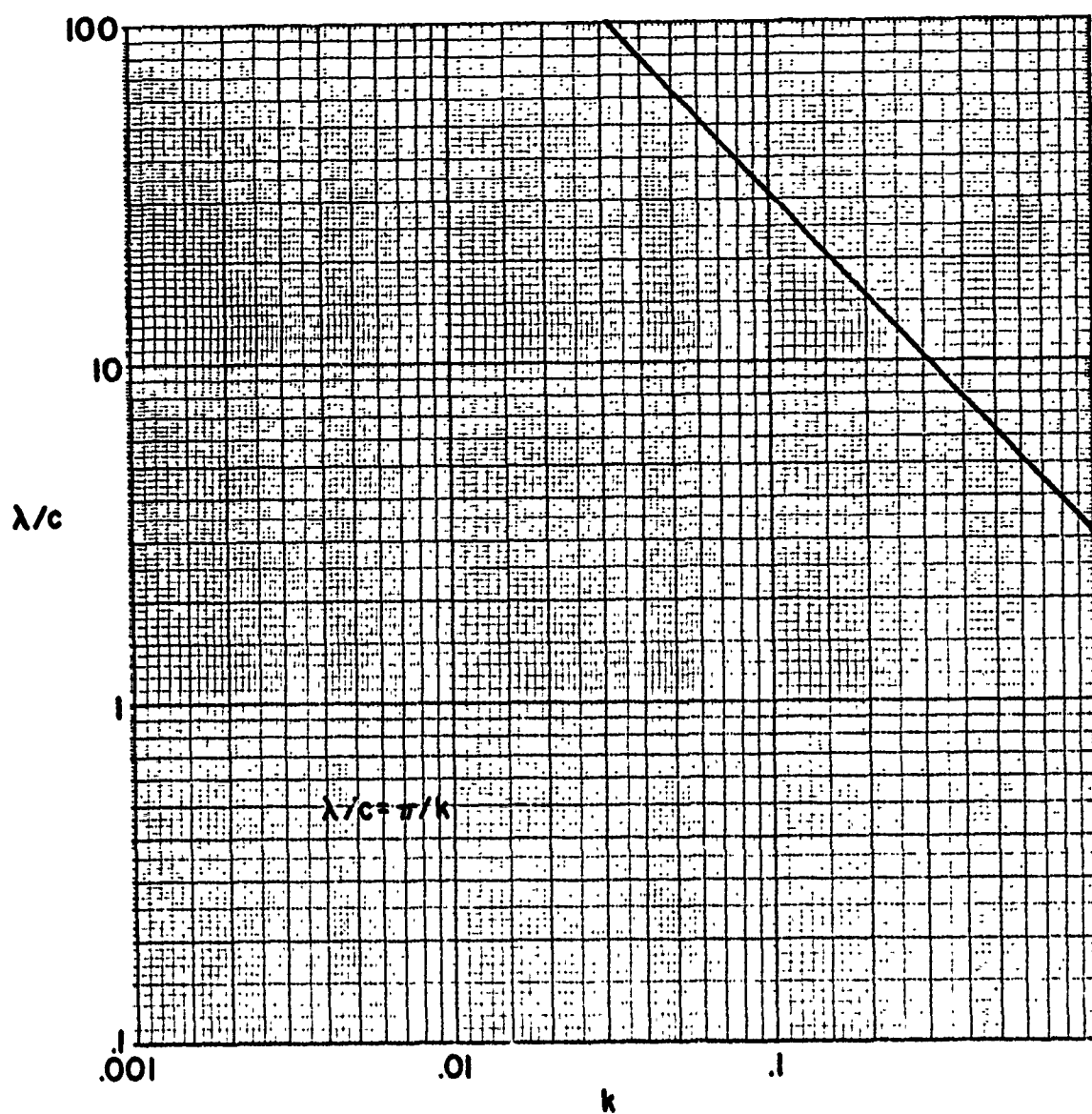
Figure A-9. Nomograph Relating λ/c and k

119

APPENDIX B

DETERMINATION OF FREQUENCY RESPONSE FUNCTIONS

Since the frequency response function plays such a central role in gust reponse analysis by power spectral methods, a review is given in this appendix of some of the ways for establishing this function. Throughout the presentation, sinusoidal motion is implied.

Structural aspects.- Two prime means are normally used to treat the aircraft structure, one a modal approach, the other a lumped-mass approach.

Modal approach:

The response or deformation of the structure is assumed to be given in terms of the natural modes of the structure, such as
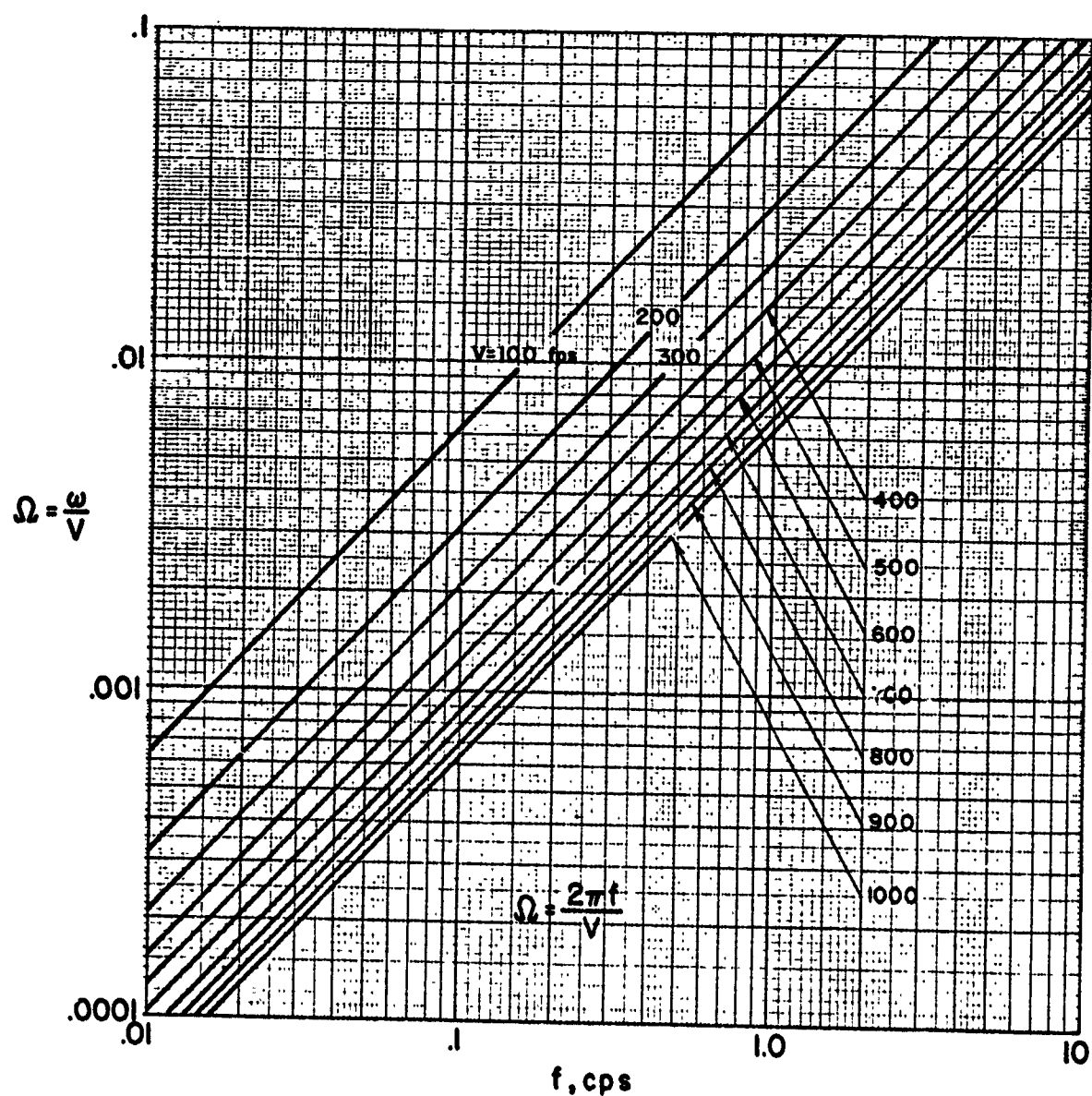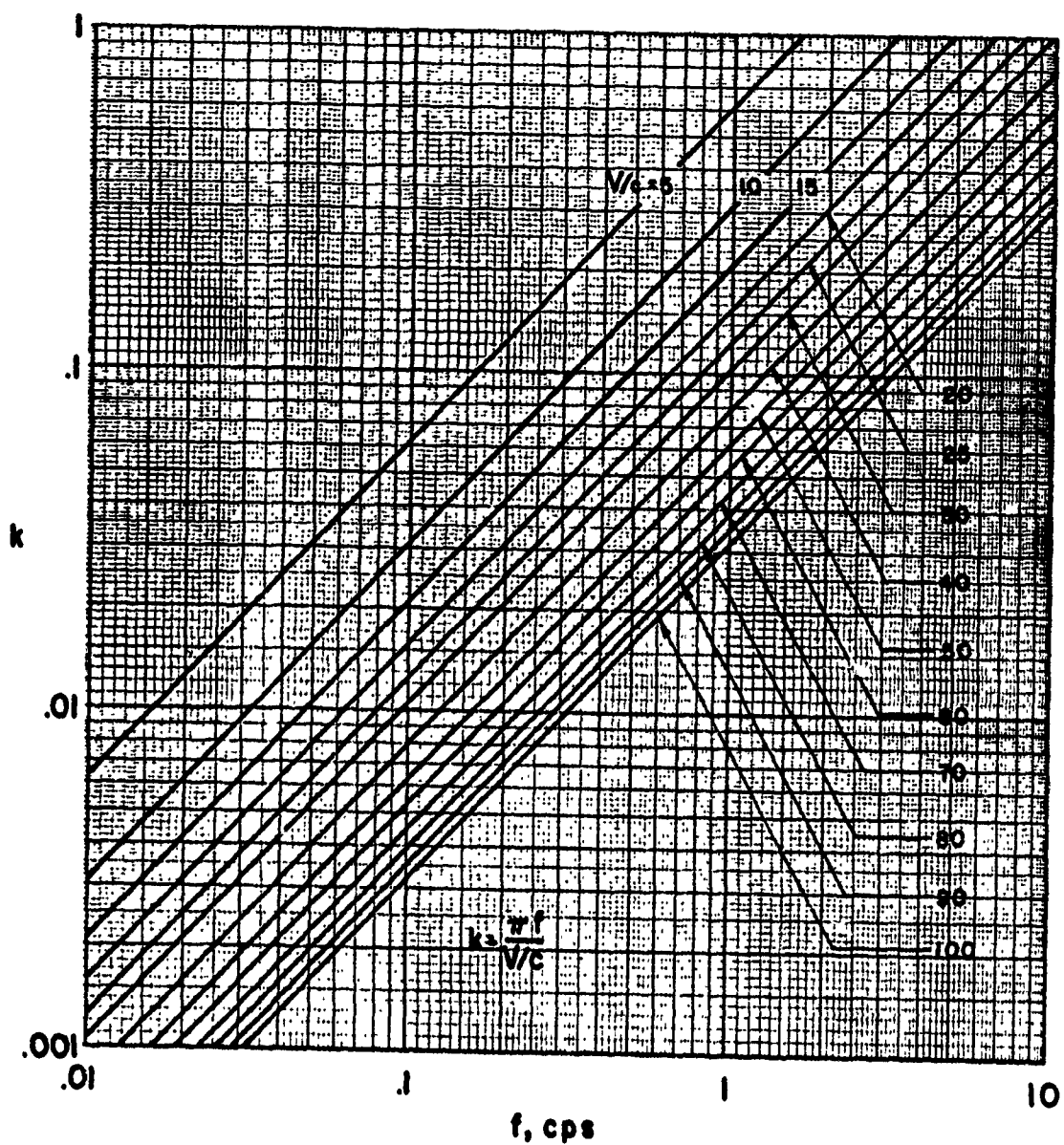
$$Z = a_1 Z_1 + a_2 Z_2 + a_3 Z_3 + \dots \tag{B-1}$$

where the Z_n's are the modes, and the a_n's are coefficients to be established. A Lagrangian dynamical treatment leads to the equation

$$M_n \ddot{a}_n + M_n \omega_n^2 a_n = \iint p \, Z_n \, dS \tag{B-2}$$

where M_n is the generalized mass of the Z_n mode , $M_n = \iint m Z_n^2 dS$, ω_n is the natural frequency of the mode Z_n , and p is the applied loading over the surface S . Structural damping is included by adding a term $2\gamma_n M_n \omega_n \dot{a}_n$ to the left side, or by modifying the second term to read $M_n \omega_n^2 (1+ig_n) a_n$.

Lumped-mass approach:

The mass of the structure is represented by "equivalent" concentrated masses; the stiffness is represented by discrete springs, or the concept of influence coefficients is introduced. The response equation takes the form of a matrix equation

$$[D]|Z_s| = \omega^2 [\text{-}m\text{-}]|Z_s| + |P_s| \tag{B-3}$$

where P_s represents applied concentrated loads. Structural damping is often introduced by multiplying the D matrix by a term $(1+ig)$.

Aerodynamics.- The aerodynamics are handled usually by a strip theory approach or by lifting surface theory; only the lifting surface theory method will be discussed here, and only for subsonic flow. Two forms of lifting surface theory have been used, one which uses a kernel function and assumed pressure modal shapes, the other which uses a modified kernel form and concentrated aerodynamic loads.

121

The basic kernel approach:

The downwash w that is produced by an aerodynamic pressure distribution p is given by the equation

$$w(x,y) = \iint p(\xi,\eta)K(x-\xi,y-\eta)dx \ dy \tag{B-4}$$

where K is a kernel function which, analogous to an influence coefficient, gives the downwash at point x,y due to a unit pressure dipole at ξ,η ; it is a function of reduced frequency $k = \omega c/2V$, and Mach number M ; see, for example, reference 31.

For a surface which is oscillating with a deflection form Z and for the condition of sinusoidal gust encounter, the downwash is given by

$$w = V \frac{\partial Z}{\partial x} + i\omega Z - e^{-i\frac{\omega x}{V}} \tag{B-5}$$

where x is the location of the downwash point relative to some convenient reference point such as the leading edge of the root chord of the wing. The problem is to combine equations (B-4) and (B-5) and to solve for the pressure p due to the motion Z and the gust input $e^{-i(\omega x/V)}$.

Modified kernel approach:

In the modified kernel approach the aerodynamic loading is assumed to be replaced by equivalent concentrated loads. In terms of these loads, equation (B-4) may be converted, see reference 3, to the matrix form

$$|w| = [\bar{K}]|P| \tag{B-6}$$

where $\bar{K}$ is a square matrix composed of terms of a modified kernel function, developed in reference 3. Reference 32 presents a related treatment which also leads to an equation similar to equation (B-6). The downwash due to the lifting surface and the gust is the same as that given by equation (B-4); for this case, solution for P can be made directly because of the fact that the K matrix of equation (B-6) can be inverted.

Frequency response function.-Four means are outlined now for establishing the frequency response function. One uses the kernel function approach; the other three are in terms of the modified kernel.

122

In terms of the kernel function:

Substitute equation (B-1) into equation (B-5) and obtain

$$w = a_1 z_1 + a_2 z_2 + a_3 z_3 + \ldots \, e^{-\frac{i\omega x}{V}} \qquad (B-7)$$

where z_n are downwash values given by $\left(V \dfrac{\partial}{\partial x} + i\omega\right) Z_n$. Assume

$$p = b_1 p_1 + b_2 p_2 + b_3 p_3 + \ldots \qquad (B-8)$$

where the p_n's are assumed pressure mode functions. Substitute equation (B-8) in equation (B-4), evaluate, and obtain

$$w = b_1 w_1 + b_2 w_2 + b_3 w_3 \qquad (B-9)$$

where the w_n's are the downwash functions associated with the p_n's . At a number of points on the wing, equal in number to the number of b_n's that are chosen in equation (B-8), equate the values of w given by equations (B-7) and (B-9); this leads to a matrix-type equation of the form

$$
\begin{vmatrix} w_1(1) & w_2(1) & w_3(1) \\ w_1(2) & w_2(2) & w_3(2) \\ w_1(3) & w_2(3) & w_3(3) \end{vmatrix}
\begin{vmatrix} b_1 \\ b_2 \\ b_3 \end{vmatrix}
=
\begin{vmatrix} z_1(1) & z_2(1) & z_3(1) & z_4(1) \\ z_1(2) & z_2(2) & z_3(2) & z_4(2) \\ z_1(3) & z_2(3) & z_3(3) & z_4(3) \end{vmatrix}
\begin{vmatrix} a_1 \\ a_2 \\ a_3 \\ a_4 \end{vmatrix}
+
\begin{matrix} c_1 \\ c_2 \\ c_3 \end{matrix}
$$

In general, the number of a_n values is different from the number of b_n values. Invert this equation to obtain

$$
\left.
\begin{aligned}
b_1 &= A_1 a_1 + A_2 a_2 + A_3 a_3 + A_4 a_4 + d_1 \\
b_2 &= \ldots. \\
b_3 &= \ldots.
\end{aligned}
\right\} \qquad (B-10)
$$

Substitute equation (B-8) into equation (B-2), evaluate the integrals, then make use of equation (B-10) to obtain final equations which are in terms of the unknown a_n's only. Solution of these

123

final equations for a_n allows the frequency response function for various quantities of interest to be evaluated. Generally, after solution is made for the a_n values, the total loading on the structure, including the inertial and aerodynamic loadings, is used to compute the section shear, moment, and torque loads. This total loading is given by

$$p_t = m\omega^2(a_1 Z_1 + a_2 Z_2 + \ldots) + p \qquad \text{(B-11)}$$

where p is given by equations (B-8) and (B-10).

By the modified kernel function:

Scheme 1.- This scheme makes use of equation (B-3); in general, the load and deflection points used for the dynamical treatment of the system, equation (B-3), may not be the same as those used for establishing the aerodynamic loads, equation (B-6). By suitable interpolation formulae, however, these two load and deflection systems may be related; suppose that the transformations from one system to the other are given by

$$|P| = [T_1]|P_s| \qquad \text{(B-12)}$$

$$|Z_s| = [T_2]|Z| \qquad \text{(B-13)}$$

where T_1 and T_2 are, in general, rectangular matrices. Combine equations (B-3), (B-5), (B-6), (B-12) and (B-13) to obtain

$$\bar{K}\, T_1 (D - \omega^2 m) T_2 Z = \left(V \frac{\partial}{\partial x} + i\omega\right) Z - e^{-i\frac{\omega x}{V}} \qquad \text{(B-14)}$$

where, for simplicity in writing, the matrix notation has been dropped. Equation (B-14), in turn, may be written

$$\left[\bar{K}\, T_1 (D - \omega^2 m) T_2 - \left(V \frac{\partial}{\partial x} + i\omega\right)\right] Z = - e^{-i\frac{\omega x}{V}}$$

or

$$D_1 Z = - e^{-i\frac{\omega x}{V}} \qquad \text{(B-15)}$$

124

Inverted, the desired result for the frequency response function
Z is found to be

$$Z = -D_1^{-1} \, e^{-i \frac{\omega x}{V}}$$ (B-16)

From Z, the frequency response function for other quantities of interest, such as acceleration or load at given points, may be determined.

The equation describing flutter of the system follows directly from equation (B-15), being simply this equation with the right-hand side set equal to zero.

Scheme 2.- If equation (B-2) is applied to each of the modes considered in equation (B-1), and if the loading p is expressed in terms of equivalent concentrated loads at various grid points, then for the sinusoidal case of a_n the following matrix equation can be written

$$\left[\left(\omega_n^2 - \omega^2\right)M_n\right]|a_n| = [Z_n]|P|$$ (B-17)

where $\left[\left(\omega_n^2 - \omega^2\right)M_n\right]$ is a simple diagonal matrix, a_n a column matrix, Z_n is a rectangular matrix built up from row matrices which express the deflection at each grid point for each mode Z_n, and P is a column matrix of the applied concentrated loads at each grid point. The simple matrix form of the generalized forces on the right side of equation (B-17) follows from equation (B-2) because of the Dirac function nature of each concentrated load. Now, make use of a matrix representation of equation (B-1) to express the deflection at each of the chosen grid points, namely

$$|Z| = [Z_n']|a_n|$$ (B-18)

where $[Z_n']$ is a rectangular matrix in which each column represents the deflection at the various grid points in a given mode.

Invert equation (B-6) and combine with equations (B-5) and (B-18) to obtain the loading as

$$|P| = [\bar{K}]^{-1}\left[V \frac{\partial}{\partial x} + i\omega\right][Z_n']|a_n| - [\bar{K}]^{-1}\left|e^{-i \frac{\omega x}{V}}\right|$$ (B-19)

The substitution of this equation into equation (B-17) leads to the result

125

$$\left[\left[\left(\omega_n^2 - \omega^2\right)M_n\right] - [Z_n][\bar{K}]^{-1}\left[V\frac{\partial}{\partial x} + i\omega\right][Z_n']\right]|a_n| = -[Z_n][\bar{K}]^{-1}\left|e^{-i\frac{\omega x}{V}}\right|$$

or

$$[E]|a_n| = -[Z_n][\bar{K}]^{-1}\left|e^{-i\frac{\omega x}{V}}\right| \qquad (B\text{-}20)$$

Solution for a_n yields the frequency response functions for a_n. With the a_ns established, various other frequency response functions such as acceleration or load at a given point follow readily.

Scheme 3.- In this version, proceed by solving equation (B-17) for $|a_n|$, or

$$|a_n| = \left[\frac{1}{(\omega_n^2 - \omega^2)M_n}\right][Z_n]|P|$$

where solution follows simply because the square matrix on the left-hand side of equation (B-17) is diagonal. The combination of this equation and equation (B-18) yields

$$|Z| = [Z_n']\left[\frac{1}{(\omega_n^2 - \omega^2)M_n}\right][Z_n]|P|$$

This equation and equation (B-5) yield

$$|w| = \left[V\frac{\partial}{\partial x} + i\omega\right][Z_n']\left[\frac{1}{(\omega_n^2 - \omega^2)M_n}\right][Z_n]|P| - |e^{-i\frac{\omega x}{V}}| \qquad (B\text{-}21)$$

Combine this equation with equation (B-6) by eliminating w and find the following equation in terms of the P values only

$$\left[[\bar{K}] - \left[V\frac{\partial}{\partial x} + i\omega\right][Z_n']\left[\frac{1}{(\omega_n^2 - \omega^2)M_n}\right][Z_n]\right]|P| = -\left|e^{-i\frac{\omega x}{V}}\right| \qquad (B\text{-}22)$$

or

126

$$[H]|P| = - \left| e^{-i \frac{\omega x}{V}} \right|$$

Inverted, the frequency response values for P are found directly as

$$|P| = -[H]^{-1} \left| e^{-i \frac{\omega x}{V}} \right| \tag{B-23}$$

It is to be noted that the matrices leading to H are all very easy to establish and, thus, this version appears especially attractive; notice also that the values of P are obtained in direct fashion.

The equations for flutter follow from schemes 2 and 3 by simply setting the right-hand sides of equations (B-20) and (B-23) equal to zero.

Example cases of frequency response functions and output spectra.- Several frequency response functions, as obtained in the study of specific aircraft, are given here to illustrate the general nature of the functions. Figures B-1 and B-2 show representative functions for the KC-135 airplane; figure B-3 for the B-58; while figure B-4 applies to the B-57. Two representative output spectra, obtained by multiplying the gust spectrum by the functions of figures B-1 and B-2, are shown in figures B-5 and B-6.

Some comment on the number of modal functions that should be included in any response treatment is considered worthwhile. In general, it is not possible to give rigid guidelines on how many modes should be included, but some observations found in practice give certain useful hints. For the larger aircraft it is usually found that the range of frequencies below 10 cps is of concern; and, more often than not, only modes below 5 cps are of importance. The mode selection is tied in with the location on the airplane where the response is being considered. For bending moment near the root, for example, the higher modes do not seem to contribute much. On the other hand, the higher modes are often found to contribute substantially when response near the outboard regions is being determined. Also, when main loads in the wing are being considered, secondary modes, such as are associated with pronounced pylon lateral motion, generally can be ignored. In computing the loads in the pylon, however, then these secondary-type modes become significant.

The main reasons why the higher modes (say modes above 3-4 cps) do not usually contribute significantly to the response is, of course, due to the rapid fall-off of the gust input spectrum in the high frequency regions. Figures B-2 and B-6 illustrate this effect rather well. In figure B-2, for frequency response, it appears that four higher modes are of concern at frequencies

127

of 3.3 , 4.2 , 5.8 and 6.6 cps . In figure B-6, however, it is seen that the two higher modes have almost disappeared, and that the response contribution of the lower two of these four modes is almost of negligible importance. The rigid body mode, the fundamental mode, and perhaps a third mode, appear to suffice for most cases.

GROSS WEIGHT: 268,000 LB   CUTOFF FREQUENCY: 10 CPS
ALTITUDE: 24,000 FT
MACH NUMBER: 0.85

WING BENDING MOMENT RESPONSE, 27 PERCENT SEMISPAN

Figure B-1. Illustrative Frequency Response Function for Wing Bending Moment for KC-135 Airplane (from reference 7)

129

GROSS WEIGHT:	268,000 LB	CUTOFF FREQUENCY:	10 CPS
ALTITUDE:	24,000 FT		
MACH NUMBER:	0.85		

WING SHEAR RESPONSE, 40.06 PERCENT SEMISPAN
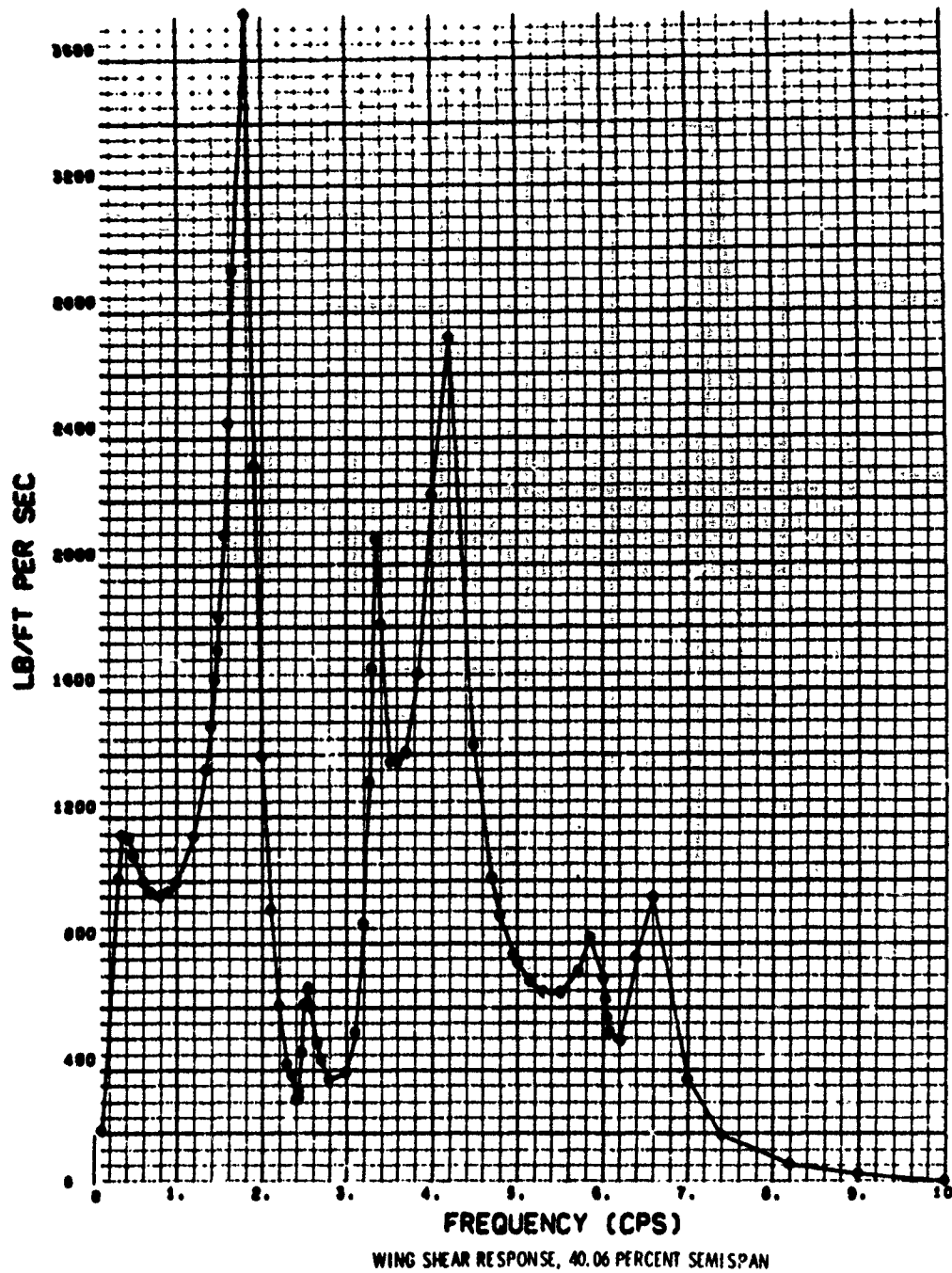
Figure B-2.   Illustrative Frequency Response Function for Wing
Shear for KC-135 Airplane (from reference 7)

130
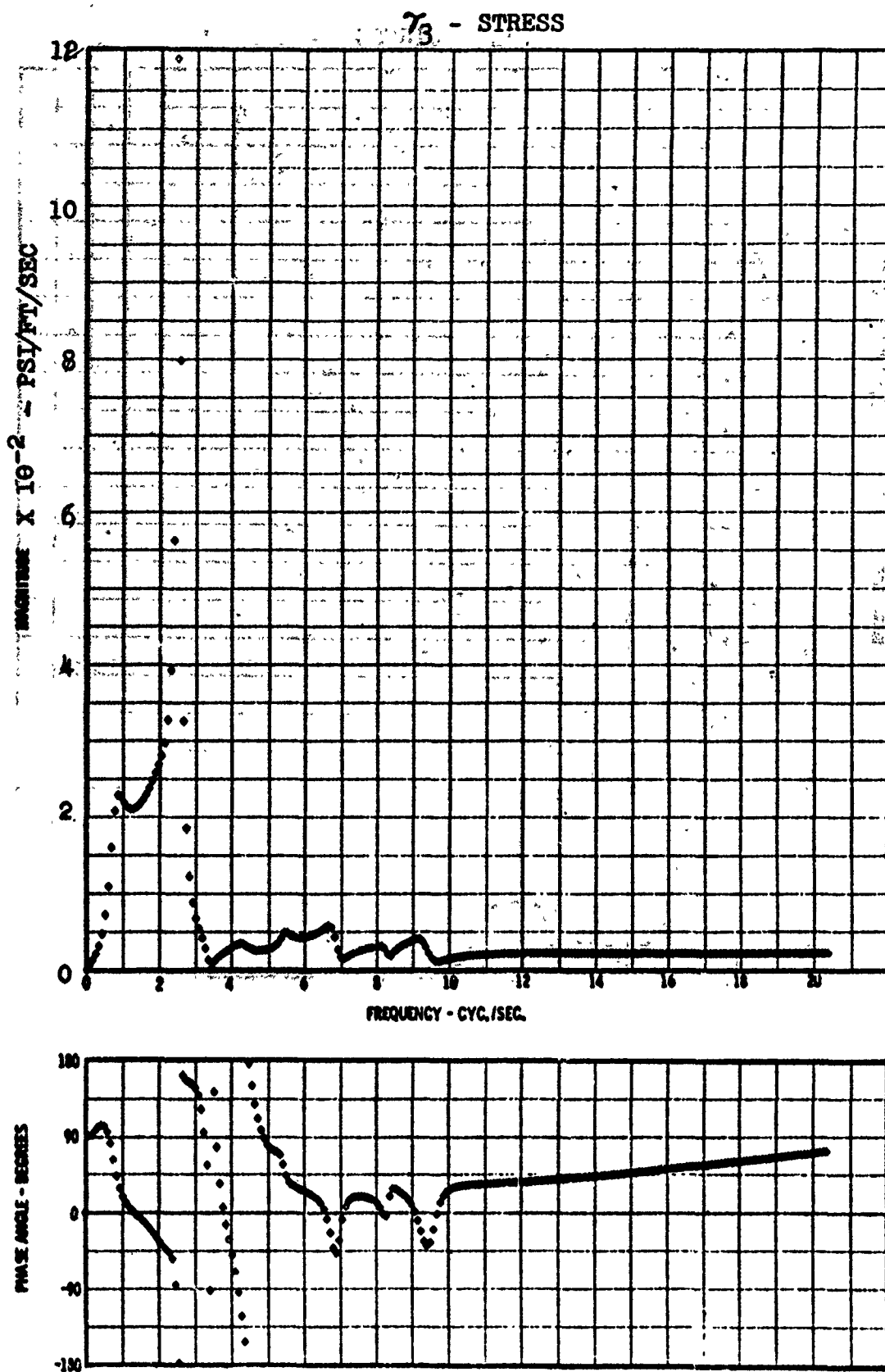
Figure B-3. Illustrative Frequency Response Function for B-58 Airplane (from reference 6)
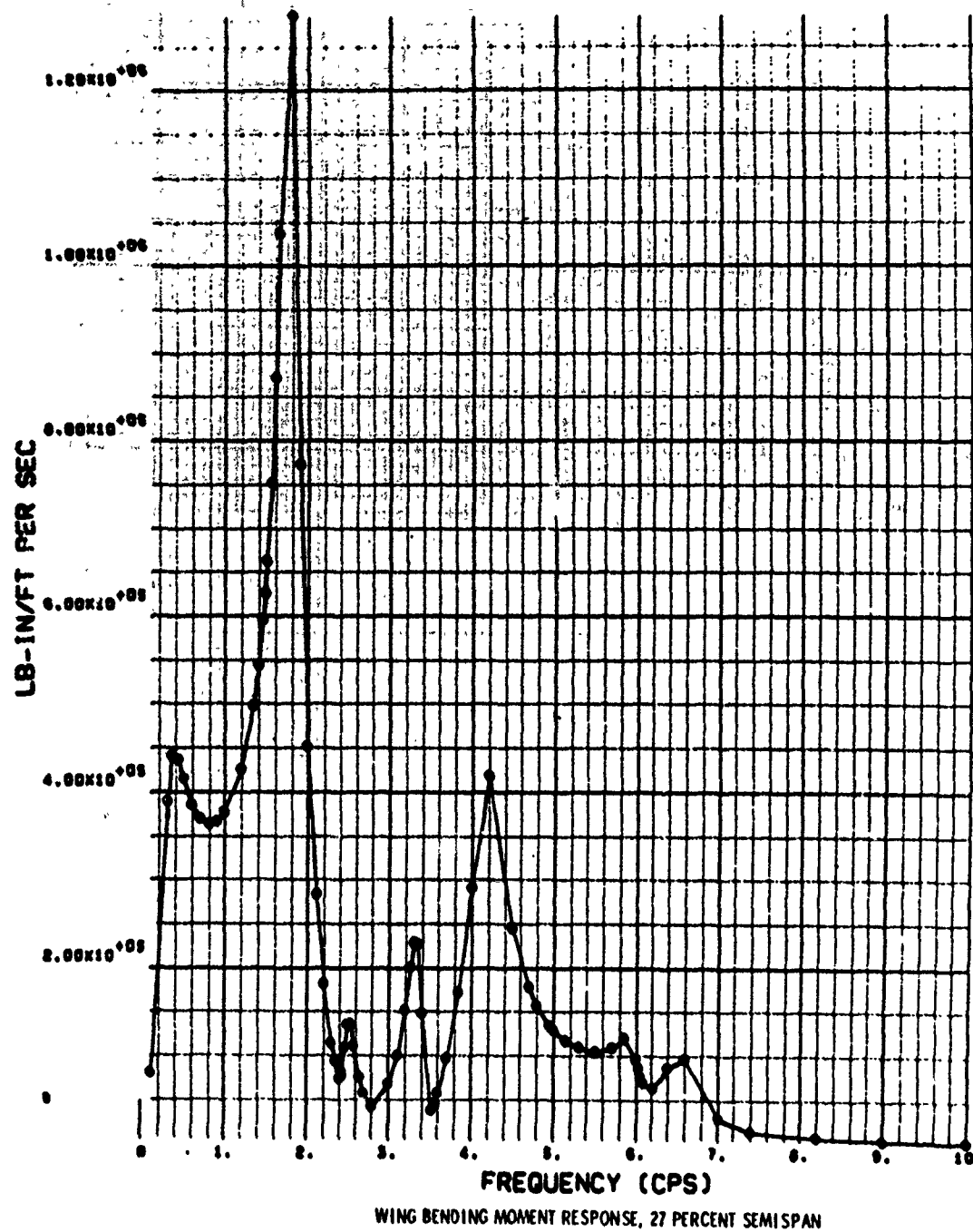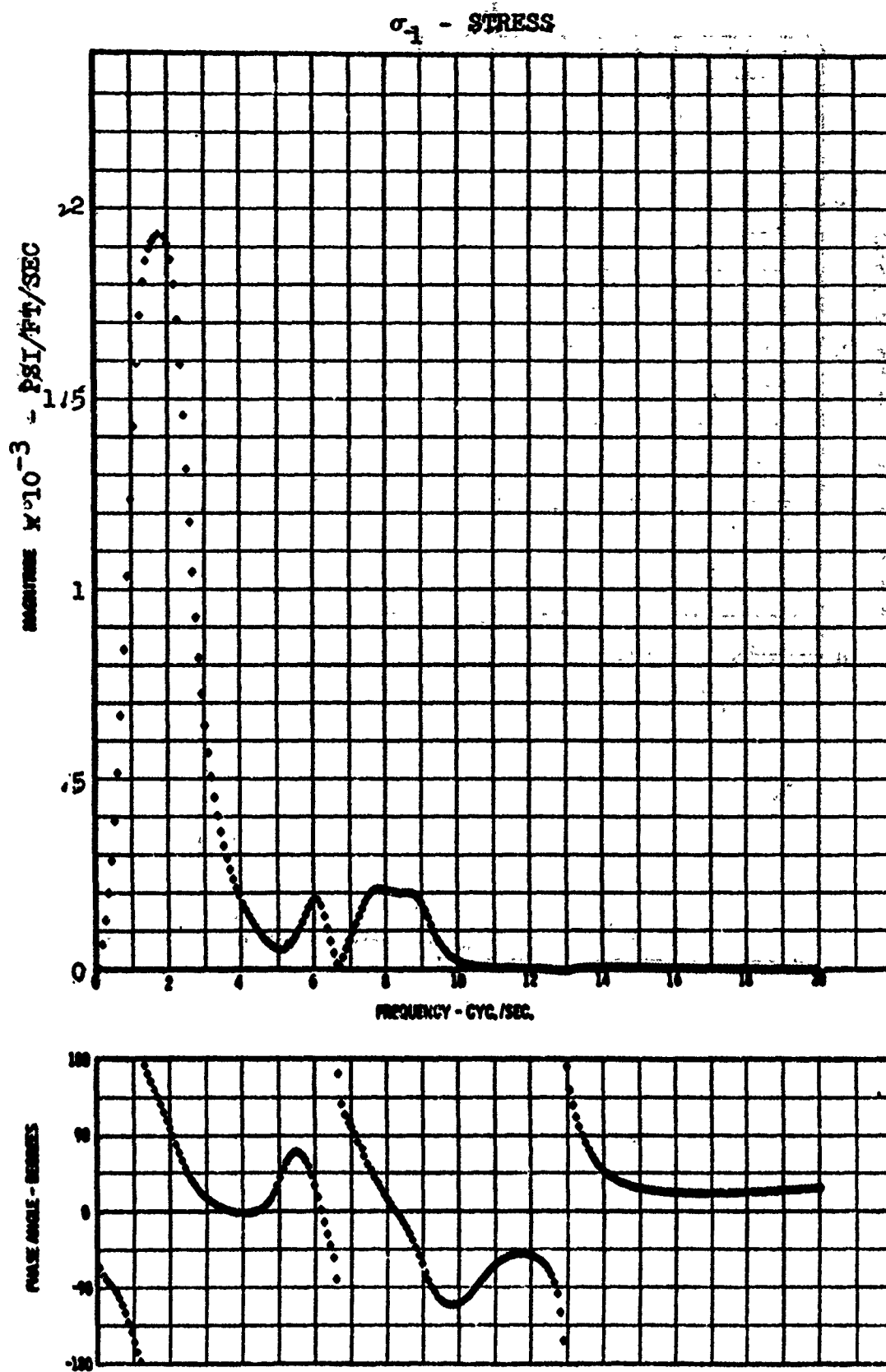
Figure B-4.   Illustrative Frequency Response Function for B-57
Airplane (from reference 6)

GROSS WEIGHT: 268,000 LB CUTOFF FREQUENCY: 10 CPS
ALTITUDE: 24,000 FT SCALE OF TURBULENCE: 1,000 FT
MACH NUMBER: 0.85

FREQUENCY (CPS)

WING BENDING MOMENT SPECTRUM, 27 PERCENT SEMISPAN
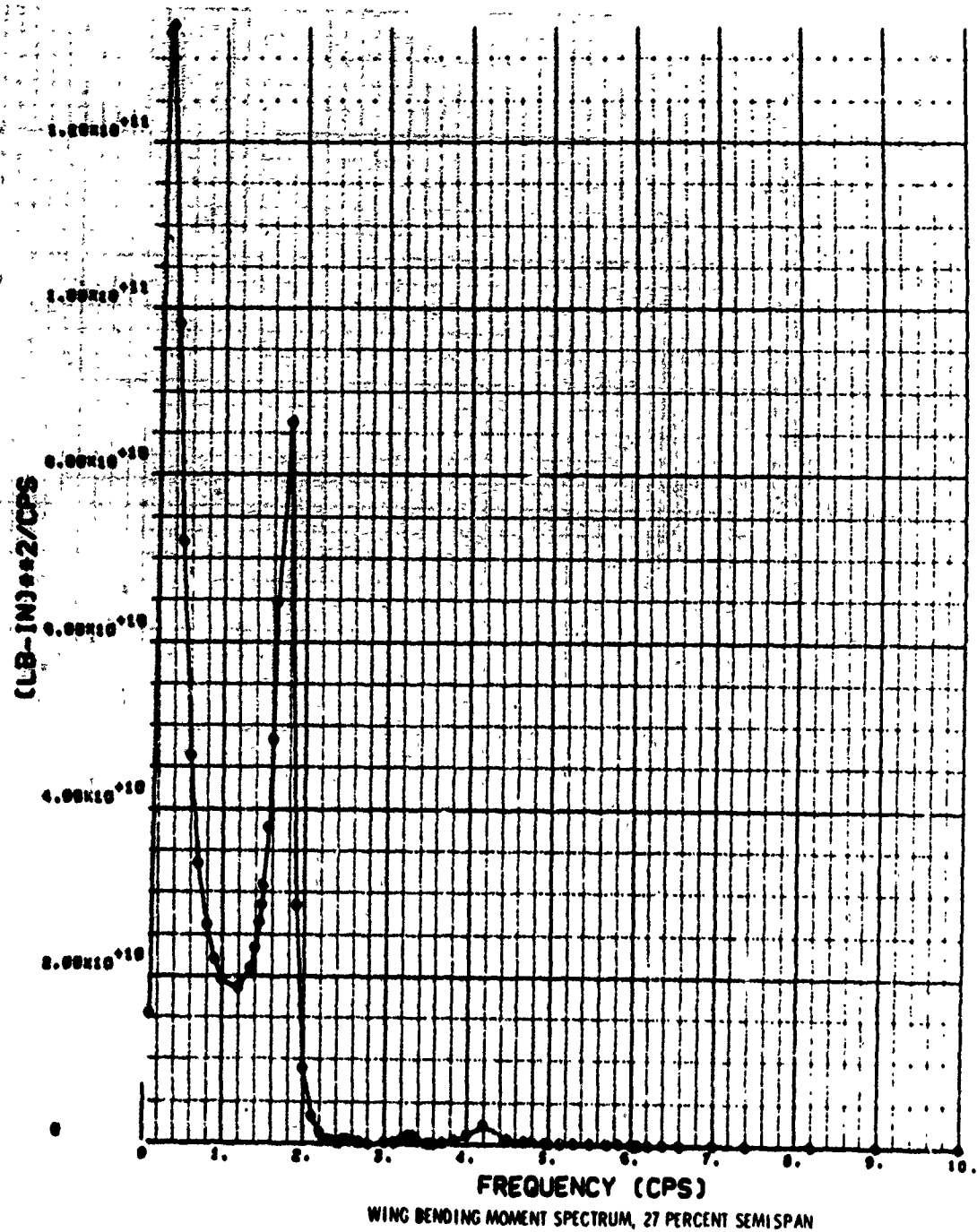
Figure B-5. Output Spectrum Associated with Fig. B-1 (from reference 7)

133

GROSS WEIGHT: 268,000 LB CUTOFF FREQUENCY: 10 CPS
ALTITUDE: 24,000 FT SCALE OF TURBULENCE: 1,000 FT
MACH NUMBER: 0.85
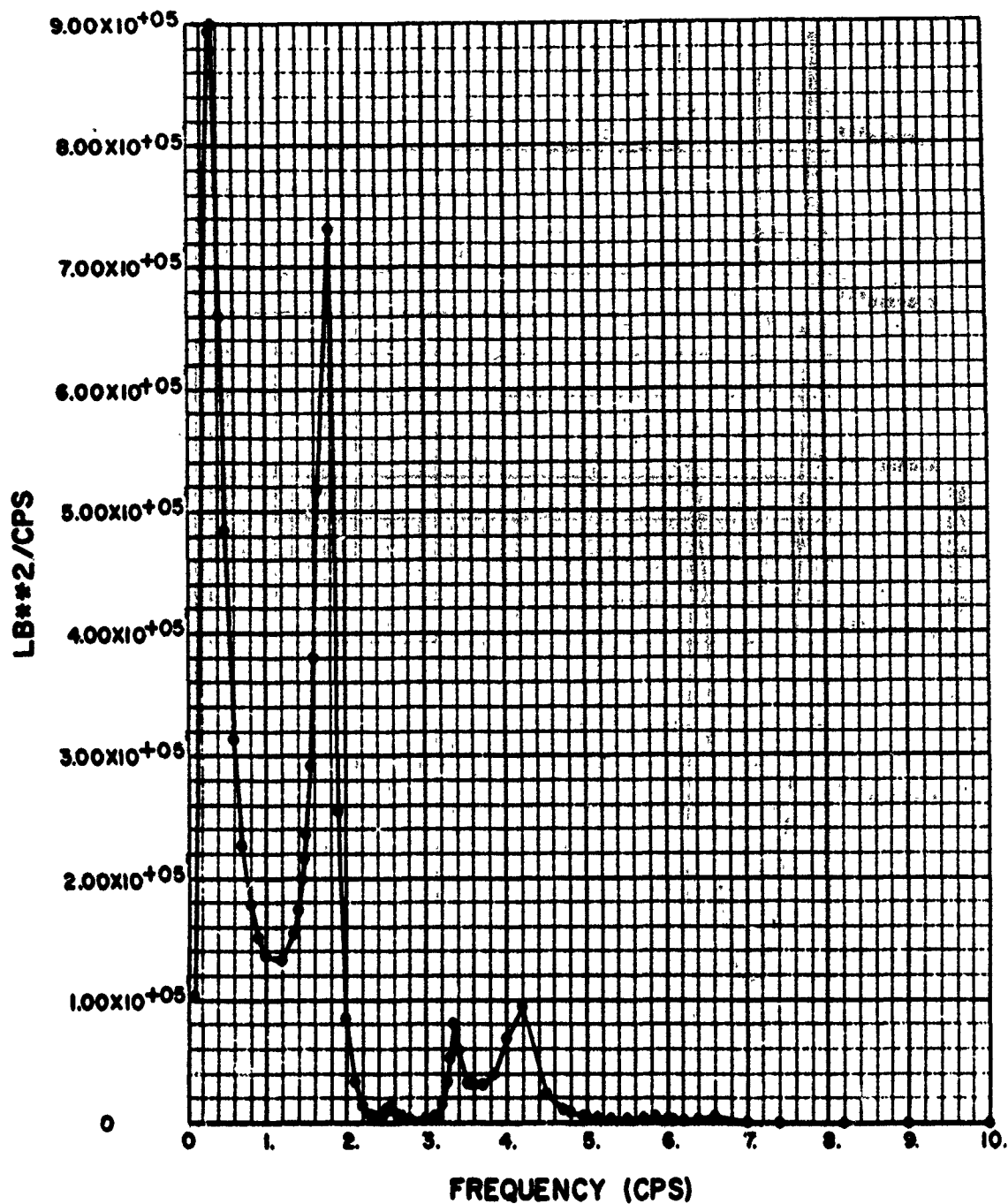
WING SHEAR SPECTRUM, 40.06% SEMISPAN

Figure B-6. Output Spectrum Associated with Fig. B-2 (from reference 7)

134

REFERENCES

1. Houbolt, J.C. "Preliminary Development of Gust Design Procedures Based on Power Spectral Techniques." Technical Report AFFDL-TR-66-58, Vol. I and II, September 1966.

2. Houbolt John C. "Gust Design Procedures Based on Power Spectral Techniques." Technical Report AFFDL-TR-67-74, August 1967.

3. Houbolt, John C. "Some New Concepts in Oscillatory Lifting Surface Theory." Technical Report AFFDL-TR-69-2, June 1969.

4. Houbolt, John C., Steiner, Roy, and Pratt, Kermit G. "Dynamic Response of Airplanes to Atmospheric Turbulence Including Flight Data on Input and Response." NASA TR R-199, June 1964.

5. Houbolt, John C. "Exceedances of Structural Interaction Boundaries for Random Excitation." AIAA Jour. Vol. 6, No. 11, November 1968, p. 2175.

6. Peloubet, R.P. and Haller, R.L. "Application of a Power Spectral Gust Design Procedure to Bomber Aircraft." Technical Report AFFDL-TR-66-35, June 1966.

7. Latz, R.N. "KC-135 Power Spectral Vertical Gust Load Analysis." Vol. II. Technical Report AFFDL-TR-66-57.

8. Hwang, Chintsun, Kambergm, B.D., Pi, W.S., and Cross, A.K. "Design Calculations on Proven Trainer and Fighter Aircraft for the Verification of a Gust Design Procedure." Technical Report AFFDL-TR-66-82, July 1966.

9. Gault, J.D. "Low Altitude Atmospheric Turbulence LO-LOCAT Mid-Term Technical Data Analysis." Technical Report SEG-TR-67-35, August 1967.

10. Crooks, Walter M., Hoblit, Frederic M., Prophet, David T., et al. "Project HICAT, An Investigation of High Altitude Clear Air Turbulence." Technical Report AFFDL-TR-67-123, Vol. I, November 1967.

11. Crooks, Walter M., Hoblit, Frederic M., Mitchell, Finis A., et al. "Project HICAT, High Altitude Clear Air Turbulence Measurements and Meteorological Correlations." Technical Report AFFDL-TR-68-127, Vol. II, Appendixes III-VI, November 1968.

12. Jones, G.W., Jones, J.W., and Monson, K.R. "Interim Analysis of Low Altitude Atmospheric Turbulence (LO-LOCAT) Data." Technical Report ASD-TR-69-7, February 1969.

13. Monson, K.R., Jones, G.W., Mielke, R.H., et al. "Low Altitude Atmospheric Turbulence LO-LOCAT Phase III Interim Report. Volume I. Data Acquisition and Analysis. Volume II. Instrumentation and Data Processing Details, Gust Velocity Data, and Test Log." Technical Report AFFDL-TR-69-63, Volume I and II, October 1969.

14. Ashburn, Edward V., Waco, David E., and Mitchell, F.A. "Development of High Altitude Clear Air Turbulence Models." Technical Report AFFDL-TR-69-79, November 1969.

15. Press, Harry, Meadows, May T., and Hadlock, Ivan. "A Re-evaluation of Data on Atmospheric Turbulence and Airplane Gust Loads for Application in Spectral Calculations." NACA Report 1272, 1956.

16. Hunter, Paul A. "Turbulence Experience in Airline Operations." Presented at Meeting on Aircraft Response to Turbulence, NASA Langley Research Center, September 24-25, 1968.

17. Pritchard, F.E., Easterbrook, C.C., and McVehil, G.E. "Spectral and Exceedance Probability Models of Atmospheric Turbulence for Use in Aircraft Design and Operation." Technical Report AFFDL-TR-65-122, November 1965.

18. Hoblit, F.M., Paul, N., Shelton, J.D., and Ashford, F.E. "Development of a Power-Spectral Gust Design Procedure for Civil Aircraft." FAA-ADS-53, January 1966.

19. Coy, Richard G. "Atmospheric Turbulence Spectra from B-52 Flight Loads Data." Technical Report AFFDL-TR-67-13, April 1967.

20. Dempster, John B. and Bell, Clarence A. "Summary of Flight Load Environmental Data Taken on B-52 Fleet Aircraft." Volume 2, Number 5. Journal of Aircraft, September-October, 1965.

21. Austin, William H., Jr. "Development of Improved Gust Load Criteria for United States Air Force Aircraft." Technical Report SEG-TR-67-28, September 1967.

22. Military Specification. Airplane Strength and Rigidity Flight Loads, MIL-A-8861(ASG). 18 May 1960. Unclassified.

23. Houbolt, John C. "Deduction of L Values from Acceleration Records." (Work for NASA, not yet published).

24. Houbolt, John C. Unpublished: "Influence of Scale Variation on Gust Spectrum Shape."

25. Houbolt, John C. and Kordes, Eldon E. "Structural Response to Discrete and Continuous Gusts of an Airplane Having Wing-Bending Flexibility and a Correlation of Calculated and Flight Results." NACA Report 1181, 1954. (Supersedes NACA TN 3006; also contains essential material from TN 2763 and TN 2897.)

26. Yates, J.E. and Houbolt, John C. Unpublished: "Oscillatory Functions for High Frequencies for Airfoils."

27. Pratt, Kermit G. and Walker, Walter G. "A Revised Gust-Load Formula and a Re-Evaluation of V-G Data Taken on Civil Transport Airplanes from 1933 to 1950. NACA Rep. 1206, 1954. (Supersedes NACA TN's 2964 by Kermit G. Pratt and 3041 by Walter G. Walker.)

28. Donely, Philip. "Summary of Information Relating to Gust Loads on Airplanes." NACA Report 997, 1950. (Supersedes NACA TN 1976.)

29. Houbolt, John C. "On the Response of Structures Having Multiple Random Inputs. Jahr. 1957 der WGL, Friedr. Vieweg & Sohn (Braunschweig), pp. 296-305.

30. Houbolt, John C. and Sen, Asim, Unpublished: "Cross Spectra for Vertical Gust."

31. Watkins, Charles E., Runyan, Harry L., and Woolston, Donald E. "On the Kernel Functions of the Integral Equation Relating the Lift and Downwash Distributions of Oscillating Finite Wings in Subsonic Flow." NACA Report 1234, 1955, (Supersedes NACA TN 3131.)

32. Albano, E. and Rodden, W.P. "A Doublet-Lattice Method for Calculating Lift Distributions on Oscillating Surfaces in Subsonic Flows." AIAA Jour., Vol. 7, No. 2, February 1969, pp. 279-285.

DOCUMENT CONTROL DATA - R & D

(Security classification of title, body of abstract and indexing annotation must be entered when the overall report is classified)

1. ORIGINATING ACTIVITY *(Corporate author)*	2a. REPORT SECURITY CLASSIFICATION
Aeronautical Research Associates of Princeton, Inc. 50 Washington Road Princeton, New Jersey 08540	Unclassified
	2b. GROUP N/A

3. REPORT TITLE

Design Manual for Vertical Gusts Based on Power Spectral Techniques

4. DESCRIPTIVE NOTES *(Type of report and inclusive dates)*

Final Report; January 2, 1969 - July 1, 1970

5. AUTHOR(S) *(First name, middle initial, last name)*

John C. Houbolt

6. REPORT DATE	7a. TOTAL NO. OF PAGES	7b. NO. OF REFS
July 1970	139	32

8a. CONTRACT OR GRANT NO. F33615-69-C-1272 *new*	9a. ORIGINATOR'S REPORT NUMBER(S)
b. PROJECT NO. 1367	A.R.A.P. Report No. 147
c.	9b. OTHER REPORT NO(S) *(Any other numbers that may be assigned this report)*
d.	

10. DISTRIBUTION STATEMENT This document is subject to special export controls and each transmittal to foreign governments or foreign nationals may be made only with prior approval of the Air Force Flight Dynamics Laboratory (FDTR), Wright-Patterson Air Force Base, Ohio 45433.

11. SUPPLEMENTARY NOTES	12. SPONSORING MILITARY ACTIVITY Air Force Flight Dynamics Laboratory Air Force Systems Command, USAF

13. ABSTRACT Recommended procedures, based on power spectral methods, are given for the design of aircraft for vertical atmospheric turbulence encounter. Four procedures are outlined. The first is a direct preliminary design type, based on specified rigid body results. The second is more detailed and makes use of composite response values, computed either from the rigid body results, or by specific frequency response analysis. A third procedure is based on comparison with a previous successful design. In the fourth procedure specific loads exceedance curves are derived in accordance with assumed missions. Recommended gust intensity values, proportion of time in turbulence, and scale values are given. For ease in application, detailed step-by-step procedures are listed throughout the manual.

The philosophy and basis for deriving the recommended design values are reviewed in part. Special sections are included throughout which summarize the basic equations that apply to gust analysis, give the means for treating structural interaction effects, and show how the problem of nonuniform spanwise gusts is treated. Appendices are included which give useful conversion and data charts, and which review various means for establishing the frequency response function.

DD FORM 1 NOV 65 **1473**

14. KEY WORDS	LINK A		LINK B		LINK C	
	ROLE	WT	ROLE	WT	ROLE	WT
gust design procedures						
power spectral techniques						
atmospheric turbulence						
aircraft dynamic response						
gust spectra						
gust intensities						
scale value						
discrete gust design						
exceedance curves						
probability density						
frequency response						